ADDIS ABABA UNIVERSITY

COLLEGE OF NATURAL AND COMPUTATIONAL SCIENCES

SCHOOL OF EARTH SCIENCES

THE PRE-VOLCANIC SEDIMENTARY UNIT IN THE KELLA SECTION, WESTERN ESCARPMENT, CENTRAL MAIN ETHIOPIAN RIFT

KALKIDAN ASMARE WORKU

A THESIS SUBMITTED TO THE SCHOOL OF EARTH SCIENCES OF ADDIS ABABA UNIVERSITY IN PARTIAL FULFILMENT OF THE REQUIREMENTS FOR THE DEGREE OF MASTER OF SCIENCE IN GEOLOGICAL SCIENCES (STRATIGRAPHY AND SEDIMENTOLOGY)

ADDIS ABABA, ETHIOPIA

JUNE, 2024

THE PRE-VOLCANIC SEDIMENTARY UNIT IN THE KELLA SECTION, WESTERN ESCARPMENT, CENTRAL MAIN ETHIOPIAN RIFT

BY:

KALKIDAN ASMARE WORKU

ADVISOR;

Dr. BALEMWAL ATNAFU

A THESIS SUBMITTED TO

THE SCHOOL OF EARTH SCIENCES OF ADDIS ABABA UNIVERSITY IN PARTIAL FULFILMENT OF THE REQUIREMENTS FOR THE DEGREE OF MASTER OF SCIENCE IN GEOLOGICAL SCIENCES (STRATIGRAPHY AND SEDIMENTOLOGY)

ADDIS ABABA UNIVERSITY

ADDIS ABABA, ETHIOPIA

JUNE, 2024

DECLARATION

I hereby declare that the thesis entitled "The Pre-Volcanic Sedimentary Unit in the Kella Section, Western Escarpment, Central Main Ethiopian Rift" is my original work carried out under the supervision of Dr. Balemwal Atnafu. It has not been submitted to any University or any other institution for the purpose of receiving degree or diploma program. All sources of materials used for this thesis are duly acknowledged.

Candidate's Name:	Signature	Date
Kalkidan Asmare Worku	_____________	______________

This thesis has been submitted for examination with my approval as university advisor.

Advisor's Name	Signature	Date
Dr. Balemwal Atnafu	______________	_____________

SIGNATURE PAGE

Addis Ababa University

School of Earth Sciences

The thesis entitled as: The pre-volcanic sedimentary unit in the Kella section, western escarpment, Central Main Ethiopian Rift, has been approved by the school graduate committee of School of Earth sciences for the partial fulfillment of the degree of Master of Science in Geological Sciences (Stratigraphy and Sedimentology).

Approved by the Examining Committee

Examiner: Prof. Worash Getaneh	___________	___________
Name	**Signature**	**Date**
Examiner: Prof. Mulugeta Fisseha	___________	___________
Name	**Signature**	**Date**
Advisor: Dr. Balemwal Atnafu	___________	___________
Name	**Signature**	**Date**

School of Earth Sciences Chairman (Postgraduate program coordinator):

___________________________	___________	___________
Name	**Signature**	**Date**

ABSTRACT

In the western flanks of the Central Main Ethiopian Rift (Kella section), the pre-volcanic sedimentary units which are the main focus of this research were investigated. In the present study, a detailed lithostratigraphic section of the area, undertake facies analysis, reconstructing the paleoenvironment, and detailed petrographic characteristics of the pre-volcanic sedimentary units are addressed. Besides; the lithostratigraphic section of the area was correlated with the regional sedimentary work. Detail field investigation and petrographic analysis were used to achieve the objective. Based on field investigation, three sedimentary units were identified. These are sandstone unit, mudstone unit, and carbonate unit. The volcanic unit overlies the sedimentary unit whereas; the basement unit underlies the sandstone unit. 31 rock samples were prepared for thin sections and examined under a petrographic microscope. The petrographic analysis results of 10 sandstone samples show that the sandstone unit is classified into Subarkose, Litharenite, Sublitharenite, and Quartz arenite. Compositionally sandstone unit is mature to supper mature and texturally it ranges from immature to mature. Based on field description and petrographic results, the siliciclastic rocks are classified into 16 lithofacies types and these are classified under 3 lithofacies association groups. The lithofacies associations are Floodplain deposit, meandering river deposit, and Peritidal environment. From the carbonate unit, 20 thin sections were examined under a petrographic microscope. The analysis results reveal that the unit is classified into 12 microfacies types and grouped under 4 microfacies associations. This is sandy mudstone (MF1), carbonate mudstone (MF2), quartz bearings bioclastic packstone (MF3), biosparite Grainstone (MF4), Packstone mudstone (MF5), Oopelbiosparmicrite Packstone (MF6), Daysclad Grainstone (MF7), biomicrite packstone (MF8) bioclastic wackestone (MF9) biomicrite wackestone (MF10**)** and bioclastic mudstone (MF11), and Radiolarian wackestone (MF12). The microfacies association of the carbonate unit is classified into three groups. Thus are; facies association 1 (MF3, MF10, MF11), facies association 2 (MF6, MF7, MF9), and facies association 3 (MF1, MF2, MF4, MF5, MF8). Generally, the carbonate unit described in the Kella section was deposited in the shallow marine environment. The overall facies stacking pattern of the study area led to the conclusion of continental to shallow marine environment.

Key Words: Depositional environment, Kella section, Lithofacies, Microfacies, Petrography

ACKNOWLEDGMENT

First of all, I would like to thank Addis Ababa University for sponsoring me to pursue my MSc. education. I would like to express my deepest appreciation and gratitude to my advisor and instructor Dr. Balemwal Atnafu for his professional and constructive comments and supervision throughout the research work including the field work. His unwavering guidance and encouragement made me strong enough to complete the research work successfully.

I extend my gratitude to my colleagues from the School of Earth Sciences Mr. Faysel S. and Mrs. Wubayehu D. who helped me during my field work. I am also grateful for the driver Ato Hailu.

I have also would like to thank the Geological institute of Ethiopia Central Laboratory for preparing quality thin sections of rock samples and the Addis Ababa University, School of Earth Science petrology laboratory and sedimentology laboratory for allowing me for thin section analysis.

Finally, I would like to express my gratitude for my family who were the source of my strength and inspiration. My Special thank is to my husband, Melkamu Adimaw (MSc.), who helped me in various ways, including the field work and other technical support.

Table of Contents

List of Figures

LIST OF TABLES

ACRONYMS

B	Bed
CMER	Central Main Ethiopian Rift
DEM	Digital Elevation Model
FA	Facies Association
FWWB	Fair weather Wave Base
FZ	Facies Zone
GPS	Global Positioning System
Km	Kilometer
KS	Kella Section
M	Meter
Ma	Million years ago
MF	Micro facies
NE	North East
PPL	Plane Polarized Light
QFL	Quartz-Feldspar-Lithic fragment
SMER	Southern Main Ethiopian Rift
SMF	Standard Microfacies
SWB	Storm Wave Base
UTM	Universal Transverse Mercator
XPL	Cross Polarized Light
YTVL	Yerrer- TuluWellel Volcano-tectonic Lineament

CHAPTER ONE

INTRODUCTION

1.1 Background

The Karroo rift system was created during the Permo-Triassic rifting of Gondwanaland due to NE–SW oriented stress. Ethiopia, Kenya, Tanzania, Mozambique, and South Africa are all parts of the Karroo rift system. There are two stages of Gondwanaland: the rifting stage and the final stage. Gondwanaland's last stages of development are included in the Gondwanaland rifting stage, which spans 300–205 Ma. During that time, long rift structures were formed, joining to form a wide depression and filled by a sequence of carbonate and clastic formations (Salman and Abdula, 1995; Ahmed Wolela, 2014).

The Mesozoic Ethiopia sedimentary history starts; following the advance of the Permo-Triassic rift systems, due to the Gondwana supercontinent breakup and subsequent sedimentation within fault-controlled depositional environments (Bosellini, 1988; Coffin and Rabinowitz, 1988; Fairhead, 1988, 1994; Scotese and Chatterjee, 1999; Gani et al., 2008).

Ethiopia's sedimentary regions occupy a large part of the country and consist of five different sedimentary basins: the Ogaden, Blue Nile, Mekelle, Gambela, and Southern Rift Basins (Ahmed Wolela, 2008). The Mesozoic sediments of Ethiopia mainly occur in: the Abay Basin (Getaneh Assefa, 1991; Russo et al., 1994; Ahmed Wolela, 2007, 2009), Mekelle Basin (Bosellini et al., 1997; Beyth, 1971) and Ogaden Basin (Bosellini et al., 2001).

The past historical evolution of the Earth can be reflected in a close investigation and analysis of sedimentary rocks, which serve as fundamental tools for paleoenvironment reconstructions. However, the pre-volcanic sedimentary unit in the Kella area of the western escarpment of the CMER is not studied independently in terms of petrographic characteristics, facies analysis, and Paleoenvironment. Few researchers have mentioned the presence of the sedimentary unit in the Kella area (Merla, 1979 as cited in Tsegaye Abebe et.al., 2010; Arno et al., 1981; Giday WoldeGabriel, 1990). The pre-volcanic sedimentary unit in the Kella area (Found in the Guraghe zone around Butajira) is therefore not well studied independently. Almost all researches that have been done around the Kella area are focused on the volcanism and structural controls of the

CMER. Therefore, in the present study the detailed sedimentological characteristics and stratigraphic works of the Pre-volcanic sedimentary unit in the Kella section, a western escarpment of CMER are investigated.

1.2. The study area

1.2.1 Location and accessibility

The specific regions of interest for the current study is situated in the east Guraghe zone of the Sodo woreda, which is close to the towns of Butajira around Kella in the Central Ethiopia Regional state. Accessing the Kella area is possible through Addis Ababa- Alem Gena-Butajira major asphalt road, which is located 110 km west of Addis Ababa. The area is geographically fond in western escarpment of the CMER. The study area is bounded by longitudes of 38˚11'0"E and 38˚42'40" E and latitudes of 8˚3'40"N and 8˚35'20" N.

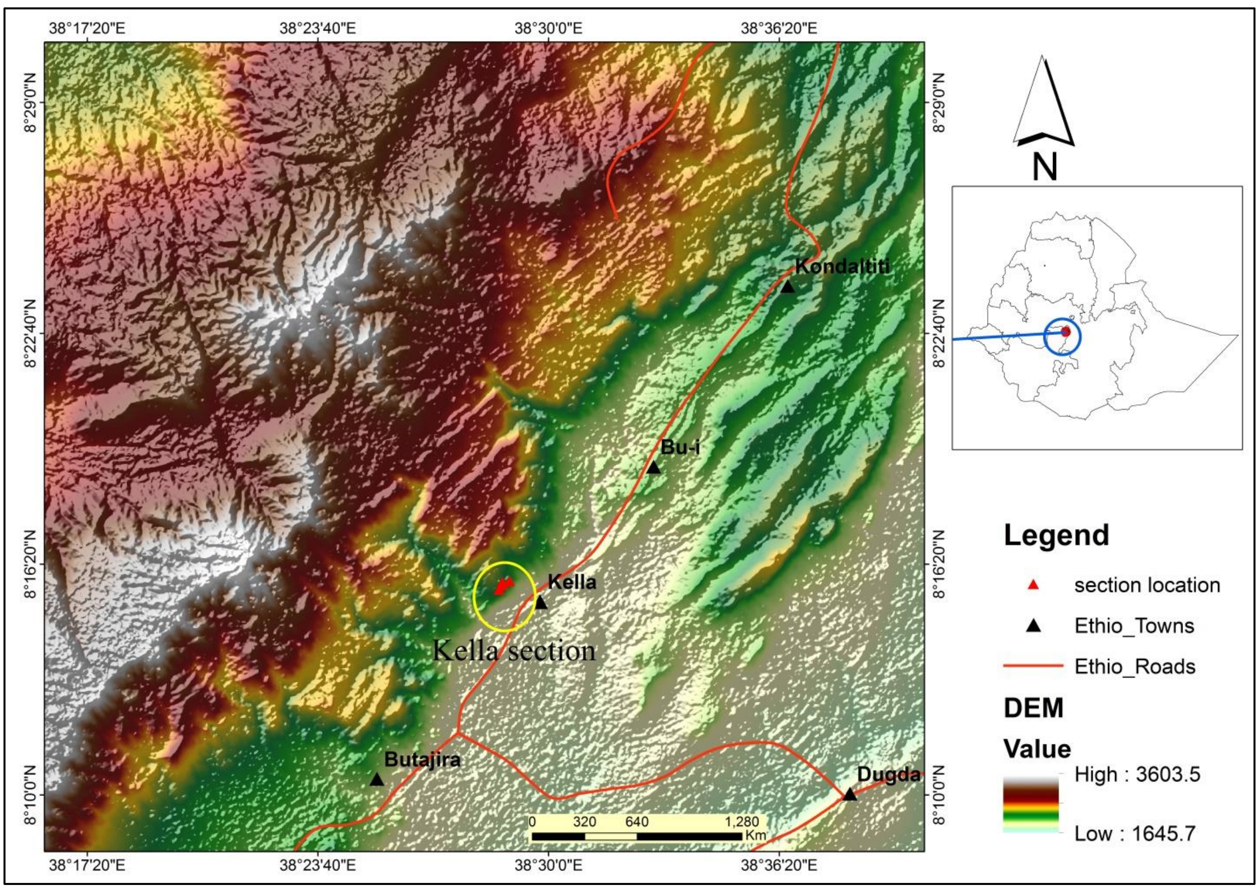

Figure 1. 1. The location map of the study area

1.2.2 Physiography

This area is part of the western margin of CMER and it is characterized by high elevation, transitional escarpment, and rift floor. The surface elevations in the Kella area and the surroundings range between 1700m – 3600 m. above mean sea level.

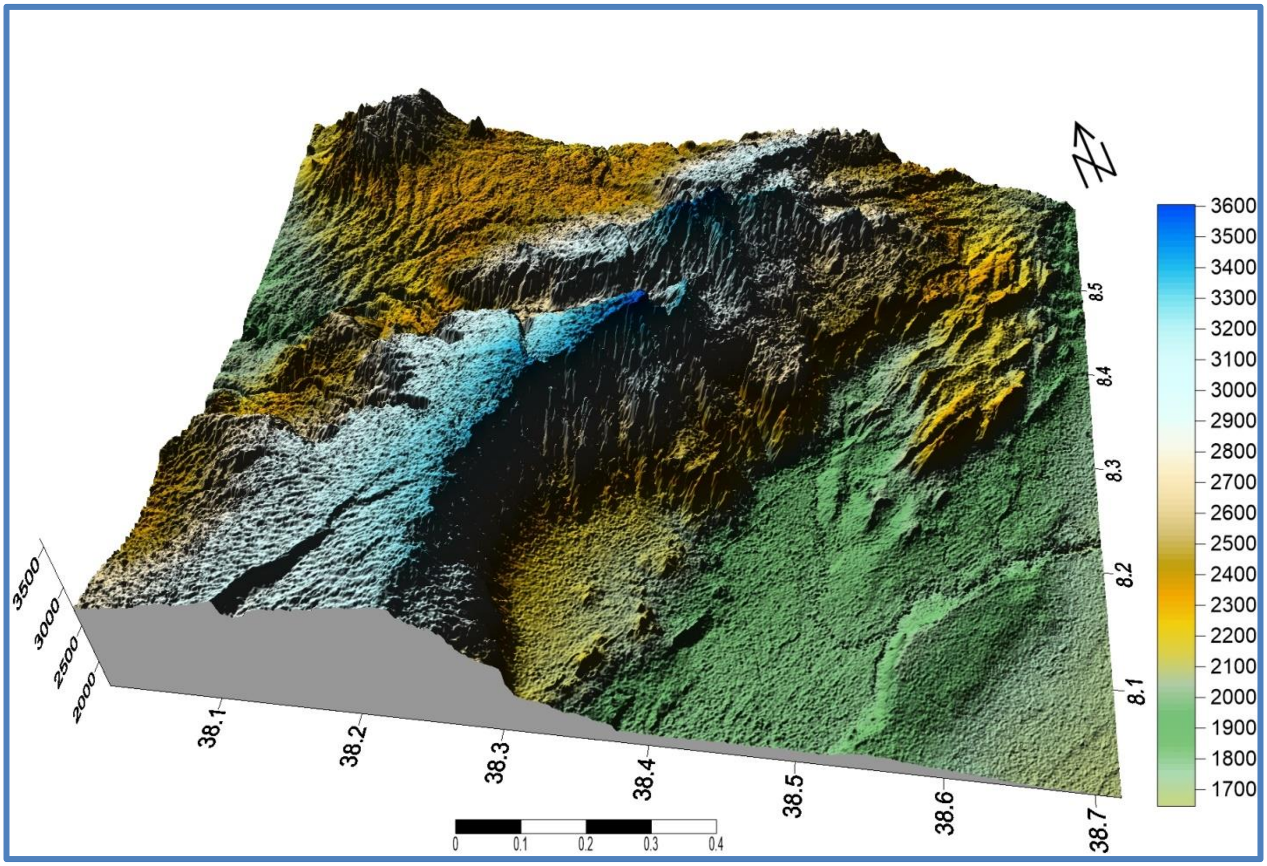

Figure 1. 2. Physiographic map of the Kella area

1.2.3 Population, climate, and vegetation

Sodo is one of the woreda in the central Ethiopia region. It is part of the eastern Gurage zone of Central Ethiopia region. Sodo administrative center is Bui, other towns include Kella. 10.19% of the 2,683,743 people living in this woreda are urban dwellers, according to the Central Statistical Agency's (2007) census, which included 1,341,000 men and 1,342,743 women. Ethiopian Orthodox Christianity is practiced by most of the population, with 93.35% of the population Ethiopian Orthodox Christianity; the reaming is Muslim and others. (https://en.wikipedia.org/wiki/ Sodo-(woreda)).

According to Tamiru Alemayehu (2006) climate classification of Ethiopia, based on altitude and temperature, the climate of the study area and its surroundings ranges from temperate to warm temperate (Woina Dega to Kola) in which the rainy season lasts from March to September. From long-term observations (2010-2024) of temperature and rainfall data, the mean minimum and maximum temperature and rainfall of the Kella area are described in the following figure as it was accessed from https://www.worldweatheronline.com/kela-weather-averages/et.aspx Accessed on Tue 16th Apr 11:42 am.

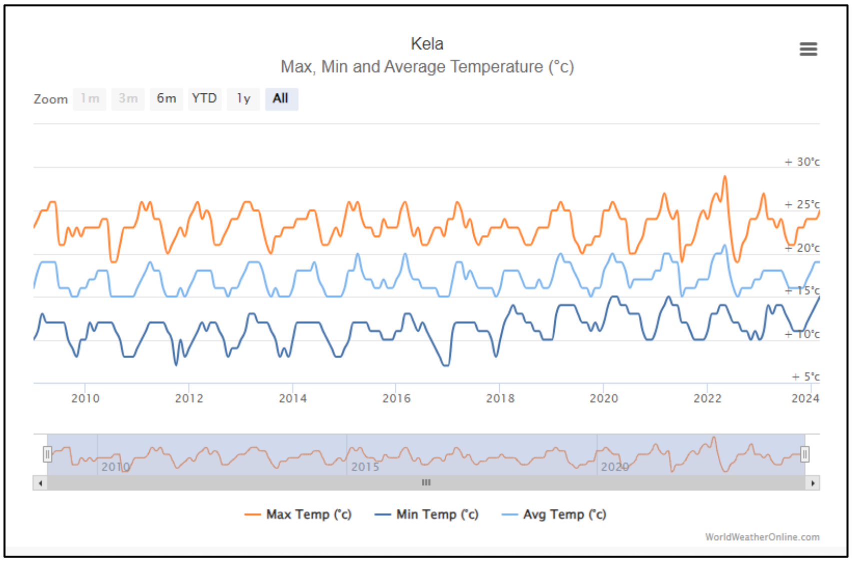

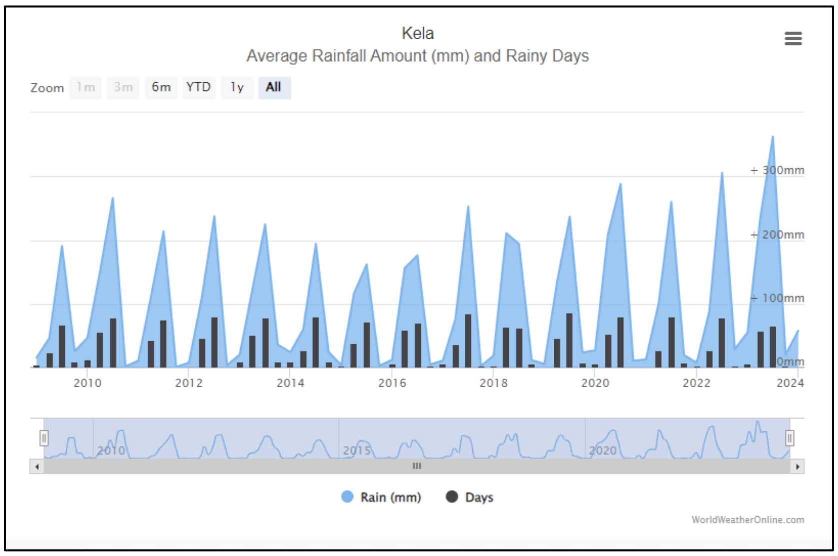

Figure 1. 3 Average rainfall and temperature from 2010-2024 in Kella area https://www.worldweatheronline.com/kela-weather-averages/et.aspx Accessed on Tue 16th Apr 11:42 am

1.3 Literature reviews

1.3.1 Overview of basic terminologies and concepts

1.3.1.1 Stratigraphy

The use of the term 'stratigraphy' dates back to d'Orbingy in 1852, but the concept of layers of rocks, or strata, representing a sequence of events in the past is much older. The superposition principle was created by Steno in 1667. It states that "any layer in a succession of layered rocks is older than the layer next above it." Stratigraphy can be considered as the relationship between rocks and time. Stratigraphy is about establishing a nomenclature for rock units of all ages and correlating them all over the world, but at another level, it is about finding evidence for climate change in the past or the movements of tectonic plates (Nichols, 2009). Previous stratigraphic studies are summarized below.

Krenkel (1926) defined limestone, gypsum, and shale units of the Abay basin. A general stratigraphic description of the region was provided together with a geological map of Ethiopia, Eritrea, and Somalia by Merla et al. (1973). The regional geology of Ethiopia was described by Mohr (1962). Ficcarelli (1968) investigate marine fossils of the Blue Nile basin section. Getaneh Assefa (1979; 1980; 1981; 1991) established lithostratigraphic units of the Abay Basin. The sedimentary development of the Blue Nile basin was described by Russo et al. (1994).

1.3.1.2 Application of facies analysis and petrographic characteristics in sedimentary rock

The term "facies" is often used when describing sedimentary rocks in terms of their depositional settings. A body of rock with particular properties that represent the conditions of its formation is called a rock facies (Nichols 2009 and referenced therein). A sedimentary facies is described by recording all the features of its lithology, texture, sedimentary structures, and fossil content that can be used to infer formation processes. Hence terms such as marine facies, clastic facies, biofacies, and lithofacies can be used (Headberg, 1976; Krumbein and Sloss, 1951). 'Facies association' refers to an approach designed to integrate different facies types with genetic relationships that might indicate a certain depositional system (Dawit Lebenie, 2010).

Climate, tectonic settings, relief, slope, and source rocks are associated with the mineralogy and compositions of clastic rocks (Tao et al., 2014). Therefore, the origin and tectonic setting can be assessed using the detrital mineralogy and composition data. The source rock characteristics can be directly identified by the clastic rocks' petrographic data (Dickinson, 1985; Wanas and Abu El-Hassan, 2006). Additionally, the petrographic data might be complemented by the geochemistry of sedimentary rocks (Armstrong-Altrin et al., 2004).

1.3.2 Overview of previous work

Over time, numerous researchers have examined various characteristics of sedimentary rocks. At Guraghe area in which the present study area is found, various researches has been done. However, the focus of the researchers is on the volcanic and structural setting of the area. Only a few researchers have mentioned the presence of sedimentary units around the Kella area. Therefore, the previous studies are summarized below;

DiPaola et al. (1993) described its origin and significance in crustal attenuation and magmatic processes in the Ethiopian Rift Valley. In their work, they have described the Mesozoic sequences found along the NE-SW trending recent fault scarp. They have described the Mesozoic sequence (150m Adigrat sandstone, 30m of shales and marls, and 20 to 30m Antalo Limestone) unconformably overlays 150m of high-grade metamorphic rocks.

Giday WoldeGabriel et al. (1990) described the geochronology, geology, and rift dynamics of the CMER. In their work, they have described the Mesozoic sequences around the Kella area. The sequence has been described as a 200-m-thick alternation of siliciclastic and carbonate beds (Arno and others, 1981, Giday WoldeGabriel et al., 1990).

The GSE (Geological Survey of Ethiopia) has studied the area at a 1:250,000 scale within the Akaki-Beseka map Sheet/NC 37–14; unpublished report (GSE, 2010). The study covers an extensive area and describes the exposed lithological units of volcanic, sedimentary, and metamorphic origin.

Tsegaye Abebe et al., (2010) explained that CMER is less than 8 Ma: verification by using apatite fission-track thermochronology. In their work, they have described that the Mesozoic sequence outcropping at Kella is only approximately 200 m thick, underlined by the basement unit.

The recent MSc. thesis work in Guraghe around the Kella area is also studied by Aberash Habtie (2023). The focus of the research was to study stratigraphy and petrography of western escarpment volcanic sequence around the Butajira-Kella area, CMER. The researcher included the Mesozoic sedimentary unit within the stratigraphic section, but the main focus was on the volcanic sequence.

1.4. Problem statement

Sedimentary rocks are archives of Earth's history as they record various physical, chemical, and biological processes operating on the surface of the Earth. Therefore, a close investigation and analysis of these rocks and their characteristics reflect the past historical evolution of the Earth and they serve as fundamental tools for paleoenvironment reconstructions. However, the pre-volcanic sedimentary unit in the Kella area of the western escarpment of CMER has not been studied independently in terms of petrographic analysis, facies, and depositional environment. However, few researchers have done only the presence of the sedimentary unit (Arno et al., 1981 cited in Giday WoldeGabriel, 1990; DiPaola et al., 1993; Merla, 1979 cited in Tsegaye Abebe et. al., 2010). The pre-volcanic sedimentary unit in the Kella area is therefore not well studied independently. The thickness of the unit is only described and compared with the Abay by the aforementioned authors. Almost all researches that have been done around the Kella area are focused on the volcanism and structural controls of the CMER. Hence, a more detailed study focused on the pre-volcanic sedimentary unit is required and has to be done to address the scarcity of petrography, facies, and paleo-environmental research which have enormous applications in broad areas of sciences and disciplines thereby in the present study the petrographic, facies analysis and paleoenvironment reconstruction for the pre-volcanic sedimentary unit of the Kella (western escarpment of the CMER) area are studied in detail.

1.5 Objective

1.5.1. General objective

The major objective of the thesis is to describe detailed sedimentological characteristics, stratigraphic works and paleo environment reconstruction of the Pre-volcanic sedimentary unit in the Kella section, a western escarpment of CMER.

1.5.2. Specific objectives

The specific objectives of this research were to;

- Construct a detailed lithostratigraphic section of the area;
- Undertake facies analysis
- Describe detailed petrographic characteristics of the pre-volcanic sedimentary units
- Compare or correlate the lithostratigraphic section of the area with the regional sedimentary work.

1.6. Basic research questions

To address the objectives mentioned above; the following few research questions are assessed:

- How to construct the lithostratigraphic section of the Kella locality?
- What kind of paleoenvironment is expected in the Kella area?
- What is the petrographic characteristic of the sedimentary unit in the Kella area?
- How to correlate the local lithostratigraphic section with the regional sedimentary work?

1.7. Methods

To achieve the above objectives, different tools, approaches, and methods were followed. Before fieldwork, different literature and relevant data were reviewed and collected that helped to understand the area. The overall procedures followed during (pre-fieldwork, during fieldwork, and after fieldwork) to achieve the objective, are described in the following section in detail.

1.7.1. Tools

The tools that are used before, during, and after the geological field work include; Field note book, pens, permanent marker, pencils, burton compass, GPS, Topo map and DEM, digital camera, a geological hammer, handheld lens, measuring tape (meter), dilute hydrochloric acid, sample bags. Software such as ArcGIS, Google earth, sedlog, strater 4, and ProSim ternary diagram were used to prepare stratigraphic log and petrographic data of the analyzed samples.

1.7.2. Literature review

Before the fieldwork is undertaken, a comprehensive review of the relevant preexisting literature were reviewed and written to understand the study area. Some of the major activities done during the revision of previous works include collecting previous technical reports, journals, and textbooks; extracting relevant information from the satellite image and reviewing, compiling literature (published and unpublished reports) related to the study area. To conduct the fieldwork successfully, preparation and collection of field equipment have also been done.

1.7.3. Field work

The most important activities done when conducting fieldwork were to observe lithological units directly following traverses, describing their appearances from hand specimens' description of all the lithological variation in color, textures, sedimentary structures, mineral composition, macrofossils based on size and morphology, trace fossil identification, and degree of bioturbation identification was done. Diluted hydrochloric acid was used to discriminate limestone from the other rock units. Carbonate rocks were classified and named using Dunham (1962) and modified Embry and Klovan (1971) carbonate classification scheme and measuring bed thickness by meter, detailed logging, and collecting fresh representative rock samples and unconsolidated sediments in a plastic bag was collected from Kella area for further petrography analysis. In addition, samples were labeled accurately, and a representative photograph and geographic coordinate point for each location were taken.

1.7.4. Petrographic analysis

After the fieldworks are finished, a laboratory study was done on the samples that were collected. The laboratory examination is undertaken on the samples that were obtained to support the macroscopic analysis of the field data, to determine the compositional and textural components of the pre-volcanic sedimentary units, and to know about the various diagenetic modifications. These are focuses on the petrographic analysis. Thin sections of representative 31 rock samples (10 Clastic samples and 20 carbonate samples and one volcanic sample) were prepared at geological institute of Ethiopia laboratory department. After receiving prepared thin sections, descriptions were done (both in plane polarized light and cross-polarized light) at Addis Ababa

University School of Earth Sciences in the petrology laboratory using Swift and Nikon polarized petrographic microscopes. A detailed petrographic study /thin section descriptions/ including the textural components. In carbonate rocks such as different types of grains, micrite, and cements were identified based on Folk (1959) Dunham (1962) and Embry and Klavan (1971) schemes. For clastic rocks, the proportion of the framework grains (Quartz, Feldspars, and lithic fragment) relative percentage of accessory mineral types, grain orientation, and packing were identified based on Folk (1980) and Pettijohn et al. (1972). These proportions are then plotted on a triangular diagram known as the "Q, F, L" triangle. This triangle is commonly used to analyze the composition and texture of sandstone for classification and naming purposes. Photographs of representative mineral assemblage and textures were taken by using a camera from the microscope.

1.7.5. Interpretation and presentation

Primary data analysis and interpretation were the main tasks for this research work. Presentation and interpretation of data collected during this study (primary data) and those from kinds of literature (secondary) are interpreted and presented in the form of text, figures, and tables. All the collected data were analyzed, discussed, and interpreted and finally, the final thesis report was written.

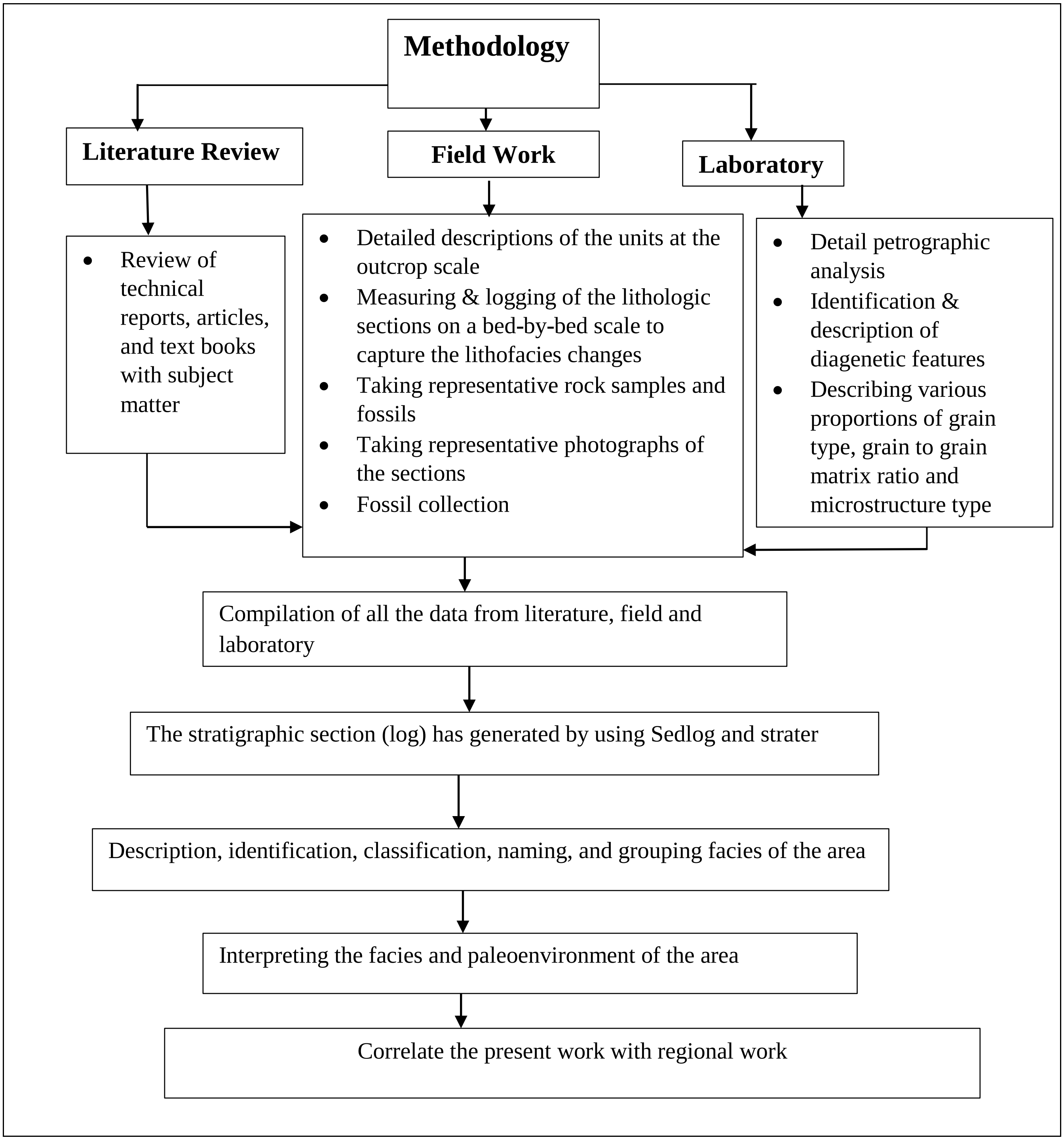

Figure 1. 4 General flow chart of the methodology

1.8. Expected outcomes and significances

1.8.1. Expected outcomes

As stated in the problem statement above, this research is the first to provide detailed research work on the pre-volcanic sedimentary unit of the Kella (western escarpment of the CMER area. Generally, the research has the following outcomes.

- A detailed description of the petrography of the sedimentary unit in the Kella area.
- An interpretation of a pre-volcanic sedimentary unit in the Kella area based on petrographic and facies analyses.
- The paleoenvironment was reconstructed.

1.8.2. Significance of the research work

Sedimentary rocks are a tool for Earth's history as they record various physical, biological chemical and processes and responses operating on the surface of the earth (Boggs, 2009). Therefore, a close investigation and analysis of sedimentary rocks and their characteristics reflect the past historical evolution of the Earth and they serve as fundamental tools for paleo-environmental reconstructions.

- The sedimentological and petrographic investigation of the pre-volcanic sedimentary unit of the Kella area was addressed in detail for the first time in this study, which close the current gap in that research.
- The pre-volcanic sedimentary unit in the Kella area has similar sedimentological characteristics and paleoenvironment to those found in the Abay or Ogaden basins, this indicates a historical link between the two basins and strengthens the previous works.

1.8.3. Thesis structure

This thesis work has seven main chapters. The first chapter introduces general information about the intentions of this study and the study area. The second chapter briefly discusses the regional geological setup of the region while chapter three introduces the geology of the area. Chapter four deals with petrographic characteristics and interpretation whereas chapter five is about facies analysis and chapter six is about the discussion and comparison with the regional work and chapter seven, conclusion and recommendation.

CHAPTER TWO

REGIONAL GEOLOGY

2.1 Introductions

The geological formation of Ethiopia is classified into three major categories namely, the Precambrian basement, Late Paleozoic to Early Tertiary sediments; and the Cenozoic volcanic and associated sedimentary rocks (Mengesha Tefera et al., 1996)

The Ethiopia sedimentary regions occupy a large part of the country and consist of five distinct sedimentary basins: the Ogaden, Blue Nile, Mekele, Gambela, and Southern Rift Basins (Ahmed Wolela, 2008).

Ethiopia's Mesozoic sedimentary history started when the Permo-Triassic rift systems formed as a consequence of the breakup of the supercontinent Gondwana and the sedimentation that followed in fault-controlled depositional conditions (Bosellini, 1988; Coffin and Rabinowitz, 1988; Fairhead, 1988, 1994; Gani et al., 2008; Scotese and Chatterjee, 1999).

The Karroo rift system was created during the Permo-Triassic rifting of Gondwanaland due to NE–SW-orientated stress. Ethiopia, Kenya, Tanzania, Mozambique, and South Africa are all traversed by the Karroo rift system (fig. 2.1). There are two stages of Gondwanaland: the rifting phase and the final stage. Gondwanaland's last stages of development are included in the Gondwanaland rifting stage, which spans 300–205 Ma. During that time, long rift structures developed, joining to form abroad plat form depression and filled by thick sequence of clastic and carbonate formations (Salman and Abdula, 1995; Ahmed Wolela, 2014).

The last stage of Gondwanaland, the period 205–157 Ma marked the end of Gondwanaland, and the starting of the breakdown of Gondwanaland into separate blocks. Parallel to this, the palaeo-Tethys Sea transgression resulted in the advance of a narrow marine embayment with barrier reefs separating some saline lagoons (e.g. Ogaden Basin, Abbay Basin, Mandwa, etc. (Hunegnaw et al., 1998; Russo et al., 1994; Salman and Abdula, 1995; Ahmed Wolela, 1997, 2008a; Tadesse Ketsela, 2007). As the last period progressed, Volcanic activity gradually decreased in the Gondwanaland region known as Afro-Antarctica, while between Madagascar and Africa, a deep depression formed, along which the palaeoTethys transgression advanced further, forming a marine seaway separating the African and Indio-Madagascar blocks (Salman and Abdula, 1995; Ahmed Wolela, 2014).

The Precambrian Orogenic belt, Karroo rifting, and Cretaceous and Tertiary rift tectonics are used to explain the distribution and rock associations. Following pre-existing lines of weakness in the basement, the Karroo rifts opened under oblique shear (Morley et al., 1999). N-S, NW-SE, and NE-SW oriented rift basins including the Ogaden and Abay Basins in Ethiopia, were formed as a consequence of the Karroo rift (Raaben et al., 1979; Tamirat Wrku and Astin, 1992; Ahmed Wolela, 1997, 2008a; Hunegnaw et al., 1998; Tadeesse Ketsela, 2007).

Mesozoic sediments have been extensively deposited in Ethiopia due to a continuous period of land subsidence in the Ogaden and sea migration from the east to the west and north, encompassing the country's central and northern regions. These Mesozoic sediments are now mostly exposed in the eastern Ogaden, Central in the Abay basin, and in the northern Tigray Mekelle basin (Aberra Mogessie et al., 2002; Bosellini et al., 2001; Russo et al., 1994; Ahmed Wolela, 2007, 2009,).

During the Mesozoic era, three major transgression and regression cycles occurred. Most of the Mesozoic sediments in Ethiopia were formed during the first cycle (Kazmin, 1972, as cited in Mengesha Teferea et al., 1996; Aberra Mogesse et al., 2002). The second and third cycles are recorded only in the Ogaden Basin by Mustahil and Ferfer Formations and the Jessoma Formation and Taleh Evaporites, respectively (Abbate et al., 2015).

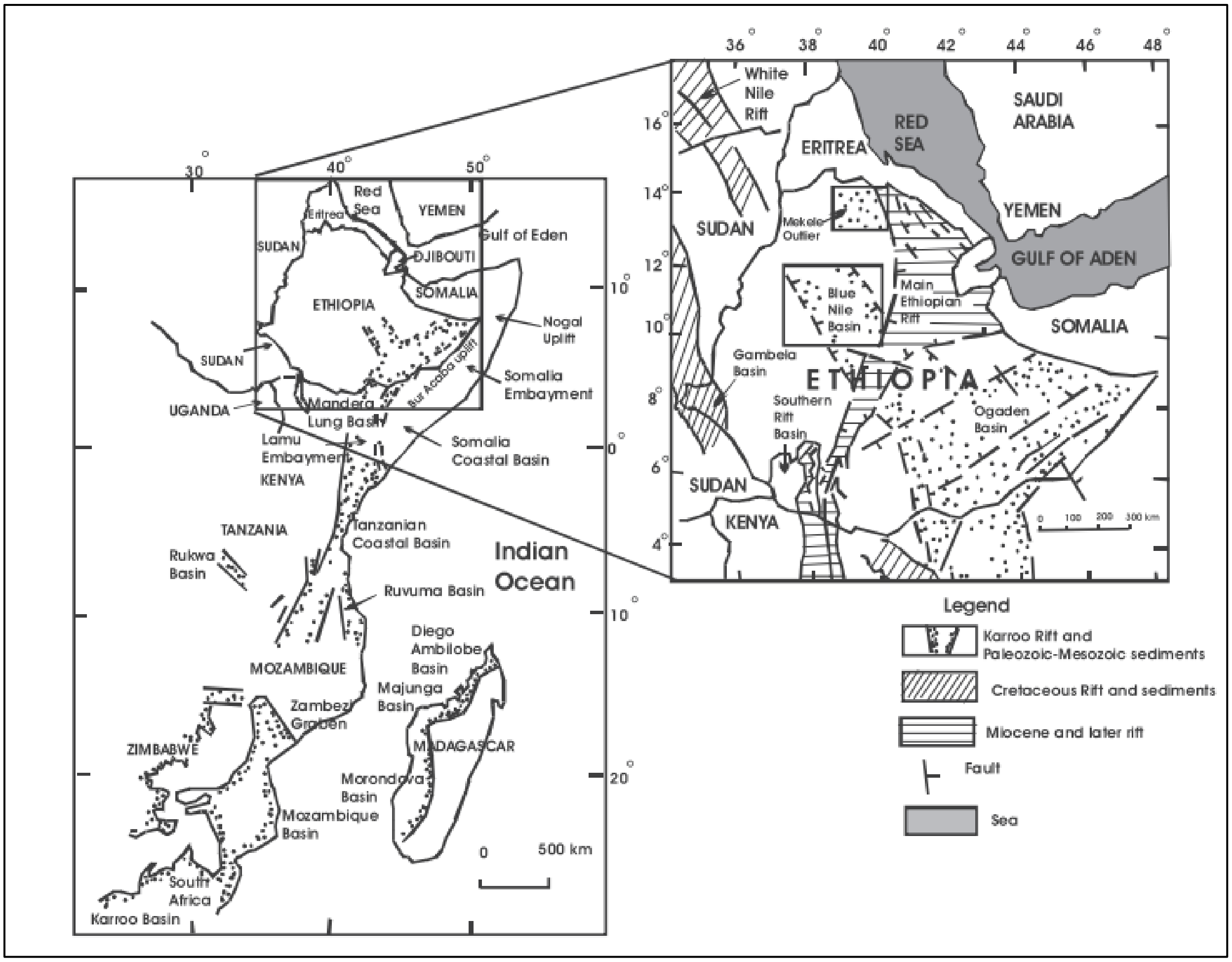

Figure 2. 1 The Karroo rifts and associated sediments in eastern and southern Africa, and the Karroo, Cretaceous, and Tertiary rifts in Ethiopia (Ahmed Wolela, 2008 and cited therein).

2.2. Regional stratigraphy

General stratigraphy of Ethiopian geology starts with a basement rock at the base covered by a Paleozoic Mesozoic sedimentary rock unit capped by a Tertiary trap series. Blue Nile basin (Abay basin) in Central Ethiopia is one of the areas where almost complete stratigraphic records of Ethiopian geological formation are found. Crystalline basement rocks (32%), Paleozoic-Mesozoic sediments (11%) and Cenozoic volcanic rocks (52%) (Ahmed Wolela, 2008; Gebrehiwot et al., 2010 and referenced therein). The main exposed lithostratigraphic units in the basin are briefly described stratigraphically below.

2.2.1. Precambrian basement rocks

The basement rocks of Ethiopia are considered to be part of the Late Proterozoic terrain of the 'Horn' of Africa where two major belts of NE Africa (the Red Sea Fold Belt) and East Africa (the Mozambique Belt) join. The Red Sea Fold Belt, also called the Arabian Nubian Shield is characterized by low-grade (greenschist facies) island arc assemblages, east-dipping sutures, and north/NW trending shear zones, while the Mozambique belt is composed of higher grade (dominantly amphibolite facies) metasediments and granitic gneisses as continental collision units (Kazmin et al., 1978)

Precambrian rocks of Ethiopia are exposed in the peripheral parts of Ethiopia; in the north, west, southwest, south, and east (Asfawossen Asrat et al., 2001). The Precambrian basement exposures are found in areas not intensively affected by Cenozoic volcanism and rifting and where the Phanerozoic cover rocks have been eroded (Mengesha Tefera et al., 1996). In Ethiopia, the Precambrian rocks comprise both the ANS in the north and the gneissic rocks of the MB (Mozambique belt) in the south (Teklewold Ayalew, 1997). In the Abay basin, the high-grade metamorphic rock assemblages are known as the Alghe group and the low-grade rocks are named as Tulu Dimtu Group (Asfaowssen Asrat et al., 2001). The Alghe group is composed of biotite and hornblende gneiss, migmatite with minor metasedimentary gneiss whereas the Tulu Dimtu Group is represented by undifferentiated metasediments and metavolcanics along with minor marble, quartzite, and ultramafics. The metamorphic rocks are unconformably overlain by either Paleozoic-Mesozoic sediments or Tertiary volcanic, except in the western part of a basin where the basement rocks are extensively exposed on the surface (Dawit Lebenie, 2010).

2.2.2. Paleozoic-Mesozoic sedimentary rocks

According to Getaneh Assefa (1979, 1991 as cited in Russo et al., 1994), the Paleozoic Mesozoic sedimentary succession that is found in the Abay basin is informally classified into five major lithostratigraphic units. These are the Lower Sandstone (Adigrat Sandstone), Gohatsion Formation, Antalo Limestone, Mugher Mudstone, and Debrelibanos Sandstone (Upper Sandstone) units. Furthermore, this classification has been modified by recent work including those of Gani et al (2008), Ahmed Wolela (2008), and Dawit Lebenie (2010). The Gohatsion Formation and Antalo Limestone units have been revised as Glauconitic Sandy mudstone (lower part of Gohatsion Formation), lower limestone (upper part of Gohatsion Formation and Lower part of Antalo limestone), and upper limestone (the remaining portion of Antalo limestone) (Gani et al., 2008). Whereas Ahmed Wolela (2008) included the 'Pre Adigrat' unit along with unnamed 'transitional units' with 50m thickness between the upper Sandstone and Antalo Limestone in addition to the lower Sandstone and Gohatsion Formation. And more recently Dawit Lebenie (2010) established eight informal stratigraphic units by adding pre-Adigrat I, pre-Adigrat II, and pre-Adigrat III onto Getaneh Assefa's (1979, 1991 as cited in Russo et al., 1994) classification. A description of each unit is given below.

Karoo sediment: The Karoo sediments were deposited in a series of rifts that marked the intention of the break-up of the eastern Gondwanaland under the influence of tectonism and climate (Tamirat Worku and Astin, 1992). The Karoo sediment is the oldest continental (floodplain, crevasse play, aeolian and alluvial floodplain) environment deposited sediment (Tamirat Worku and Astin, 1992; Ahmed Wolela2008 and Dawit Lebenie 2014). It overlays on the basement unit and consists of conglomerate, sandstone, silt stones and shales. The equivalent of the Karoo sediment described the Pre-Adigrat I, II and III unit in the Central Ethiopia, the Enticho Sandstone and Edaga Arbi glacial in the northern Ethiopia (Mekele Basin) and the Calub, Bokh and Gumburo formation in the Ogaden basin. The thickness of the this sediment reached 250-650m eroded part in the Central Ethiopia and 800-1200m in Ogaden Basin.(Ahmed Wolela 2012). The age of Karoo Sediments is allocated by many authors with various pieces of evidence and debated geologic time. Mohr (1963) as cited by Dawit Lebenie (2014) reported a Permo– Triassic age based on lithologic similarities with the South African Karoo while, Kazmin (1975) suggested sand, silt and shale filled sediment below the Adigrat sandstone in the Blue Nile Basin is possibly deposited in Carboniferous–lower Mesozoic interval. Geleta & Wille (1998) emphasize the existence of Middle Triassic age continental sediments.

Adigrat Sandstone: The Adigrat formation was named for the first the lower sandstone of the Adigrat town (Blanfored, 1869). This Formation is widely distributed in Abay Basin, Ogaden Basin, and Mekelle Outlier (Ahmed Wolela, 2008). It covers a wide area in Abay Basin and forms cliff exposures. The unit thickness ranges from 100-700 m, in the Abay Basin it is about 300 m. It is unconformably underlain by either the basement or the Pre-Adigrat units and conformably overlain by Gohatsion Formation. However, Dawit Lebenie (2010) redefine the presence of conformable contact between Adigrat sandstone and Gohatsion Formation due to the presence of widespread pedogenesis and lateritisation in Mekelle Basin and proposed that the abrupt change in facies form coarse sandy upper shoreface facies to evaporite dominated Gohatsion formation in the Abay Basin. It consists of dominant sandstone beds intercalated with siltstones, mudstones, conglomerates, and rare wood fragments and is interpreted as having continental origin (Aberra Mogessie et al., 2002; Russo et al., 1994; Ahmed Wolela, 2008,). However in recent work, Dawit Lebenie (2010; 2016) within this unit, three stratigraphic units bounded by unconformity were defined. According to these works, the lower of this formation, informally named as Unit I, represents a tide-dominated estuarine and storm-dominated shoreface deposit whereas the second unit informally named Unit II represents a barrier/inlet spit origin. Unit III, which is only found in the Mekelle Basin, represents a transgressive barrier lagoon system. Based on Palynological evidence the age of Adigrat sandstone unit is Permian–Triassic (Jepsen and Athearn 1961, 1964; Mohr 1962; as cited in Russo et al. 1994).

Gohatsion Formation: It was first named by Getaneh Assefa (1981) after its type section in the town Gohatsion in Central Ethiopia. The thickness of this Formation is up to 450 m. It is conformably overlain by Antalo Limestone Formation and underlain by Adigrat Sandstone. According to Getaneh Assefa (1981) and Russo et al. (1994), it is composed of cyclical successions of facies that are composed of lower to upper, alternating dolostones, marlstones, and shales, bioturbated mudstones with thin siltstone intercalations, fine-grained coquinoid cross-laminated sandstones, and the thick gypsum beds. The presence of scattered small bivalves and gastropods (Corbiculinae, Lucinids, Arcomytilus, Protocerithium) suggests a peritidal environment with associated lagoonal and pond water bodies (Russo et al. 1994). Getaneh Assefa (1981) identified four informal groups of the Gohatsion Formation based on lithostratigraphy. However more recent work by Samuel Getachew (2018), the formation is divided into three informal members named the Lower Mudstone Member, Gypsum Member, and Upper Mudrock Member. Russo et al. (1994) suggested that the Gohatsion Formation corresponds to the early marine transgression, which is largely associated with the rifting and subsiding of the future African continental margin.

Antalo Limestone: The term Antalo Limestone was originally assigned by Blanford (1870) to the limestone unit in the northern Ethiopia. This carbonate succession in the Central Ethiopia is

420 m thick and conformably overlies the Gohatsion Formation as described by Russo et al. (1994). Based on fossil assemblages this unit can be divided into three parts that represent different stages of sea transgression. At the base 180 m and composed of burrowed mudstones that grade upwards into oolitic and coquinoid limestones without or with intercalated marl beds, and then into massive limestones with scattered patches of corals, nerineids, and stromatoporoids, for which a shallow water environment was inferred. In the middle part, a 200 m thick succession consists of fossiliferous interbedding of marly limestone and marls. This group represents a shelf to an open marine environment. The top part which is 50 m thick comprises laminated oolitic and reefal limestones, which suggested that shallow water conditions would be returning. This unit was formed by major transgression due to African continental margin formation and the eustatic increase in sea level (Russo et al., 1994).

Mugher Mudstone: The name “Mugher Mudstone” was adapted after a type section was created by Getaneh Assefa (1991) along the bank of the Mugher River in the eastern part of the Blue Nile canyon. The sequence is 15 m thick in the Gohatsion area and 320 m thick in the Jema valley. It conformably overlies the Antalo Limestone (Getaneh Assefa, 1991, Russo et al., 1994). It conformably overlays Antalo Limestone Formation and is overlain by the Debre Libanos Sandstone. According to Russo et al. (1994) and Getaneh Assefa (1991), this succession can be subcategorized into two based on lithofacies. The lower part (15m) is composed of alternating beds of nodular and vein-filling gypsum, dolomites, and shales, interpreted as supratidal and lagoonal environments. The upper part (240m) consists of interbedded sand, silt, and mudstone with localized occurrences of lignite and scattered plant fragments interpreted as meandering river system deposits. In terms of fossil record, this formation is the most productive unit in the entire basin with several species of both invertebrate and vertebrate fossils along with different plant species (Russo et al., 1994; Dawit Lebenie, 2010). In some works, this unit is inferred as “Ambaradem Sandstone Formation” in connection with the sandstone formation that it overlays, with the aim of correlating it with a formation found in northern Ethiopia (Ahmed Wolela, 2008).

Debre Libanos Sandstone: Also known as Upper Sandstone, ranges in thickness from a few m to 280 m and represents sandy braided river deposits on a broad alluvial plain (Russo et al., 1994). The bottom boundary is marked by a change from alternating beds of mudstone and fine-grained sandstone that form gentle slopes (Mugher Mudstone) to a generally massive, cliff-forming coarse-grained sandstone. The top boundary is unconformable as it is overlain by the Tertiary flood basalts. The succession is characterized by cross-bedded pebbly sandstones and fine conglomerates with rare occurrences of mudstones (Dawit Lebenie, 2010).

2.2.3 Tertiary volcanics

The eruption of the Ethiopia-Yemen flood-basalt province (Trap series) at the Red Sea-Gulf of Aden-East African rift triple junction initiated volcanic activity in Ethiopia during the Eocene–Late Oligocene (Corti, 2009). The Tertiary trap sequence of Ethiopia was extruded within a short period (1 million years) around ~30 Ma ago (Hofmann et al., 1997, Kiffer et al., 2004). This volcanic activity is a result of the rift that opened along the Red Sea and Gulf of Aden separated the Arabian and African continents (Hofmann et al., 1997; Pik et al., 1998; Kiffer et al., 2004; Abbate et al., 2015). The Oligocene volcanics originally covered over 600,000 km^2 area. They are overlain by several Oligo-Miocene shield volcanos, the most notable ones being the Simien Shield, Choke Shield, and Guguftu Shield (Keiffer et al., 2004, Dawit Lebenie, 2010). Geochemical analysis of these series indicates either theolitic (high or low Ti basalts) or alkaline magma sources (Hofmann et al., 1997; Pik et al., 1998; Keiffer et al., 2004). Their distribution throughout the plateau indicates spatial control rather than temporal evolution (Pik et al., 1998), where the low Ti basalts are exposed around the northern part of the plateau while high Ti basalts are dominantly exposed in the eastern and southern parts.

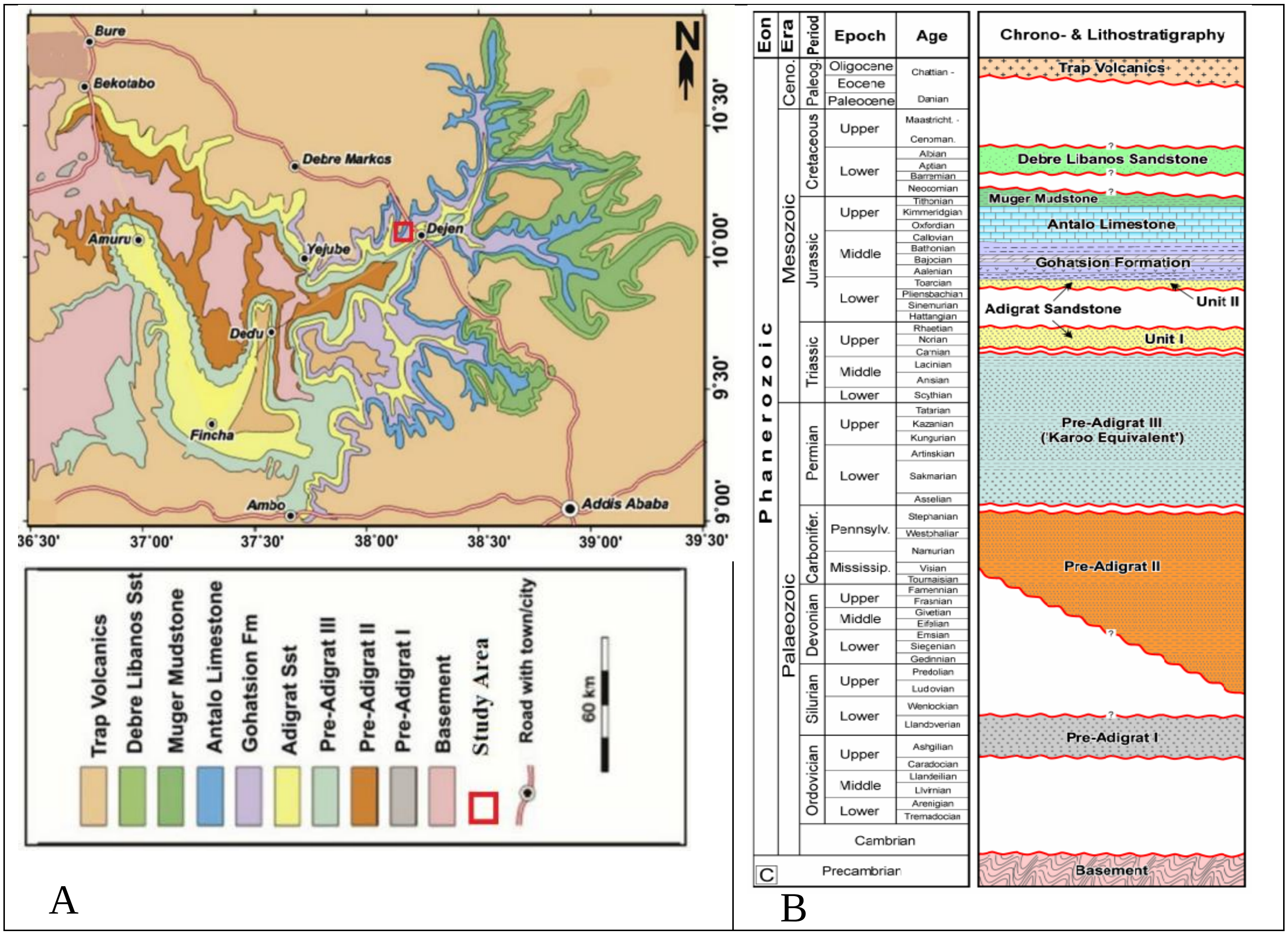

Figure 2. 2 A. Generalized geological map of the Abay Basin canyon. B. Chronolithostratigraphy of the Abay Basin (Dawit Lebenie, 2010)

2.3 Rifting and volcanism

Determining how volcanism may be influenced by regional tectonics is essential to understanding how rift zones have evolved and this requires the explanation of overall rift structure and associated volcanic features (Bekele Abebe et al, 2007). The general scale variation in volcanism type with extension amount, which reflects the involvement and differentiation of different volumes of magma, is an interesting characteristic of the evolution of the continental rift (Bekele Abebe et al, 2007 and referred therein). EARS provide the chance to study the compositional difference of erupted magma with the magnitude of extension, which is the age of the rift. The general trend for the EARS is N-S, but there are other trends like NW-SE due to the line of basement weakness (Klerkx et al., 1998).

2.3.1 Main Ethiopian Rift (MER)

The Main Ethiopian Rift is a key sector of the East African Rift system that connects the Afar depression, at the Red Sea–Gulf of Aden junction, with the Turkana depression and Kenya Rift to the south (Chorowicz, 2005 and Corti 2009). The Ethiopian Rift was formed by an active expansion between the plates for Somalia and Nubia, which extends approximately 1000km south of the afar junction intersection to the Kenyan Rift (Boccaletti et al., 1999; Bonini et al., 2005; Corti, 2009). The enormously long rift trends are almost in an N-S direction. The MER is about 80km wide around its center, with a general trend of N-S to NNE/SSW. According to (Corti, 2009) MER is split into (SMER), (CMER), and (NMER) depending on the direction and timing of the faults (Bonini et al., 2005; Corti et al., 2013; Corti, 2009 ;) (Fig.2.3). The boundary faults of the NMER, which have formed during 10–11 Ma, trend on average at N50°E and stretch south from the Afar valley to the area around Lake Koka Around 10–11 Ma, first volcanism also started (Wolfenden et al., 2004). With border faults that typically trend between N30°E and N35°E, the CMER stretches from Lake Koka through the lakes region to Lake Awasa. The age at which extension begins in the CMER is still debated. Giday WoldeGabriel et al. (1990) suggest that 8.3–9.7 Ma is when faulting first began, with the earliest syn-rift volcanics occurring at about 8 Ma. Whereas Bonini et al. (2005), suggest 5-7 Ma for the beginning of extension and volcanism. The SMER extends south from Lake Awasa into the broadly rifted zone of southern Ethiopia (Ebinger et al., 2000) with faults trending north-south to N20°E. Faulting in the Southern MER was well established by ∼18 Ma (Ebinger et al., 1993; Giday WoldeGabriel et al., 1991), and volcanism started around 18– 21 Ma (Ebinger et al., 1993; George and Rogers, 2002).

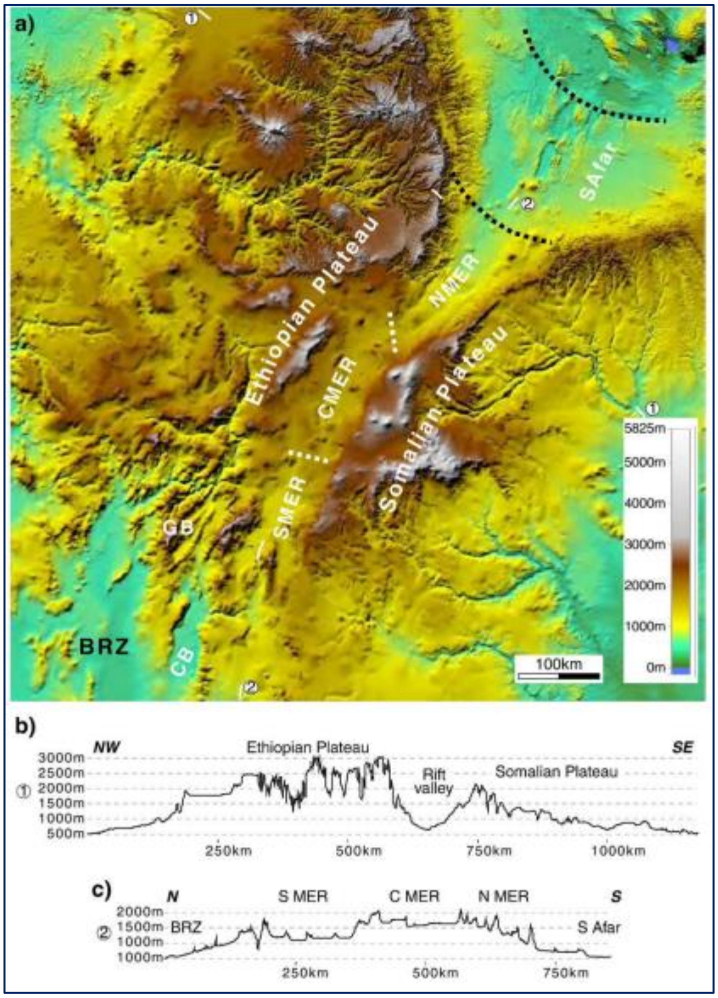

Figure 2. 3 a) An Ethiopian Rift digital elevation model displaying the main rift segment: southern Afar (Safar), (NMER), (CMER), and (SMER). BRZ: Broadly Rifted Zone; CB: Chow Bahir Rift; GB: Gofa Basin and Range. b) Topographic profile across the Rift Valley. c) The rift valley's topographic profile (Corti, 2009).

2.3.2 Volcanism in Main Ethiopian Rift

According to Gidey WoldeGabriel et al., (1990), magmatic activity in MER appears to be been episodic rather than continuous and showed different characters in the different rift segments, which is mainly what occurred broadly in two geologic periods: the Late Tertiary and the Quaternary. Magmatic activity in Ethiopia generally started following the eruption of Oligocene (30–35 Ma) voluminous flood basalts (Mohr and Zanettin, 1988; Ebinger et al., 1993; Gezahgn Yirgu et al., 2006), followed by a complex shield volcano activity. However, within the Southern

MER, the Tertiary volcanic activity started earlier than other MER sectors at 45 Ma. Close to the rift margin, the two escarpments are distinguished by Miocene-Pliocene volcanic activity. The majority of volcanic activity on the western edge is confined to YTVL, which creates aligned core silicic volcanoes (Tsegaye Abebe et al., 1998). These volcanoes become younger towards the rift, from the 7 Ma Nekemt edifices to the Pliocene-Quaternary volcanoes (Wenchi, Wechacha, Furi, and Yerer) (Tsegaye Abebe et al. 1998). Huge volcanic eruptions throughout the Quaternary stages of the MER opening were noticeable. The eruption is distinguished by a high proportion of silicic rocks, a small amount of basalt, and a lack or absence of intermediate compositions this suggested by (Peccerillo et al., 2007).

2.3.3 Volcanism in the CMER

According to Tsegaye Abebe et al. (2010), the CMER is surrounded by the Yerer-Tullu-Wellel volcanotectonic lineament to the north and Goba–Bonga lineament to the south. It is also surrounded to the east and west by fault escarpments (some of them with an offset of more than 1500 m) such as the Munesa and Guraghe rift margins. Tertiary to Quaternary volcanic rock is exposed in the MER, apart from minor fluvio-lacustrine sediments, mostly of Quaternary age, that were deposited on the rift floor. One exception is an outcrop of Mesozoic sediments covering Precambrian crystalline rocks at the foot of Guraghe escarpment, close to the village of Kella (Tsegaye Abebe et al. 2010). Apart from Kella, basement rocks in the MER are exposed only in its extreme south and northern Afar. Low-temperature thermochronological data related to rift-induced exhumation are available only from the SMER (Pik et al., 2008). the stratigraphy of CMER according to Tsegaye Abebe et al. (2010), from youngest to oldest are Quaternary central volcanics (Quaternary, ~< 1.6 Ma), rift-shoulder trachytic–rhyolitic volcanics and pyroclastic layers (Miocene–Pliocene), rift floor volcanics (Pliocene,4.2-3 Ma), Gurage basalts (plateau volcanics) lower Miocene (12–8 Ma), Shebele trachyte (Mid-Miocene, 17-12 Ma), Kella basalts (Oligocene,31-29 Ma), Pre-Tertiary units (Mesozoic and Precambrian). According to Gidey WoldeGabriel et al. (1990), the western escarpment is made up of huge basalts, tuffs, and rhyolites that are covered lava flows made of basalt interbedded ignimbrite layers. According to Di Paola (1972), the composite escarpment exposures nearly all of the lacustrine deposits on the rift base as well as volcano-clastic and fluvial sediments, while exposing a small portion of the crystalline basement with its cover of Mesozoic sedimentary strata and a 1.5 km thick section of basalt-dominated volcanic rocks.

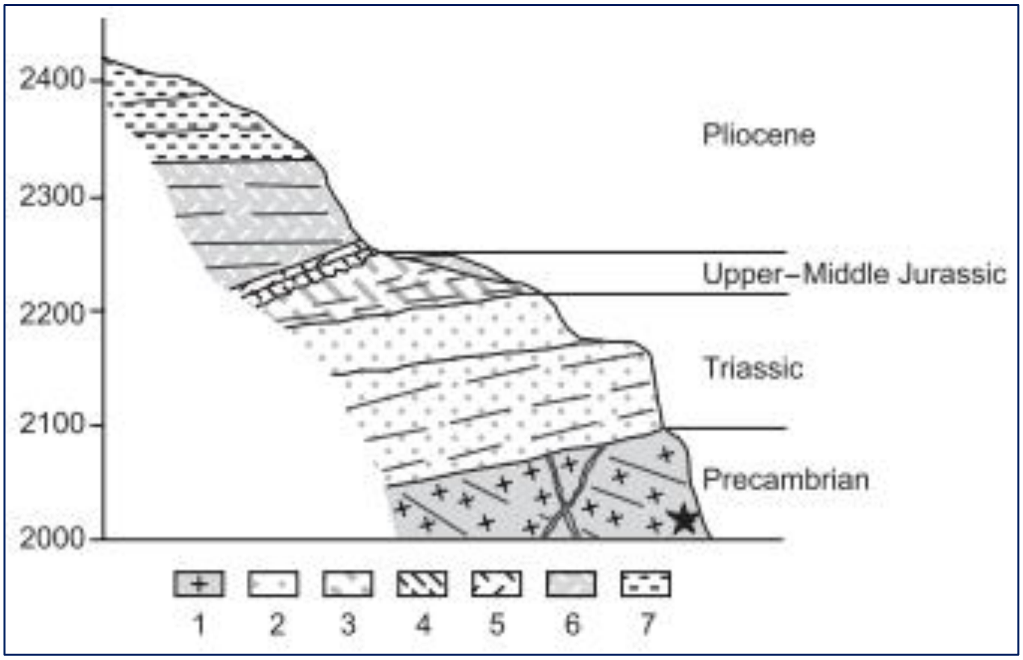

Figure 2. 4 a) An Ethiopian Rift digital elevation model displaying the main rift segment: (1) Precambrian biotite gneiss, (2) Adigrat sandstones, (3) claystones, shales, and minor limestones, (4) palaeo-fluvial deposits, (5) stratified ash layer, (6)compacted crystal-rich pyroclastics, (7) rhyolitic lava flows. Altitude in metres above sea level: location of Kella Precambrian basement rock samples (Tsegaye Abebe et al., 2010).

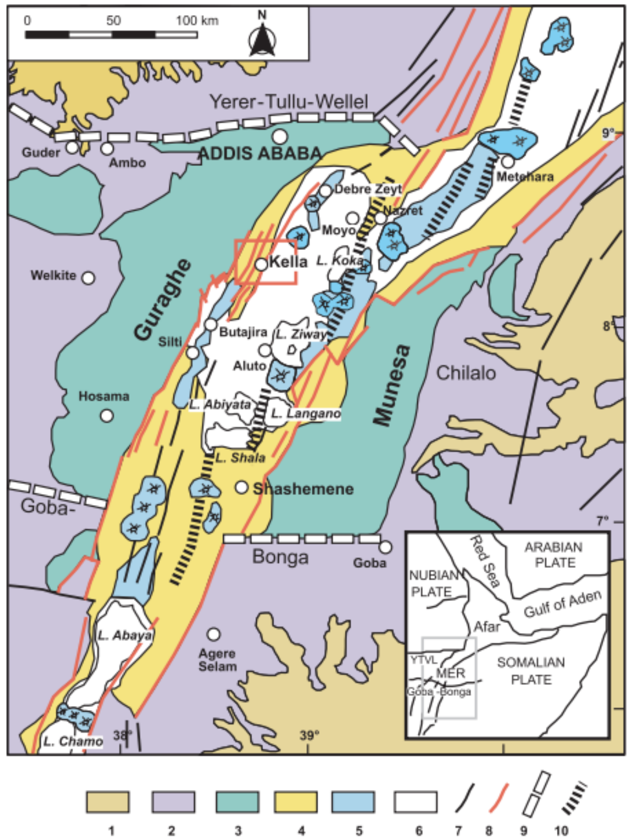

Figure 2. 5 The geological map of Central Ethiopia, modified after Jepsen and Athearn (1997) as cited in Tsegaye Abebe et al. (2010)

(1) Pre-Tertiary sediments and crystalline basement, (2) Oligocene (32–29 Ma) and lower Miocene (12–8 Ma) plateau volcanics, (3) Miocene–Pliocene rift-shoulder trachytic–rhyolitic volcanics and pyroclastic layers, (4) Plio-Pleistocene rift floor, (5) Quaternary central volcanics and basaltic lava flows, associated scoria cones and phreatomagmatic deposits, (6) Quaternary lacustrine sediments and interbedded pyroclastics, (7) faults, (8) major rift border faults, (9) major transversal tectonic lineaments in the basement, (10) Wonji Fault Belt segments. Red square: area shown in Fig. 2. In the inset: YTVL, Yerer-Tullu-Wellel volcanotectonic lineament, MER.

CHAPTER THREE

GEOLOGY OF THE KELLA AREA

3.1. Introduction

The pre-volcanic sedimentary unit is exposed along the road between Kella town and Keshite, at the foot of the CMER's western margins. The Kella area has a diverse lithology, including sandstone, mudstone, shall, marl, limestone, and volcanic rock (Fig. 3.1). Volcanism and tectonic structures have a general impact on the region. Because of this, the sedimentary unit observed there is not continuous and horizontal. As evidenced by field observations, the sedimentary units exposed in the Kella area are tilted (25^{o} degrees). To achieve the objectives outlined in section 1.5, a thorough field investigation was conducted. During the field investigation, exposures of sedimentary and volcanic units were described, and representative samples were collected for petrographic analysis. Based on field observations, four sections in this locality were chosen for detailed description (sections A, B, C, and D), which are described in the next section.

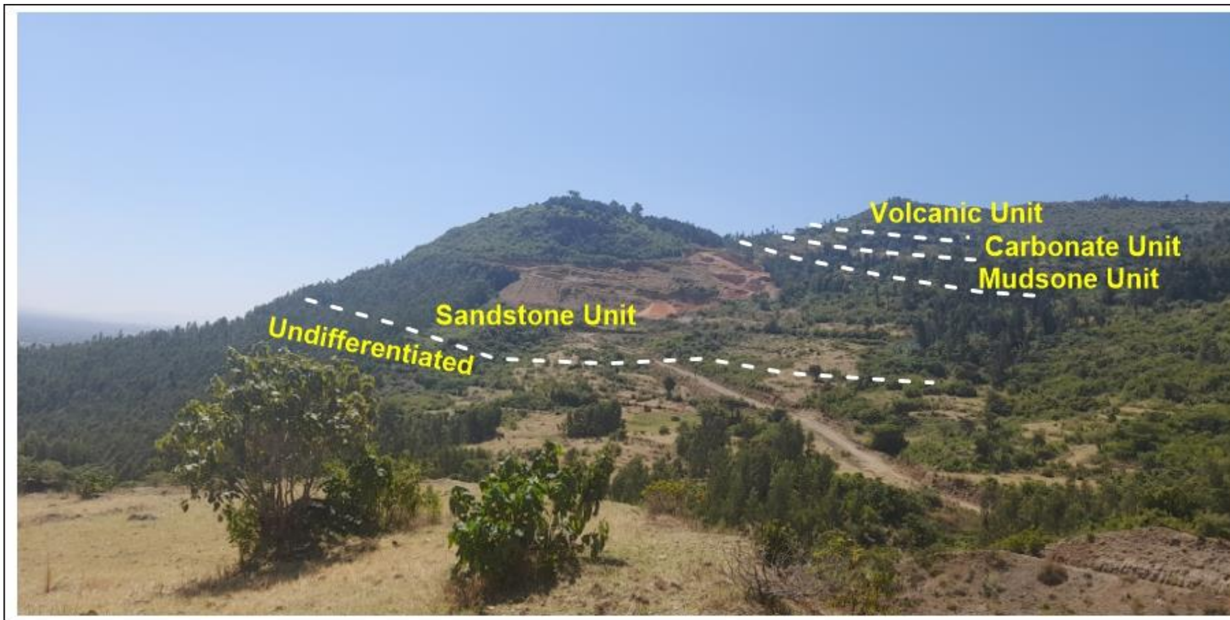

Figure 3. 1 The exposed lithological unit in the Kella area.
The upper part consists of volcanic unite, while the carbonate unit is found below them. Between the carbonate unit and the sandstone quarry site, there is a mudstone unit. Below the sandstone unit, the area is covered with vegetation, making identification difficult.

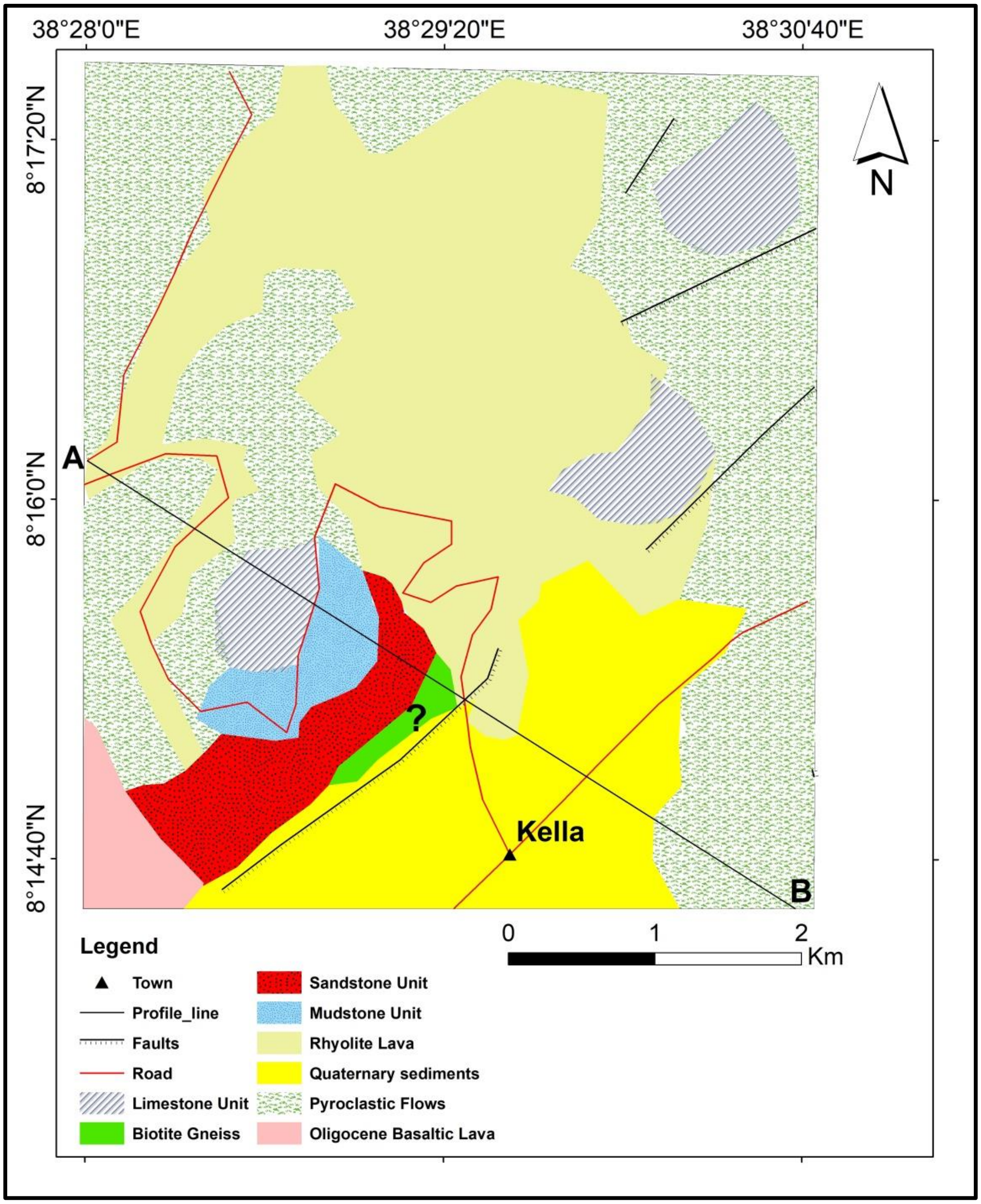

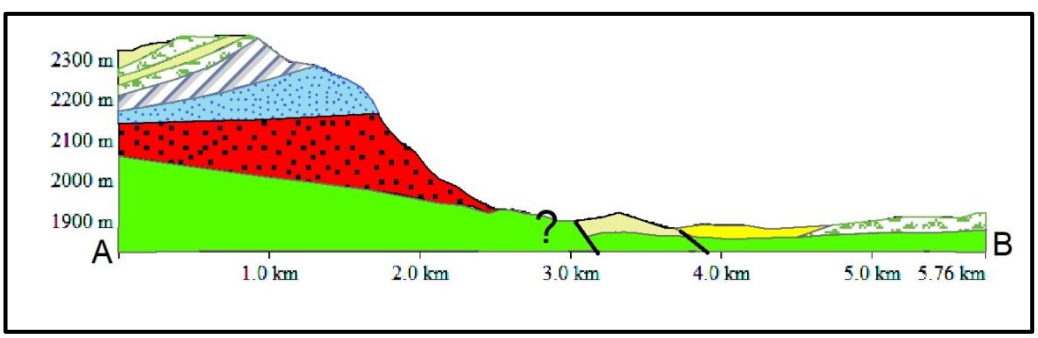

Figure 3. 2 The geological map of Kella and the surrounding area (A) and Geological cross section from A to B (B) (Modified after, GSE, 2010, Sileshe Negussia, 2019).

3.2 Section- A

Section-A is located between the UTM coordinates 0442830 Easting and 0913438 Northing, with an elevation of 2230m above sea level. The section was taken at the quarry site and includes vertical cliff-forming exposure (fig 3.3). This section is conformably overlying by the mudstone unit as it was observed during field work and unconformably overlies the basement unit (DiPaola et al 1993; Giday Woldegabriel et al., 1990 and Tsegaye Abebe et al., (2010). In this section, as well, the sedimentary unit's bedding is not continuous and tilts. The section is 165.5m thick. It Consist a coarse to very coarse-grained sandstone bed containing randomly distributed pebbles, which then grades into medium-fine-grained sandstone, conglomerate lenses sediment, and unconsolidated sandstone beds. Sandstone beds are made up of crudely developed planar cross-beds, wave-convolute beds, massively bedded, horizontally laminated sandstone sheets thinly bedded sandstone. Overall the section is divided into 11 beds based on sedimentary structure, texture, and stratigraphic position (fig 3.4).

Figure 3. 3 Quarry site and a cliff forming exposure of section A (sandstone),
This is a sandstone lithological unit. The cliff-forming exposure is mostly covered by vegetation so it was challenging for identification.

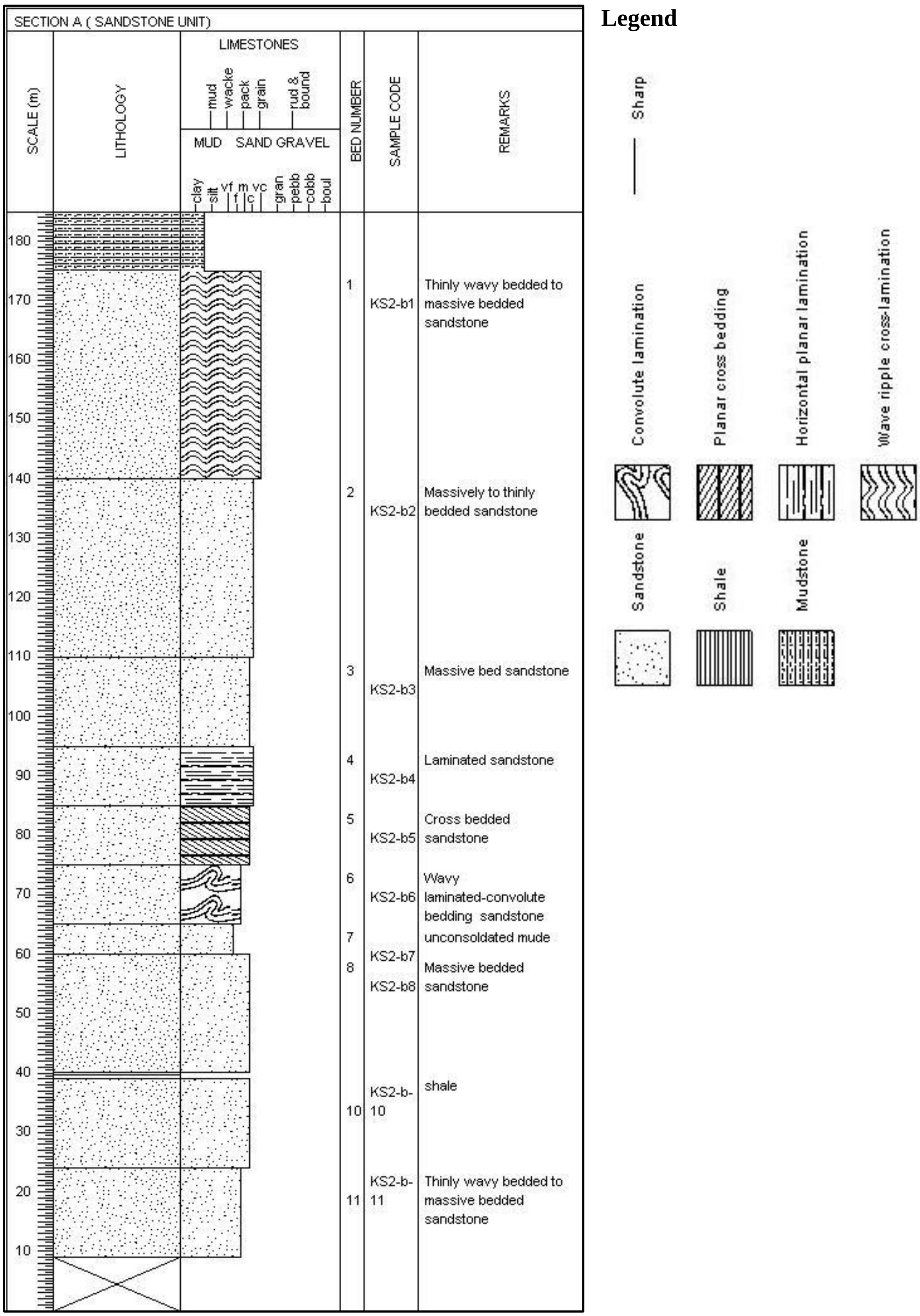

Figure 3. 4 Stratigraphic logs for section A (sandstone unit) of the Kella area,

3.3 Section-B

Section-B is located between the UTM coordinates 0442681 Easting and 0913383 Northing, at an elevation of 2254m sea level, and has road cut exposure. This section is unconformably overlain by volcanic rock (Unwelded tuff), whereas as you move northeast, the section is conformably overlain by the carbonate unit and conformably overly on the sandstone unit (fig 3.6). The section is made up of variegated color fine grain poorly consolidated mud and thinly wavy bedded siltstone, as well as a silty sand bed with a reddish to light gray color and variable thickness. The bed in this section is not continuous, but rather tilted and of variable thickness; from the section to the southwest, the mudstone unit disappears, whereas to the northeast, the thickness increases and then disappears. This section has a maximum thickness of 24m. The bottom part of the section is covered by vegetation and it is difficult for identification. However, the contact between the mudstone unit and the sandstone unit was identified. Based on filed observations, this section is divided into six beds (fig 3.5).

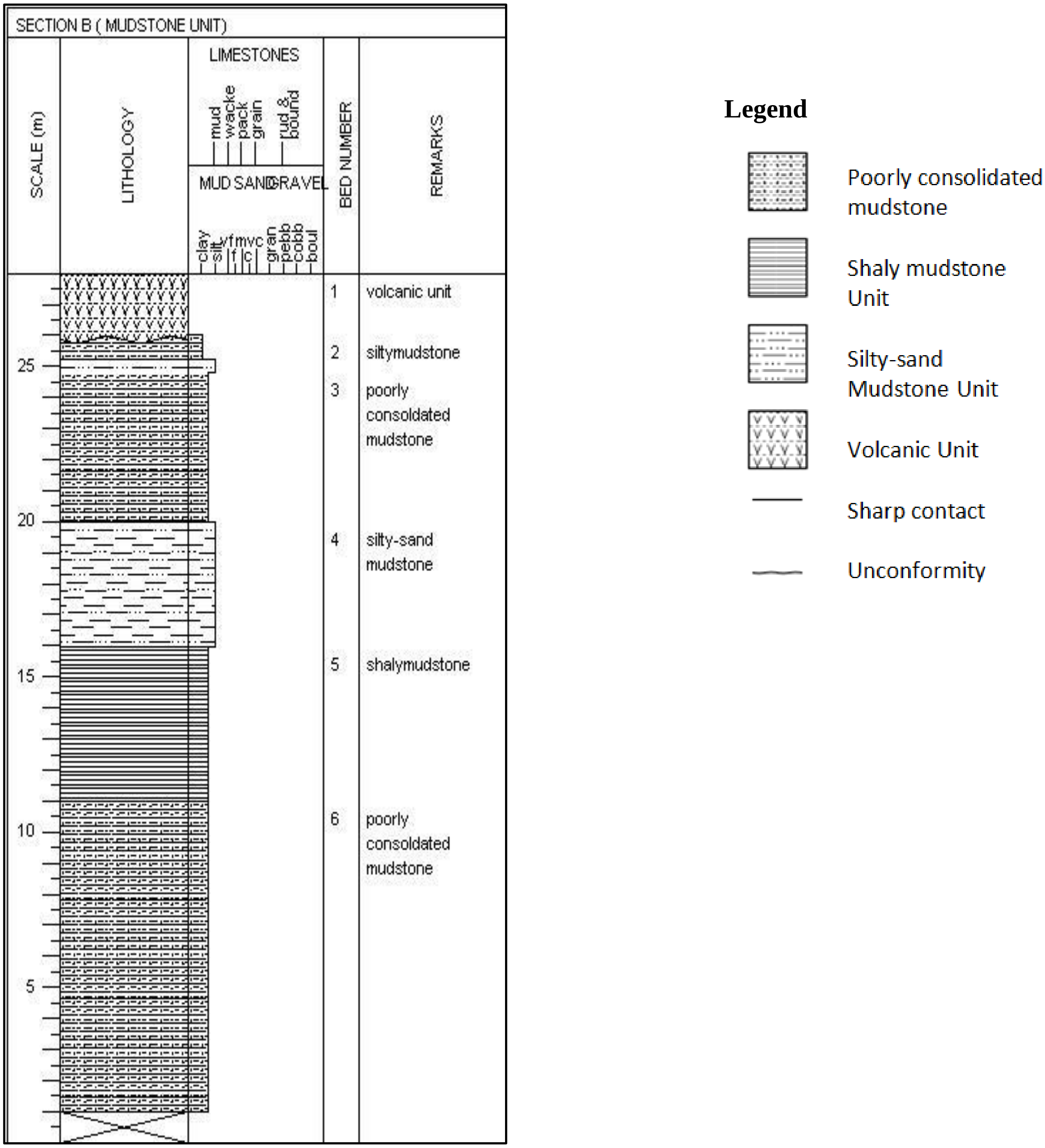

Figure 3. 5 Stratigraphic logs for section B of the Kella Area (Mudstone Unit)

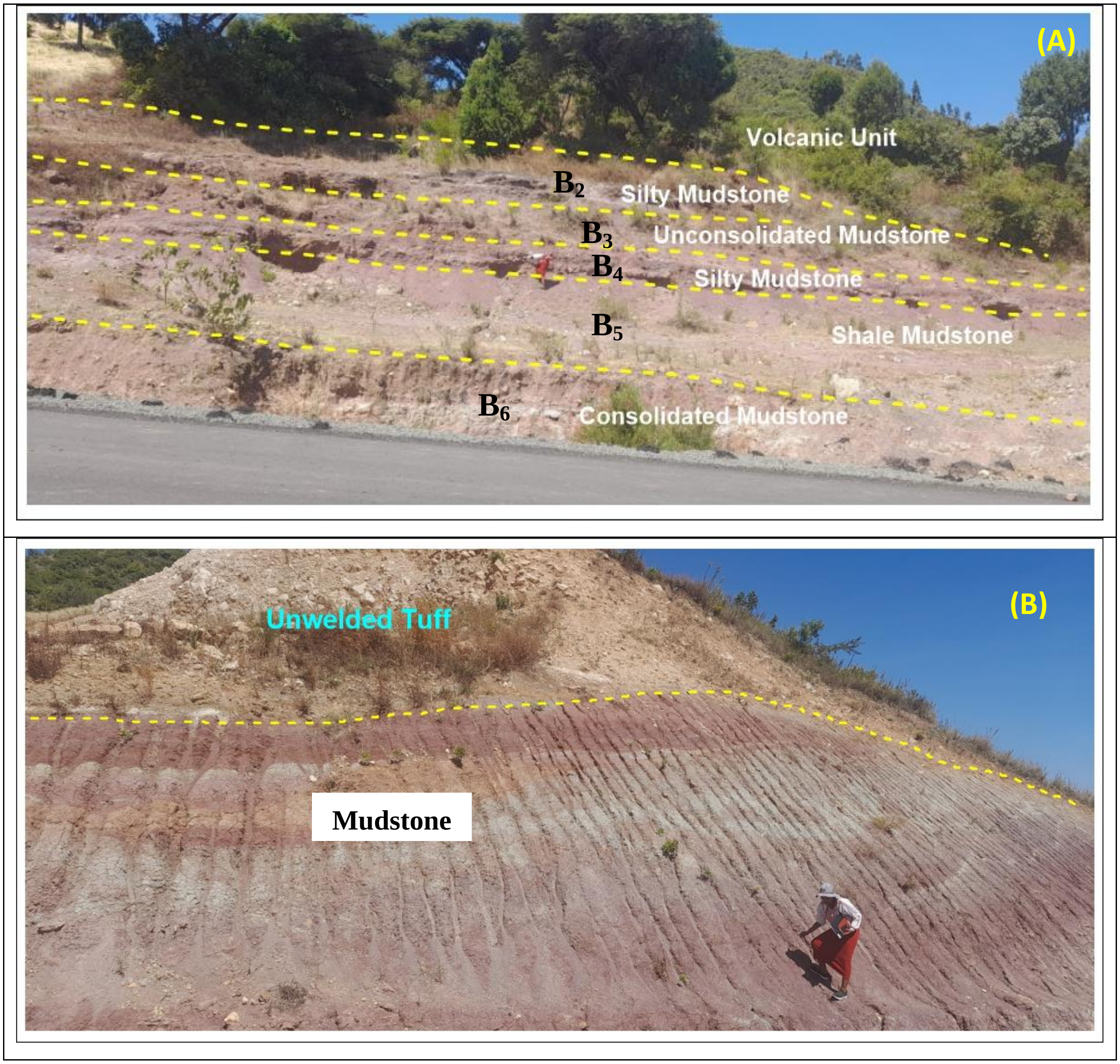

Figure 3. 6 Shows section B of the Kella area
Where (A) shows the whole section exposure and constituent beds and (B) shows the contact between the volcanic units (Unwelded tuff) and mudstone unit. Here the mudstone unit disappears directly after the road cuts the western part of the figure. Where B, bed

3.4 Section-C

Section-C is located between the UTM coordinates 0442599 Easting and 0913188 Northing, at an elevation of 2250m above sea level, and contains road cut exposure. This section is unconformably overlying by the volcanic (ignimbrite) unit and conformably overlays on the mudstone unit. The bed in this section is not continuous, but rather tilted and of variable thickness. The measured section has a maximum thickness of 17.3m. This section contains limestone intercalation with marl and shale lithology, which has variable thickness. The limestone is reddish, gray, or light gray in color, and it has fossil and calcite precipitation at the bed's surface as well as a silicified limestone bed. The marl bed is gray to dark gray. The shale bed has fissility and a light to dark gray color. The upper part of the section is dominated by limestone lithology, while the lower part is dominated by shale lithology. Based on filed observation the section is divided into nine beds from bottom to top (fig 3.8).

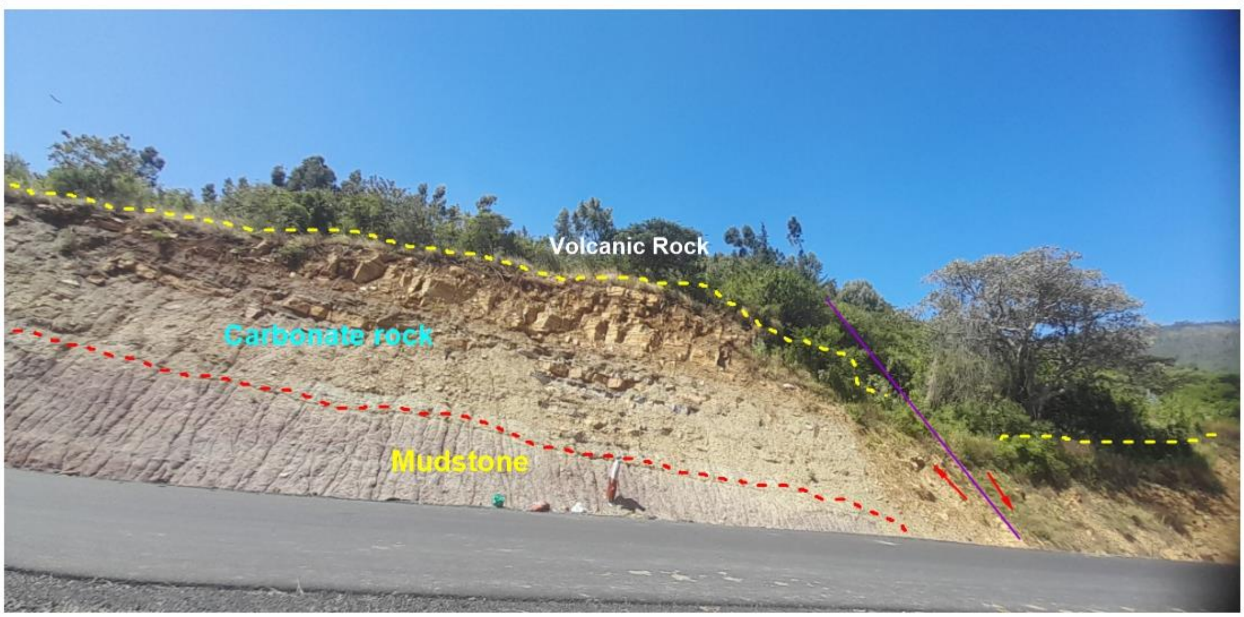

Figure 3. 7 The figure shows section C of the Kella area with exposed units of volcanic, carbonate rock and mudstone at the bottom

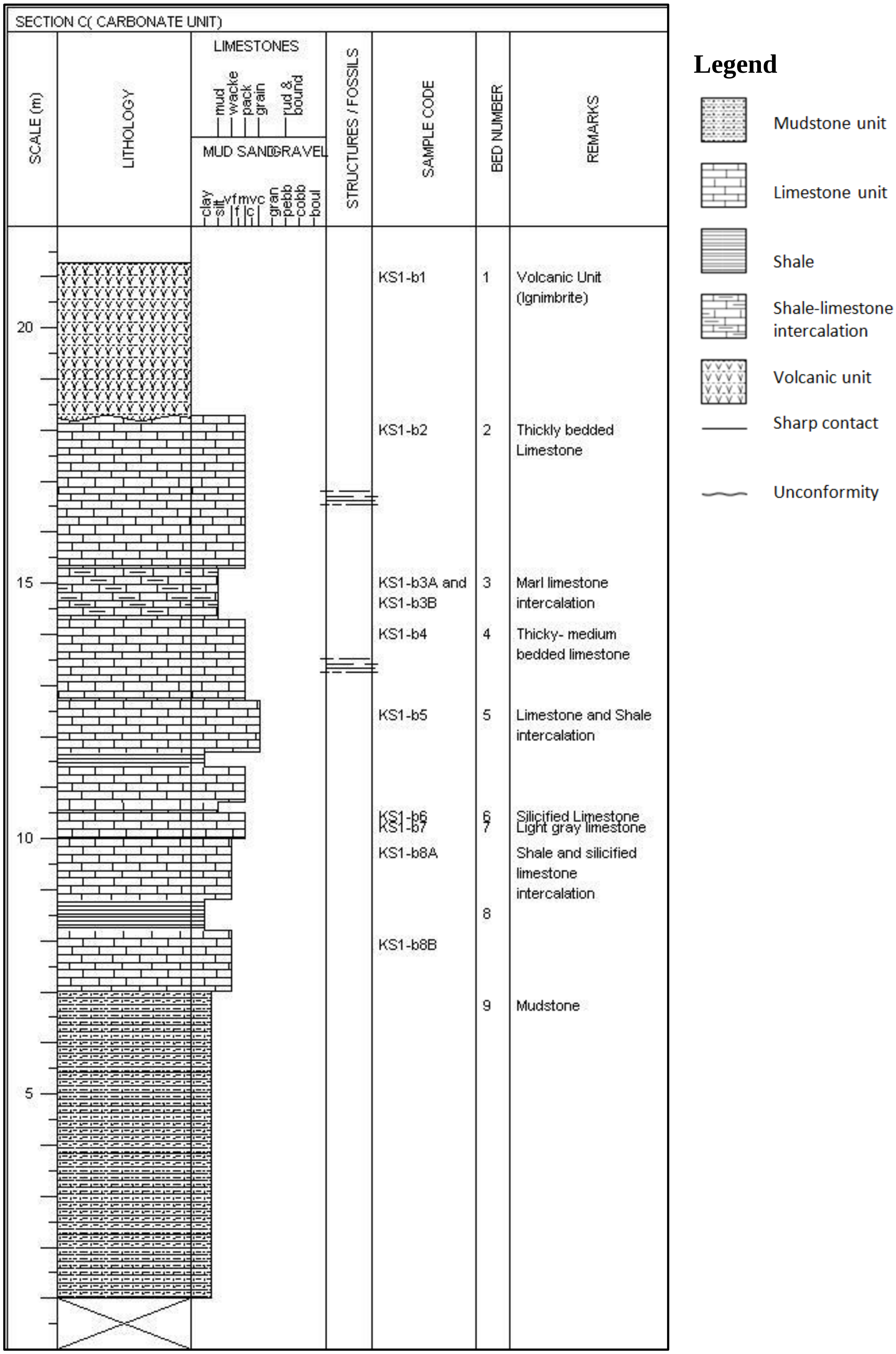

Figure 3. 8 Stratigraphic logs for section C of the Kella Area

Poorly consolidated mudstone (b-9): This is the bottom part of the section, measuring 6m in thickness. It exhibits variegated colors and a fine grain size, with gray shale that displays fissility.

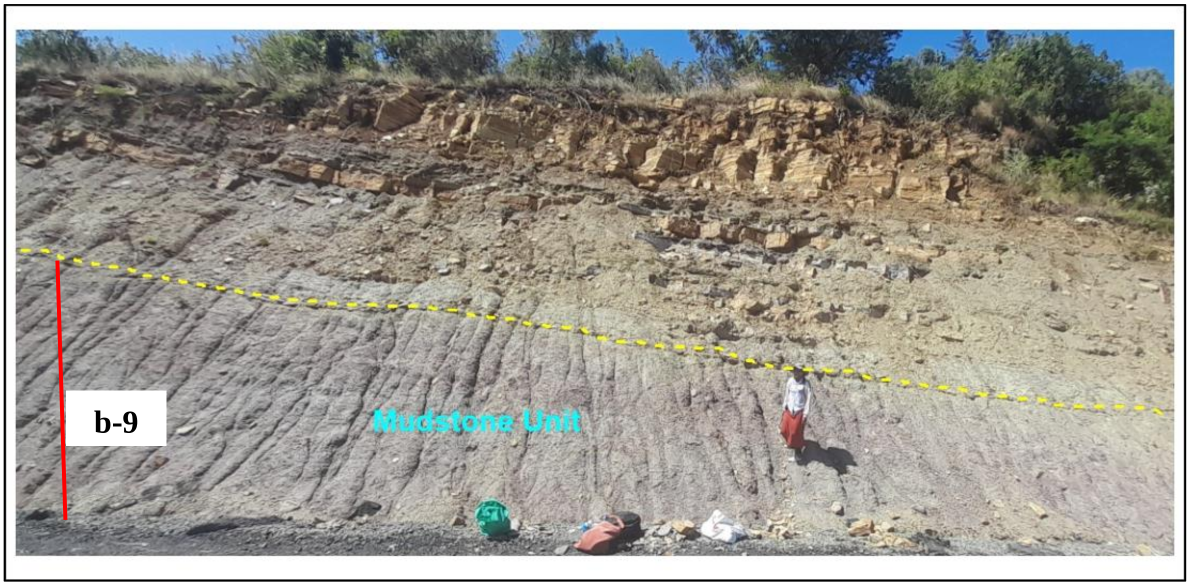

Figure 3. 9 Shows the bottom-most part of the section (unconsolidated mudstone unit) where the contact between the overlying carbonate units is shown by a yellow broken line.

Silicified limestone intercalation with shale (b-8): this bed is overlays the poorly unconsolidated mudstone bed and has a thickness of 3m. Three different silicified limestone beds are found with variable thickness (ranges from 0.2 to 0.6m.) and have light gray to reddish color with small grains. The shale sub-beds are thick relative to the silicified limestone layer with a gray color and fissility.

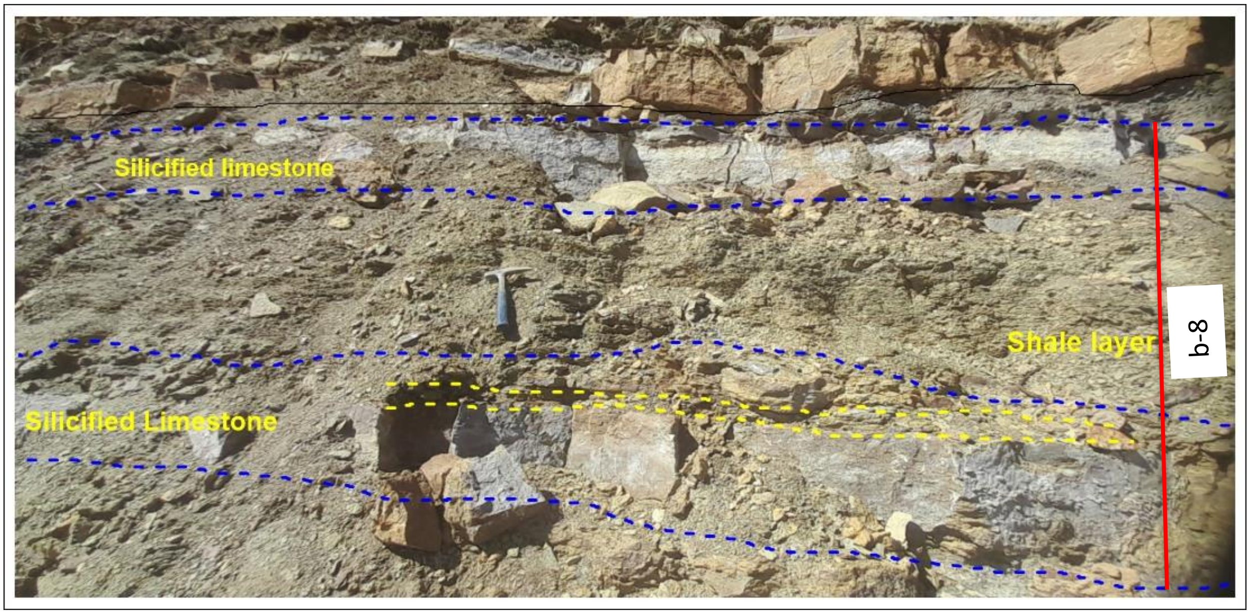

Figure 3. 10 The figure shows the intercalations of silicified limestone with the shale where the silicified limestone is indicated by the blue broken lines

Light gray Limestone bed (b-7): This bed is 0.5m thick and has a light gray color. However, the weathered part appears brownish in color (Fig. 3.11, b-7).

Silicified limestone (b-6): The bed has a thickness of 0.2m and displays a range of colors from light gray to reddish to brownish. It contains clasts and also shows calcite precipitation on its surface. At the bottom part it contains thin shale layer with gray color.

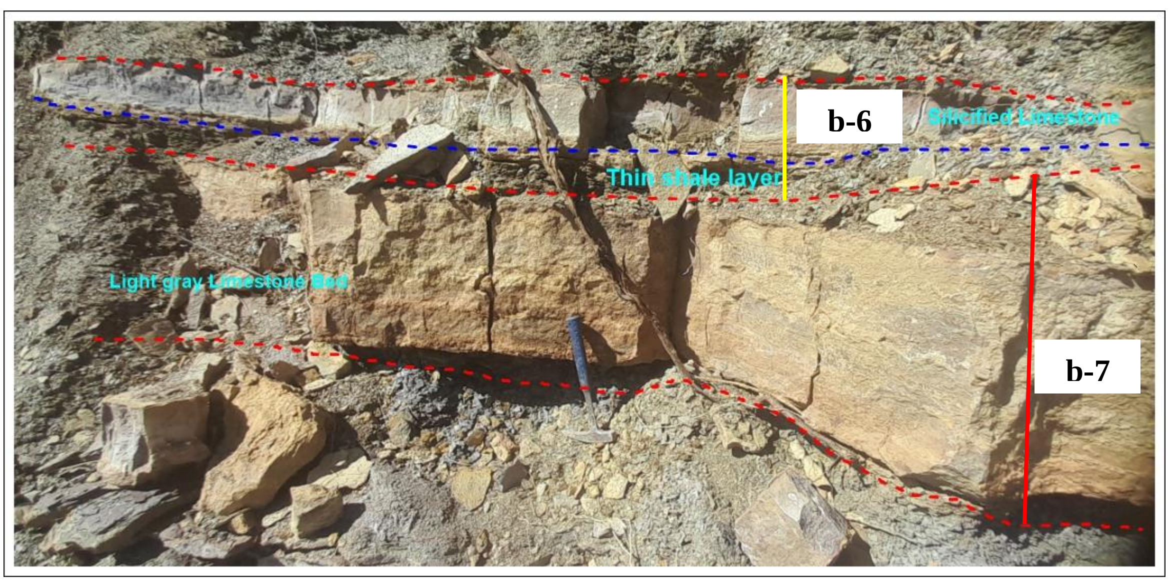

Figure 3. 11 The figure shows the intercalations of silicified limestone with the shale where the silicified limestone is indicated by the blue broken lines

Limestone-shale intercalation bed (b-5): The bed has a total thickness of 2m. It consists of alternating layers of limestone and shale. The shale layer is divided into four sub-beds with varying thicknesses ranging from 0.2m to 0.4m. The shale exhibits a variegated color and has a fissility characteristic. The limestone has three sub-beds with variable in thickness, ranging from 0.2m to 0.3m. It has a gray to reddish color and contains veins filled with cement material, and elongated gray clasts.

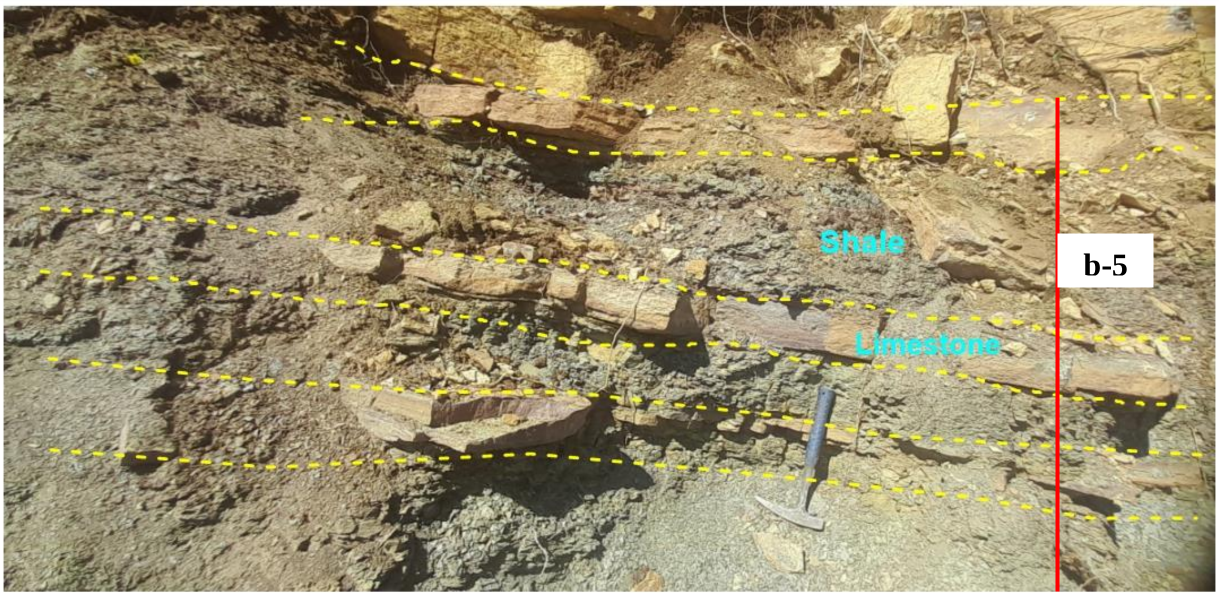

Figure 3. 12 Shows limestone intercalations with variegated shale where the shale sub bed sows variable thickness and each subbed of the limestone is indicated by a yellow broken line.

Thickly to medium bedded Limestone (b-4): The bed has a total thickness of 1.6 meters and has a gray to reddish brown color. The weathered sections of the bed show a yellowish color. Inside the bed, there are three subbed layers with thicknesses ranging from 0.2 to 0.7 meters. The top surface of the bed displays calcite precipitation. Furthermore, it contains fossil grains that appear gray in the hand specimen scale.

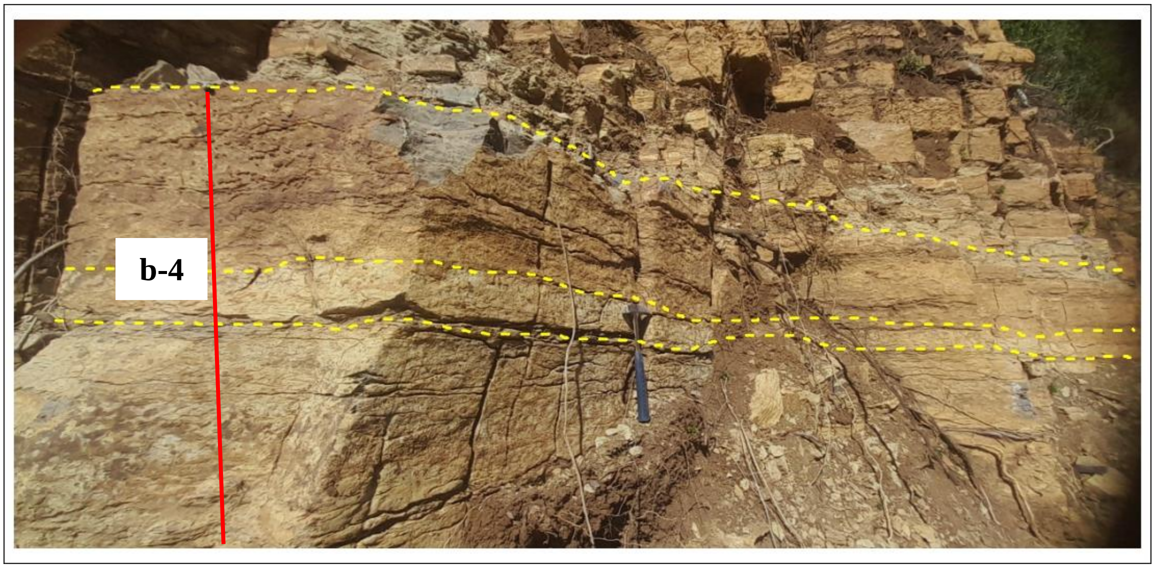

Figure 3. 13 Shows the thickly to medium bedded limestone
Where the upper and lower part is thickly bedded of similar character whereas the middle part is medium sub-bed thickness indicated by yellow broken lines.

Marl limestone intercalation (b-3): This bed is composed of three layers and has an overall thickness of 1m. The top section of the bed is made of gray-colored marl lithology, which measures 0.5m in thickness. The middle portion is composed of light gray limestone and has a thickness of 0.2m. In this section, no grains are observed at the hand spacemen level, indicating that it is micritic. The lower portion of the bed is characterized by gray-colored marl and has a thickness of 0.3m. It also contains fissile dark gray shale.

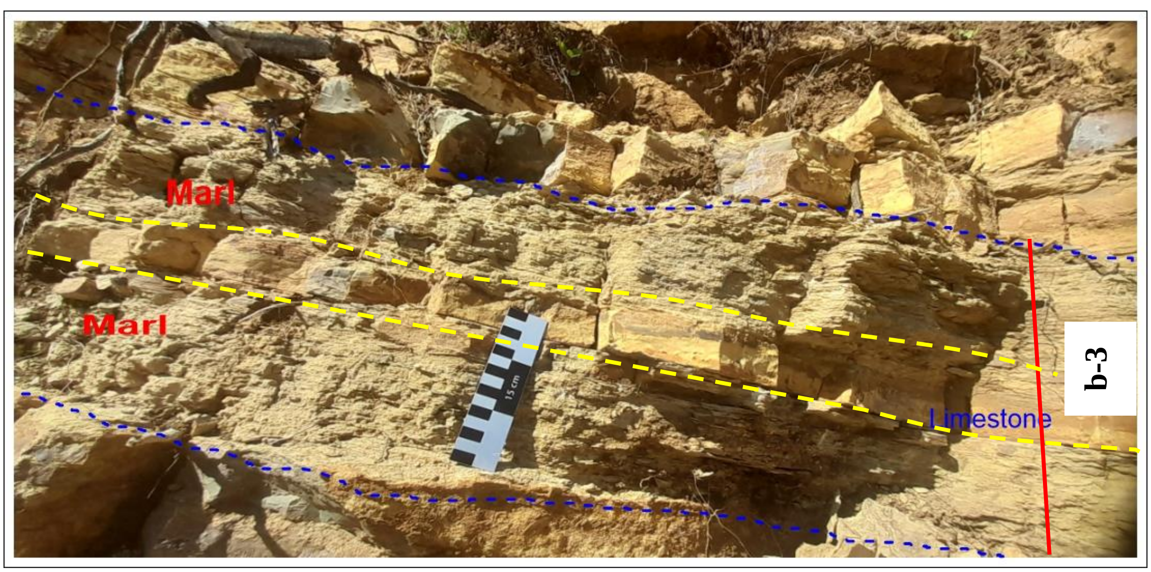

Figure 3. 14 Show Marl limestone intercalation indicated by the blue broken lines where the light gray limestone is intercalated with marl.

Thickly bedded limestone (b-2): The top part of the limestone unit is represented by this bed, which can reach a thickness of up to 3m. This bed consists of six sub-bedding, each with a varying thickness ranging from 0.3 to 1m. The clasts within the bed have a dark gray color, while the overall bed appears light gray to brown in color and the weathered color is yellowish.

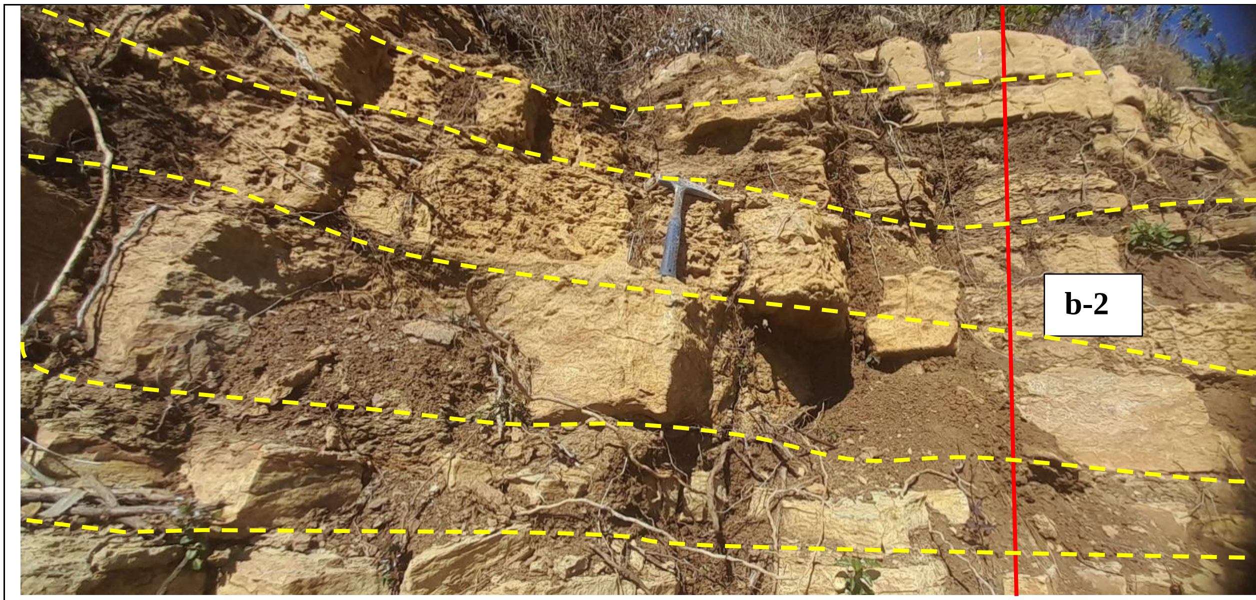

Figure 3. 15 The figure shows the bedded limestone, highly weathered with six sub-beds. This bed is the upper part of the carbonate unit in section C. the yellowish broken line separates each sub-beds.

Ignimbrite unit (b-1): Compared to other lithology, this unit is widespread and rests unconformably on top of the carbonate unit. It has an estimated thickness of around 400 meters. The pyroclastic unit consists of layers that vary in color, ranging from light to dark gray in fresh samples, and weathered samples may exhibit shades of reddish, yellow, or pink. This rock is fine-grained and tightly welded, composed of fractured basalt, lithic fragments, larger basalt pieces, ash, and unwelded tuffs.

3.5 Section-D

Section-D is located between the UTM coordinates of 0442610 Easting, 0913422 Northing, with an elevation of 2240m above sea level. It is characterized by road cut exposure. The section is unconformably overlain by volcanic rock (an ignimbrite) and conformably overlays the mudstone unit. The beds in this section are not continuous; instead, they are tilted and display fold-like or bed-load-like structures. The measured section has a maximum thickness of 20m

.The lithology of the section consists of limestone, marl, shale, and unconsolidated mudstone. Based on the lithological units and their stratigraphic positions, the section is divided into 19 beds, which are described below from bottom to top.

Figure 3. 16 Shows section D of the Kella area with exposed rocks
Volcanic rock at the top, carbonate rock at the middle and mudstone at the bottom, where the cyan broken line indicated the volcanic contact with the carbonate and the red broken line contact between the carbonate unit and mudstone unit.

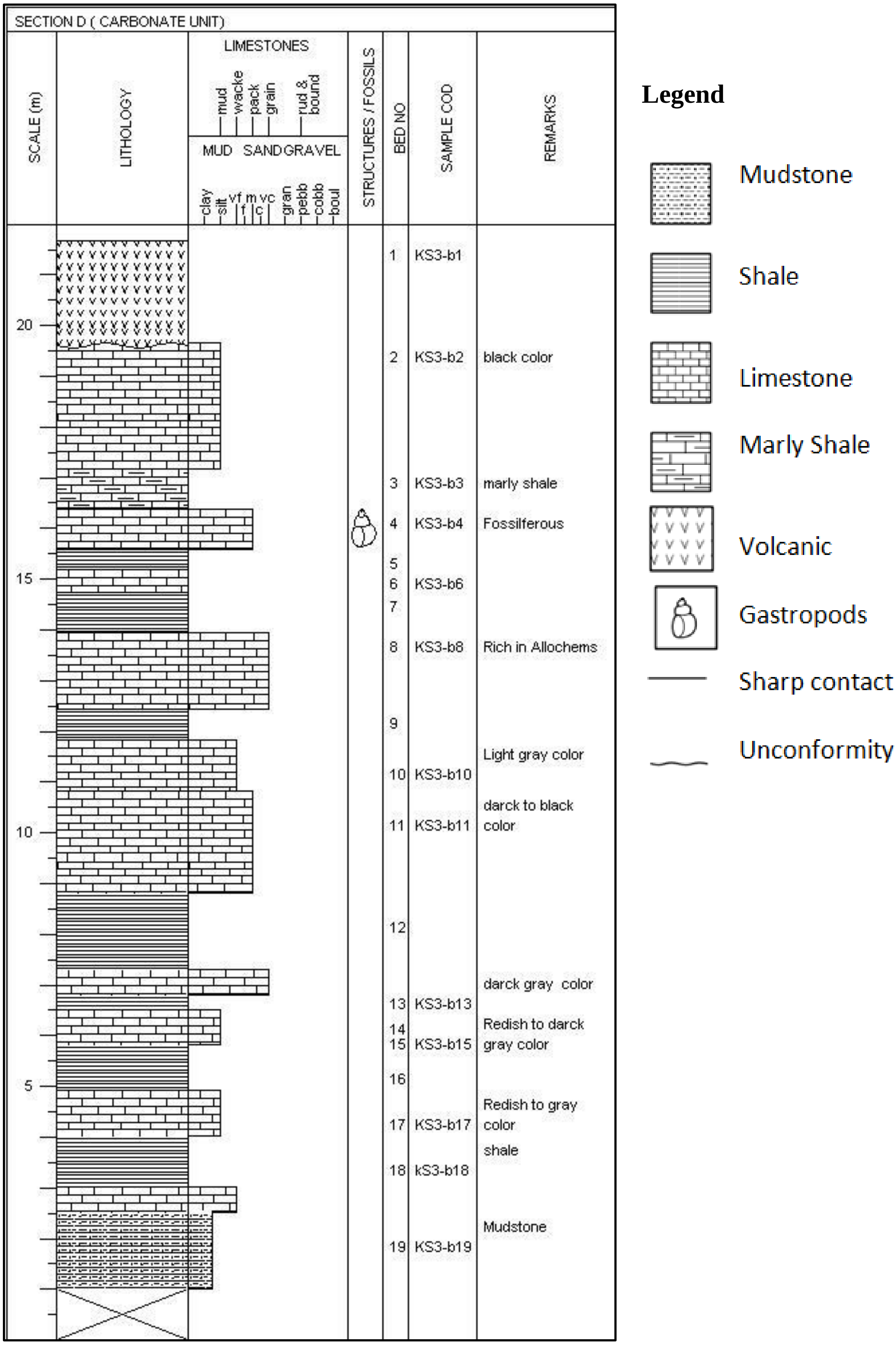

Figure 3. 17 Shows the stratigraphic log of section-D of the Kella area

Friable mudstone (b-19): The bed is the bottom part of the section and it has a thickness of 1.5m and has a variegated color. It is composed of fine-grain mud and it contains light gray shale which has a fissile nature (fig. 3.18 b19).

Shale (b-18): This shale bed is overlays on the friable mudstone bed and overlaying by the gray-reddish limestone bed with a thickness of 1.5 m. It is made up of fine grain mud with a gray color and it has a fissile nature (fig. 3.18 b18).

Gray to reddish limestone (b-17): This bed is overlaying by the shale bed and has an overall thickness of 0.9m, with reddish to gray color (fig. 3.18 b17).

Shale (b-16): This bed is overlaying by the reddish-dark gray limestone bed and has a thickness of 0.9m. It has a dark gray color which is made up of fine grain mud (fig. 3.18 b16).

Reddish to dark gray limestone (b-15): It has a thickness of 0.7m and it contains shiny material. Additionally, it has precipitated calcite on the bedding surface (fig. 3.18 b15).

Shale (b-14): This bed overlay on the reddish-dark gray limestone bed and a thickness of this bed is 0.3m, a dark gray color with fissility (fig. 3.18 b14).

Dark gray limestone (b-13): This bed overlay on the shale bed (b14) the thickness of this bed is 0.5m and it is gray to dark gray in color. It has calcite precipitation on the surface of the bedding (fig. 3.18 b13).

Shale Layer (b-12): This shale bed is overlay on the dark gray limestone bed and it has a thickness of 1.5m. It shows fissility with gray color (fig. 3.18 b12).

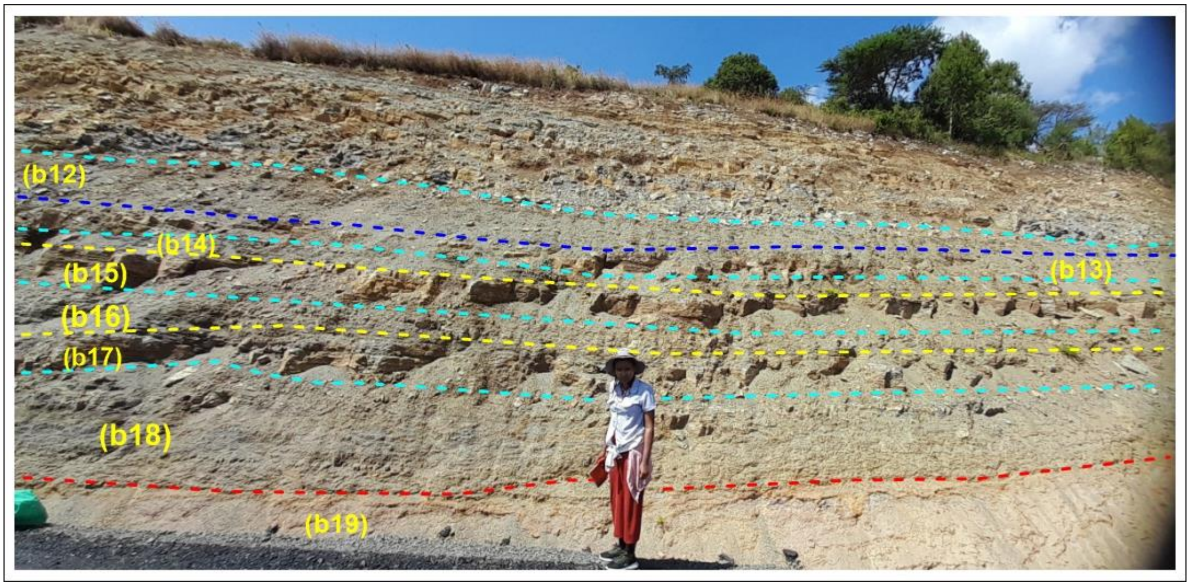

Figure 3. 18 The figure shows the exposures of bed 12 to bed 19;
Where, b12= shale unit, b13=dark-gray limestone, b14=Shale unit, b15=reddish to dark-gray limestone, b16=Shale unit, b17= gray to reddish limestone, b18=shale unit and b19=friable mudstone.

Dark to Black limestone (b-11): This limestone bed is overlays on the shale layer (b-12) and overlaying by the light gray limestone bed and it has a thickness of 2m.it has a black color with some shiny materials (fig.3.19 b11).

Light gray limestone (b-10): This bed has a thickness of 1m and is light gray in color. It consists of two sub-beds with different thicknesses. It also contains a vein that is filled with cementing material and the cement has brownish to whitish color (fig. 3.19 b10).

Shale (b-9): This bed is overlays on the light gray limestone bed and it is 0.6m thick with dark brown in color. It is made of fine-grain mud with fissility (fig.3.19 b9).

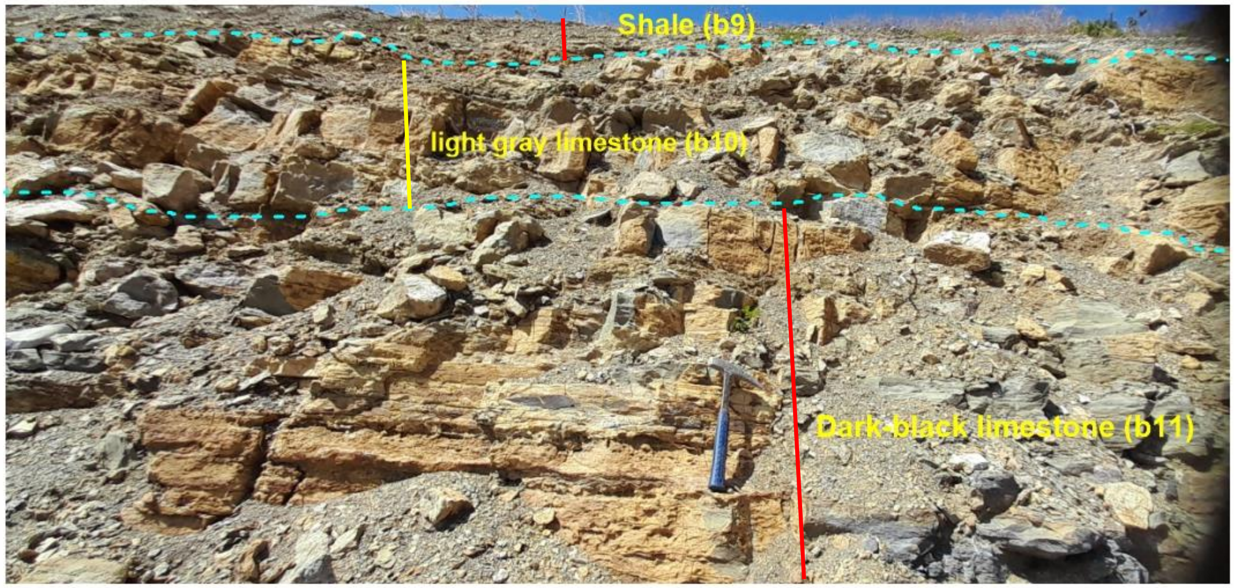

Figure 3. 19 Shows the beds of shale (b9) at the top, light gay limestone (b10) at the middle, and dark-black limestone bed at the bottom (b11)

Allochemical limestone (b-8): This bed has a thickness of 1.5m and it is rich in allochems. It is divided into three sub-beds. The upper part is 0.6m thick and black in color while the middle part is 0.5m thick with reddish color. The lower part is made of 0.4m thick and gray in color **(**fig. 3.20 b8).

Shale unit (b-7): This bed has a thickness of 0.8m and is similar to bed 5 (fig. 3.20 b7).

Grayish limestone (b-6): the bed is 0.45m thick and has reddish to gray color. It consists of clasts and veins filled with cement material that has a light brownish color. Additionally, there is calcite precipitation on the bedding surface (fig. 3.20 b6).

Shale unit (b-5): the bed is 0.4m thick and has a dark brown color. It is composed of fine-grin mud with fissility (fig. 3.20 b5).

Fossiliferous limestone (b-4): the bed is 0.8m thick and has a gray color. It is abundant in gastropod shells on the top surface, with a small diameter in millimeters (fig. 3.20 b4).

Loosely consolidated Marl (b-3): The thickness of the layer is 0.8m and it has a gray to brownish color. It is composed of fine-grain unconsolidated carbonate mud and it is found below the black limestone bed (fig. 3.20 b3).

Black limestone (b-2): The bed, which has a thickness of 2.5 m, is overlaid by the volcanic (ignimbrite) unit in an unconformable manner. It consists of six sub-bedding layers with varying thicknesses ranging from 0.2 to 0.8m. On a hand specimen scale, no grains are observed, and it is black in color (fig. 3.20 b2).

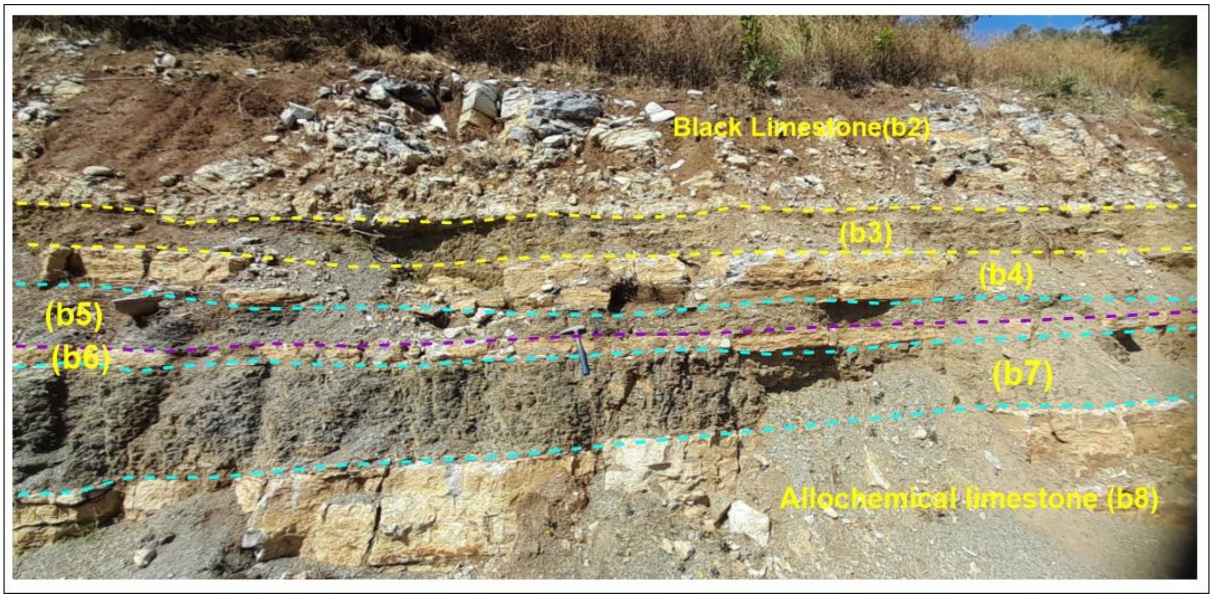

Figure 3. 20 The figure shows the exposures of bed 2 to bed 8;
Where, black limestone, b3=loosely consolidated marl, b4= fossiliferous limestone bed, b5= shale bed, b6= grayish limestone bed, b7=shale unit, bed 8=allochemical limestone

Ignimbrite unit (b-1): This unit is similar to the bed one (b1) of the section C. The unit unconformably overlies the carbonate unit.

3.6 Limestone exposures north-east of the section

A different outcrop of limestone lithology is found in the northeast of the section. Each of the three locations exhibits unique characteristics and exposers. Each of them is described in the following section.

3.6.1 Exposure one

This limestone unit is located between the UTM coordinates of 442968 Easting, 913499 Northing with an elevation of 2135m above sea level. It is 5m thick and has been exposed by a seasonal stream. No clasts were observed in the hand spacemen scale, and it has a light gray color. The limestone is highly weathered, displaying a karst structure and thickly bedded. It is surrounded by a volcanic unit.

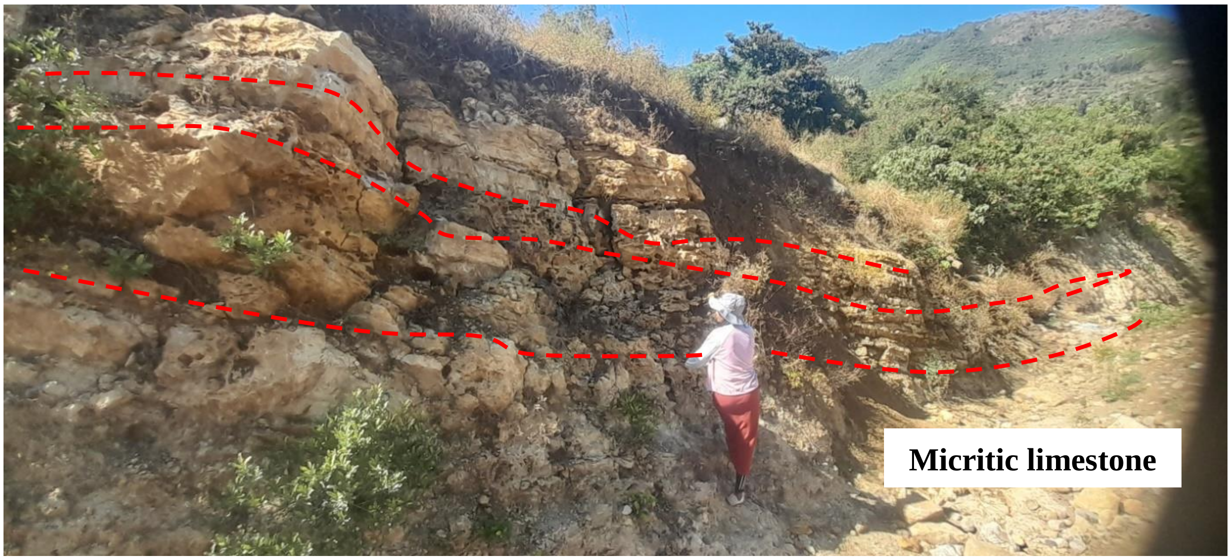

Figure 3. 21 Micritic limestone exposure with karst structure exposed north east of the sandstone quarry site.

3.6.2 Exposure two

This limestone unit is located in the northeast (NE) directions of the Kella to Keshite asphalt road; at UTM coordinates of 044389 Easting, 0914965 Northing with an elevation of 2125m above sea level. It is weathered with no clear exposure, has a gentle slope, and transitions into cultivated land. It has a yellowish to whitish color and no grain was observed in hand spacemen scale.

Figure 3. 22 Deeply weathered yellowish limestone exposure north east of Kella- Keshite asphalt road. The units have no clear exposure and were dominantly covered by vegetation and cultivated land

3.6.3 Exposure three

This limestone unit is located in the northeast (NE) of the Kella to Keshite asphalt road; at UTM coordinates of 0444498 Easting, 0915388 Northing with an elevation of 2130m above sea level. It is similar to exposure two highly weathered with no clear exposure, has a gentle slope, and changes into cultivated land. It has a light gray color, no grain was observed in the hand spacemen scale.

Figure 3. 23 Light gray limestone exposure north east of Kella- Keshite asphalt road. The units have no clear exposure and were dominantly covered by vegetation and cultivated land.

3.7 Composite stratigraphy

The present study comprises four section which is found in the central Ethiopia regional state, east Guraghe zone of the Sodo woreda, Kella section these are section A (165.5m thick sandstone unit), section B (24m thick mudstone unit), section C (17.3m thick carbonate unit), and section D (20 m thick carbonate unit) were identified. Based on the lithologic unit and the base of vertical succession the present studied section is correlated within the Kella section and finally produced the composite stratigraphy of the Kella section.

Figure 3. 24 Correlation between the four sections of the Kella area (section A, section B, section C and Section D)

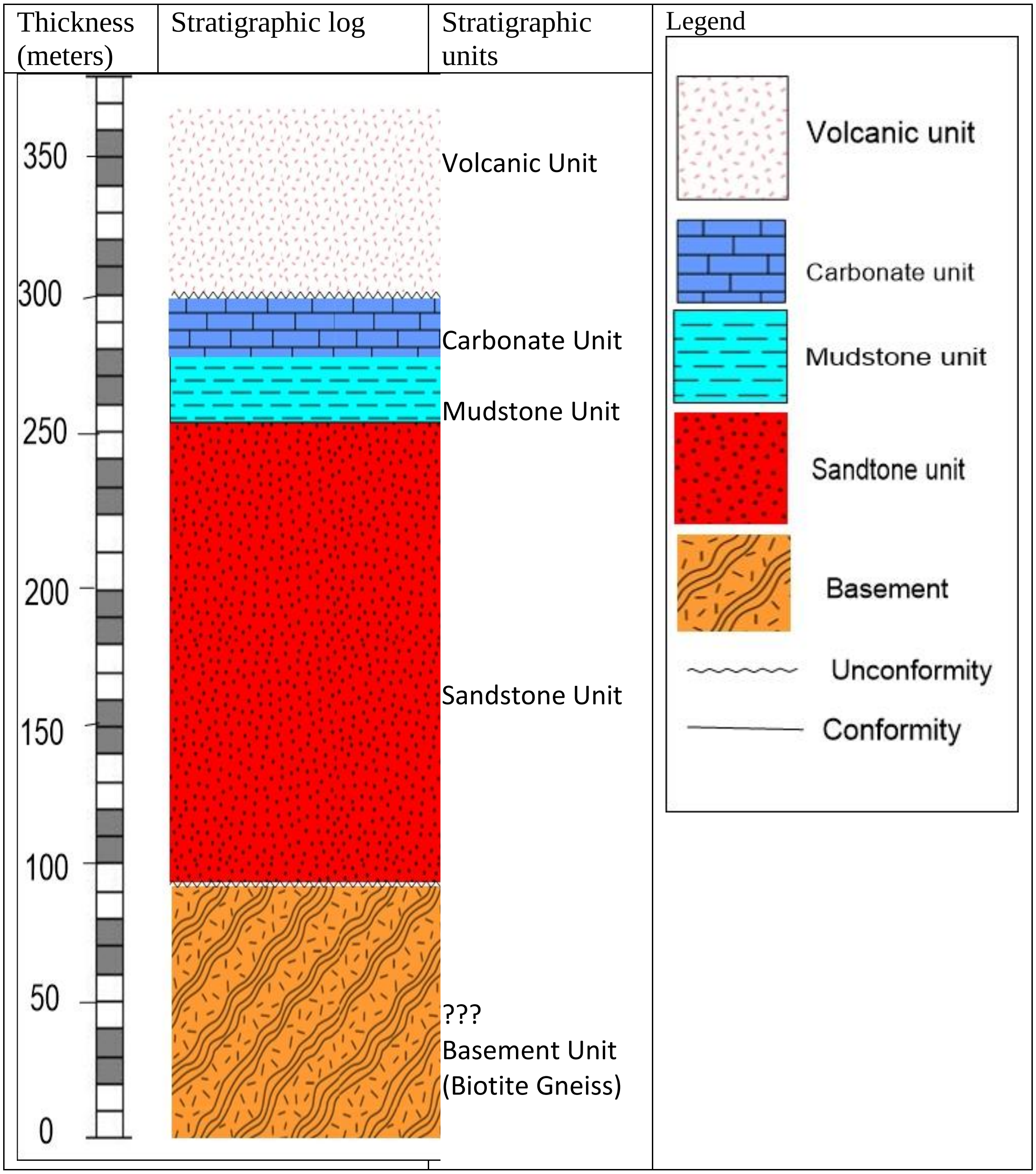

Figure 3. 25 Composite stratigraphy of the Kella section.

CHAPTER FOUR

PETROGRAPHIC ANALYSIS

4.1. Introduction

In geological science, petrographic analysis is conducted to provide support for data obtained from field observation. This analysis allows for the examination of the detailed compositional and textural properties of rock samples. In addition to filed observations made in the studied outcrop section of the Kella area, a total of thirty one (31) representative samples analyzed, specifically there were ten (10) samples of sandstone from section A, nine (9) carbonate samples from section C, nine (9) carbonate samples form section D and two (2) carbonate samples from exposure two and three and one volcanic rock sample were analyzed and described under petrographic microscope. Therefore, all the thin sections are analyzed using a petrographic microscope and the details are described in the following sections.

4.2. Sandstone (section A)

Ten (10) sandstone samples were analyzed. During thin section analysis, the composition of rock-forming minerals is identified. This is done by using point counting the modal proportion of the framework grain. The result is then plotted on a QFL diagram, following the classification scheme established by Folk (1980) and Pettijohn et al (1987). In addition to the compositional analysis, this study also discusses the detailed textural and diagenetic features observed in the rock. The matrix and cementing minerals consist of fine-grained material that binds the framework grains together, as well as the materials filling the pore spaces between the grains, as identified. There are also accessory minerals present, including a sheet of mica (biotite and muscovite) flake. In addition, a small number of opaque minerals have been observed in certain thin-section samples.

4.2.1 Compositional description

In thin section analysis, various types of detrital mineral compositions were identified in the sandstone. The predominant minerals found in the framework grain are quartz while feldspars and lithic fragments make up a small percentage of the overall mineralogy of sandstone.in addition to the framework grains; there are also minor accessory minerals such as sheets of mica and opaque minerals observed. The space between the grains of sandstone is filed with a finer muddy matrix mixed with very fine quartz and the cement. Under the thin section, the observed cementing minerals include calcite, silt-sized quartz, and oxide minerals.

Quartz: is the main mineral grain present in all thin sections, making it a significant component of sandstone. The quartz grains consist of both monocrystalline and poly crystalline grains. When comparing polycrystalline quartz grain with monocrystalline quartz grain, the polycrystalline quartz grain contains a smaller proportion. The individual grains have a sub-angular to sub-rounded morphology. In some samples, the quartz grains, along with the other detritus, are coated with poikilotopic autogenetic spari-calcite. Micro cracks and undulose extinction are the most common. Additionally, certain quartz grains contain needle shaped incorporated minerals.

Feldspar: one of the key components used in the compositional classification of sandstone. In comparison to the quartz grain, the feldspar grain contains a significantly smaller proportion according to the modal analysis result obtained from point counting. The feldspars grains exhibit signs of alteration and have angular to sub angular with few crystals having well-rounded morphology. In some samples, microcline feldspar exhibits cross-hatched twining. Among the feldspars group, potassium feldspars (K-feldspars) are more commonly observed.

Lithic fragments (rock fragments): are the other key components used in the compositional classifications of sandstone. In comparison to the quartz grain, the lithic fragment grain contains a smaller proportion according to the modal analysis result obtained from point counting. Often it is formed in multiple quartz grains and sutured together (in the form of polycrystalline quartz).

Matrix: it is a type of clay and silt-sized material with a fine-grained texture, which is the framework grains are embedded and adhere to one another. Based on the analysis, the matrix is relatively high. The extremely fine-grained nature of the matrix poses challenges when studding its composition in detailed through petrographic analysis.

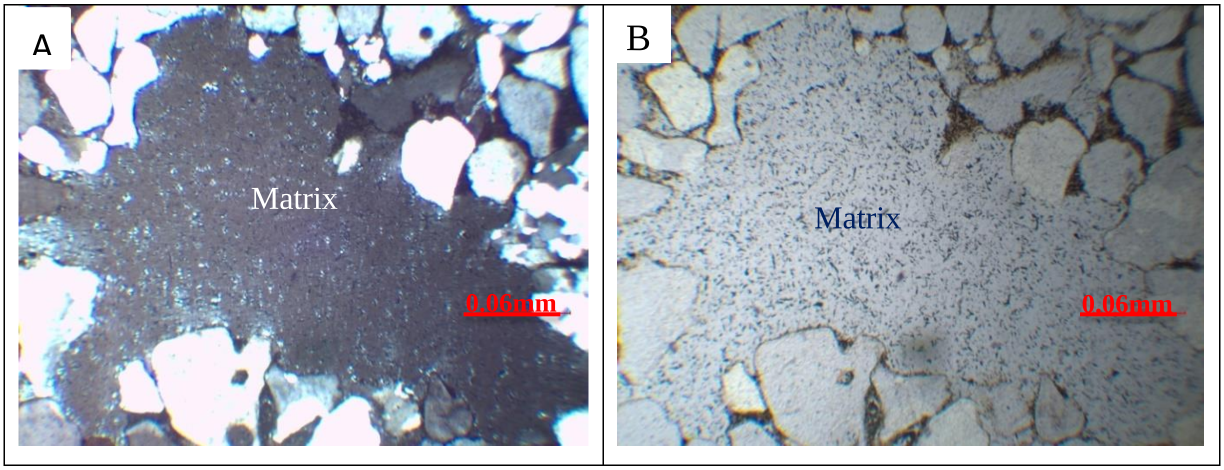

Figure 4. 1 The photomicrograph shows a matrix which (sample KS_2-b8) is difficult to identify of the matrix type, the photo has undertaken XPL; A, PPL; B

Cement: The most common cementing mineral is reddish to brownish oxide and calcite. In one sandstone sample (KS_2-b1) there is no cementing material rather the matrix is much more (40%). in some thin sections, only oxide cement is dominant.

Other trace minerals: this includes mica minerals (biotite and muscovite) and opaque minerals. Opaque minerals like oxides are found in the form of inclusions within quartz grain and between grain boundaries.

4.2.2 Textural description

The textural description of sandstone depends on the shape, size, roundness surface feature, and sorting of each grain. There is various grain size distributions observed in the thin section analysis. These grains vary in size ranging from fine sand to pebble size. The size of the grain has been determined using the Wentworth (1922) grain size classification. The shape of most grains is discoid-bladed with some elongated, road-like grains and the grains have angular to sub-angular with ranges of well to poorly sorted. Sample (KS_2-b8 and KS_2-b11) has fine grain size angular to sub angular and well sorted, (KS_2-b6, KS_2-b4, KS_2-b5 has medium to coarse grain with poor sorting).

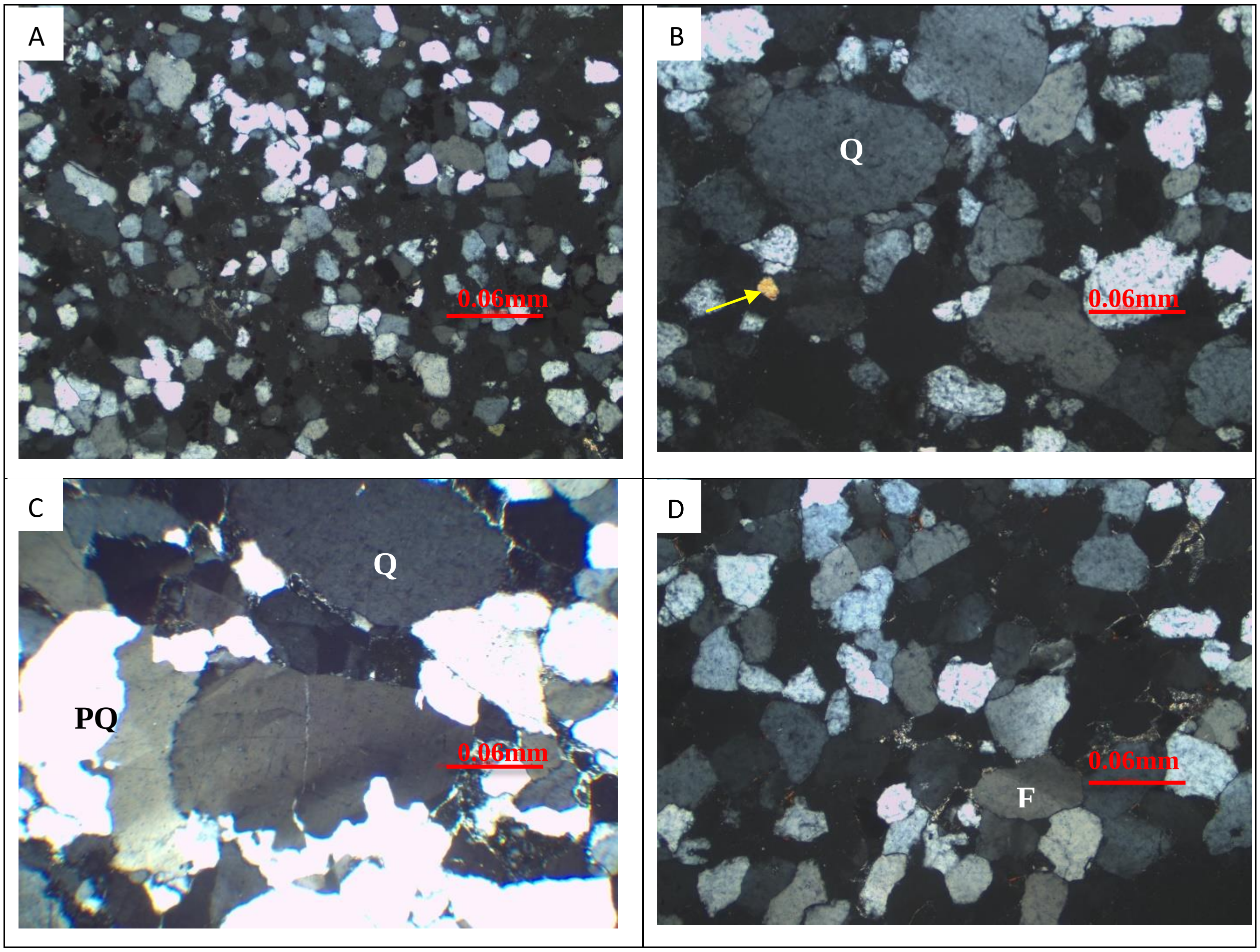

Figure 4. 2 The photomicrograph shows the texture of sandstone.
A (KS_2-b11) shows fine grain rounded-subrounded quartz with well-sorted B) (KS_2-b3B) fine to coarse grain with rounded to sub-rounded grains and the yellow arrow indicates biotite minerals. C (KS_2-b2A) coarse, angular grain with poor sorting, D (KS_2-b2B) fine-medium grain with good sorting and has rounded-sub-rounded grain. All photos under taken XPL. PQ = polycrystalline quartz, Q = quartz, F =feldspar

4.2.4 Compositional and textural maturity

The textural maturity of the studied samples ranges from immature to mature. The samples KS_2-b1, KS_2-b2A, KS2-b2B and KS_2-b11 are described as texturally immature. Whereas, the samples KS_2-b3A, KS_2-b3B, KS_2-b4, KS_2-b5, KS_2-b6 and KS_2-b8 are texturally mature.

The compositional maturity of sandstone described in the Kella section ranges from mature to super mature. The sample KS_2-b11 is described as compositionally supper mature as it is dominantly composed of quartz grains and the remaining samples are grouped as mature.

4.2.5 Sandstone classification

The classification of sandstone is a broad concept, as there are many different classification systems for this type of rock. In this study, a classification of sandstone was determined by using a modal proportion of framework grain. a classification of sandstone major frame work grains are quartz (Q), Feldspars (F), and lithic fragments (L) were counted under a petrographic microscope and their relative proportion is determined from hundred percent. The relative proportion of matrix and cement was also determined. Based on the Folk (1980) classification scheme, most of the selected samples (simple KS_2-b1, KS_2-b2A, KS_2-b2B, KS_2-b3A, KS_2-b3B, and KS_2-b5) represent Subarkose, two samples fall under Litharenite (sample KS_2-b4 and KS_2-b6), one sample is categorized under Sublitharenite (sample KS_2-b8) and one sample is categorized under quartz arenite (sample KS_2-b11) (fig. 4.3).

Table 4. 1 point count data of sandstone sample under petrographic microscope analysis.

Sample No.	**Components of sandstone in percent (%)**						
	Q	**F**	**L**	**Matrix**	**Cement**	**Others**	**Rock Name**
KS_2-b1	50	5	3	40	0	2	Subarkose
KS_2-b2A	41	5	1	40	10	3	Subarkose
KS_2-b2B	45	10	2	30	10	3	Subarkose
KS_2-b3A	65	5	3	15	10	2	Subarkose
KS_2-b3B	62	10	2	20	2	4	Subarkose
KS_2-b4	50	2	18	15	14	1	Litharenite
KS_2-b5	60	5	3	20	10	2	Subarkose
KS_2-b6	42	1	20	25	10	2	Litharenite
KS_2-b8	47	2	5	4	40	2	Sublitharenite
KS_2-b11	46	1.5	0.5	40	3	9	Quartz arenite

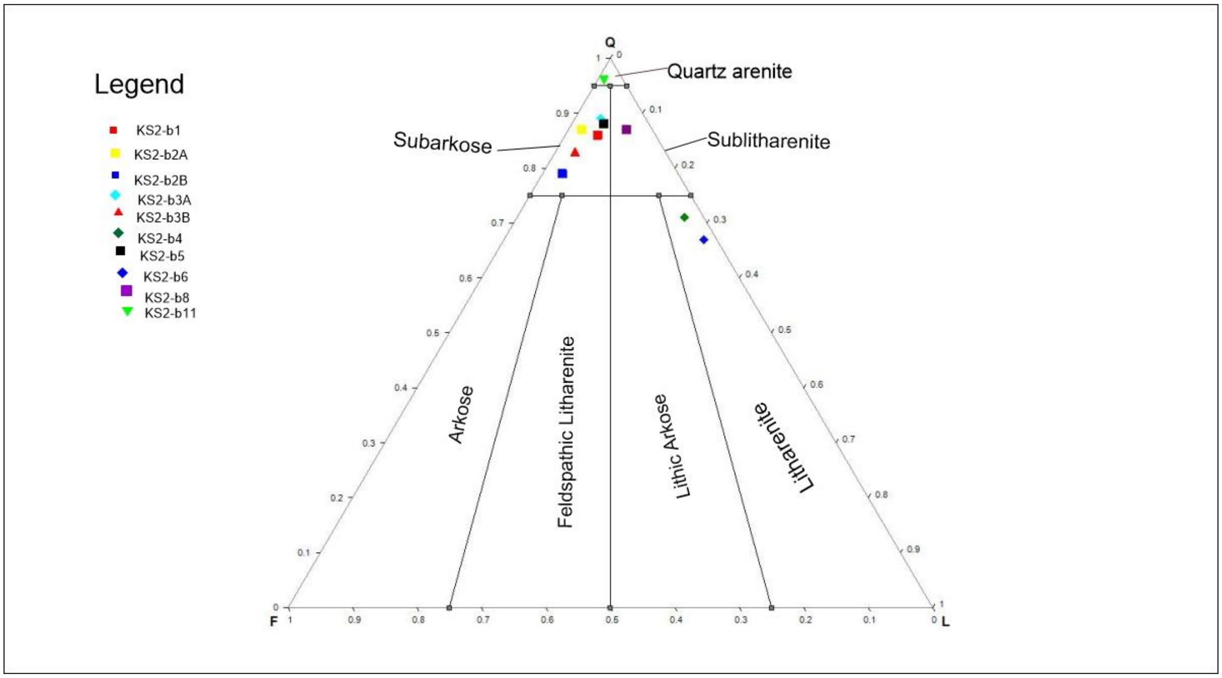

Figure 4. 3 The QFL (Quartz-Feldspar- lithic fragments) ternary diagrams showing the compositional classification of sandstone of the Kella area (After Folk, 1980)

4.3 Limestone

Microscopic study is essential for a thorough understanding of facies analysis and interpretation of the depositional environment of carbonate units. Field observation alone is insufficient to fully describe all the properties of carbonate rocks. Hence A total of twenty (20) samples were analyzed and described through a petrographic microscope. The detail thin section description and identification were conducted based on Folk (1959), Dunham (1962), and Embry and Klavan (1971) schemes. The fossil content and composition of each sample were determined and using this data, microfiches types and depositional environment were identified. The detailed analyses are described below (see table 4.2).

Table 4. 2 Petrographic data of carbonate unit in the Kella section.

Section	Sample cod	Petrographic data										Rock name		MFT
		Allochems (%)				Quartz (%)	Oxide (%)	Micrite (%)	Cement		Porosity (%)	Dunham (1962)	Folk (1959)	
Section C		Peloids	Ooids	Bioclast	Intraclast				Sparite	Calcite (%)				
	KS_1-b2			65		5		30				Packstone	biomicrite	3
	KS_1-b3A					3		97				Mudstone	Micrite	1
	KS_1-b3B					2		98				Mudstone	Micrite	1
	KS_1.b4			70		2		20	8			Packstone	Biosparmicrit	3
	KS_1-b5			65					35			Grainstone	Biosparite	4
	KS_1-b6			60				35	5			Packstone/Mudstone	Biosparmicrite	5
	KS_1-b7	20	15	20				30	10		5	Packstone	Oopelbiosparmicrite	6
	KS_1-b8A		2	75					23			Grainstone	Oobiosparite	7
	KS_1-b8B			30		10		40		20		Wackestone	Biomicrte	10
Section D	KS_3-b2							98		2		Mudstone	Micrite	2
	KS_3-b4			80				18			2	Packstone	Biomicrite	8
	KS_3-b6			55				30		10	5	Packstone	Biomicrite	8
	KS_3-b8	5	5	40			5	37	5	3		Packstone	Oopelbiomicrite	6
	KS_3-b10			20				60			20	Wackestone	Biomicrite	9
	KS_3-b11			5		25	10	60				Mudstone	Biomicrite	11
	KS_3-b13			60	5		5	15	5	10		Packstone	Intrabiomicrite	6
	KS_3-b15		5	55					10	30		Grainstone	Oobiosparite	7
	KS_3-b17			60				30		5	5	Packstone	Biomicrite	9
Out of section	LS-S1					10		60			30	Mudstone	Micrite	1
	LS-S2			20				70		10		Wackestone	Biomicrite	12

Section	Sample code	Quartz	Alkali Feldspar	Olivine	Texture	Rock Name
D and C	KS_3-b1	30%	65%	5%	Porphyritic	Ignimbrite

4.4 Diagenesis feature

Diagenesis refers to the processes that affect sediments immediately after deposition and continue until metamorphism occurs at high temperatures and/or pressures. Sedimentary rock encompasses a range of biological, chemical, and physical processes that determine the texture, mineralogy, and fluid flow properties of the rock (Tucker and Wright 1990).

4.4.1 Sandstone diagenesis

The diagenetic processes that have influenced the sandstone include cementation, compaction, recrystallization, replacement, mineral overgrowth, and dissolution (Hayes, 1979).

4.4.1.1 Grain deformation

Grain deformation typically occurs during the compaction stage of diagenesis (Tucker, 2001). Under petrographic analysis, some of the grains in the sandstone, especially the quartz grains, showed slight deformation, indicating prolonged contact between grain frameworks. The grains were tightly packed together due to overburden pressures, resulting in liner convex-concave contact as a result of compaction (fig 4.3 A and B).

4.4.1.2 Cementation

Cementation is the process of welding together the clastic sediment framework grains through the precipitation of mineral matter within the pore space. This diagenetic process involves the autogenic precipitation of minerals in the loose sediment pores. The primary outcome of cementation is the reduction of porosity. In the thin section analysis, three types of cementation were identified: calcite cementation, oxide cementation, and silica/quartz cementation. Calcite cement is a type of cement that is used to reduce porosity between framework grains (fig. 4.3 C). It fills the large crystals with a poikilitic texture, both replacing and growing over the existing grains. Oxide cementation is the process that involves reducing the porosity by filling the space between the grains (fig.4.3 D). The common silica cement found in this study is quartz mineral overgrowth. This fine-grained quartz mineral fills the open space between the framework grains.

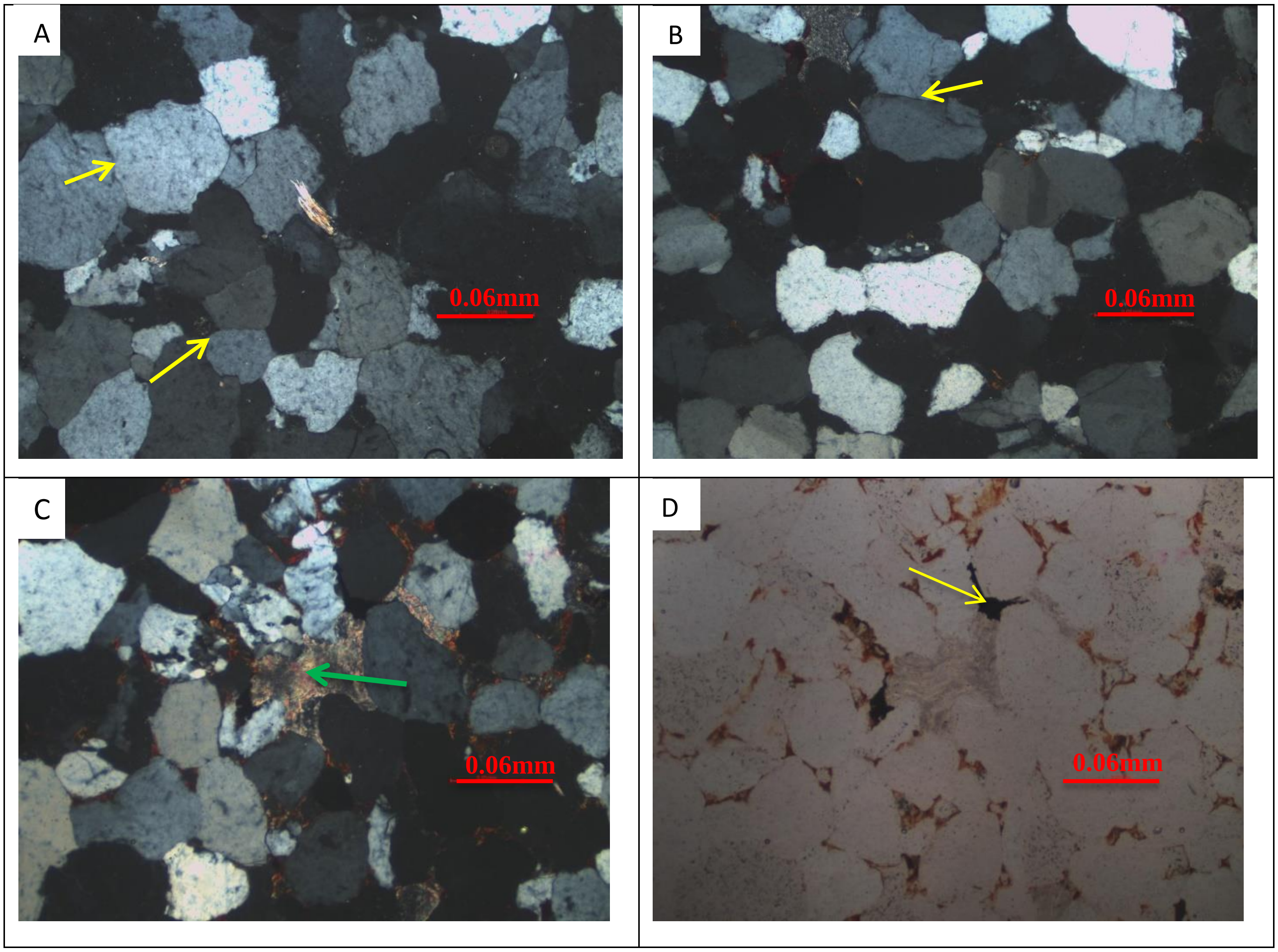

Figure 4. 4 The photomicrograph of different samples
A) The quartz grains, showed slight deformation, indicating prolonged contact between grain frameworks (sample KS_2-b1) and B (sample KS_2-b5). C) The green arrow indicates the calcite cement (Sample KS_2-b6) and D) the yellow arrow shows the oxide cement (sample KS_2-b6), the photomicrograph taken under XPL; A, B, C and PPL; D.

4.4.2 Carbonate diagenesis

The carbonate units in the study area are influenced by various diagenetic processes, such as micritization, dissolution cementation, physical compaction, pressure solution recrystallization/ neomorphism, and the replacement of carbonate grains and matrix with non-carbonate minerals (silicification). This section discusses the different types of diagenetic processes that occur in the carbonate unit being studied.

4.4.2.1 Compaction

During the progressive burial of the carbonate mineral, an increase in overburden pressure leads to a reduction in the sediment thickness and the formation of compaction textures. Compaction process can be categorized as either mechanical (physical) or chemical (pressure solution) Tucker and Wright (1990).

4.4.2.1.1 Physical compaction

Physical compaction involves tighter packing and deformation of grains due to overburden pressure as burial into the subsurface proceeds. Grains are deformed by brittle fracturing and breaking and by plastic or ductile squeezing which reduces porosity, permeability, and sediment thickness dewatering and fracturing, reorientation, breakage of allochems and closer packing of grains (Shinn and Robbin, 1983 Choquette and James, 1981). This type of diagenetic alteration is found in section D from the Kella area (KS_3-b4) (fig 4.4 A).

4.4.2.1.2 Chemical compaction

Chemical compaction involves the process of pressure solution occurring between the rains, resulting in the formation of interpretation or sutured contacts. These phenomena can also give rise to pressure-solution seams known as stylolite. These are characterized by the presence of clay minerals and other fine non-carbonate minerals, often referred to as insoluble residues. This type of diagenetic feature was identified in section D sample KS_3-b15 (fig 4.4B).

4.4.2.2 Cementation

Cementation is the process by which minerals precipitate within the pore space of sediment rich in grain or cavity. Cementation is the most dominant diagenetic process throughout the study section (fig 4.4 D).

4.4.2.3 Micritization

Micritization completely replaces the entire skeletal fragments with micrite, this leads to the obliteration of rains and the disappearance of the original strictures. However, some fossil fragments preserve the original structures and are less affected by the micritization process. The completely micritized bioclast are the shells of bivalves, that have prismatic microstructure, making the clasts susceptible to micro borings, intensive micritization, and complete replacement of the original skeletal fragment (Flugel, 2004). On the other hand, there are few skeletal fragments with well-preserved delicate original structures covered by thin layers of micrite envelope, as a result of constrictive micritization.

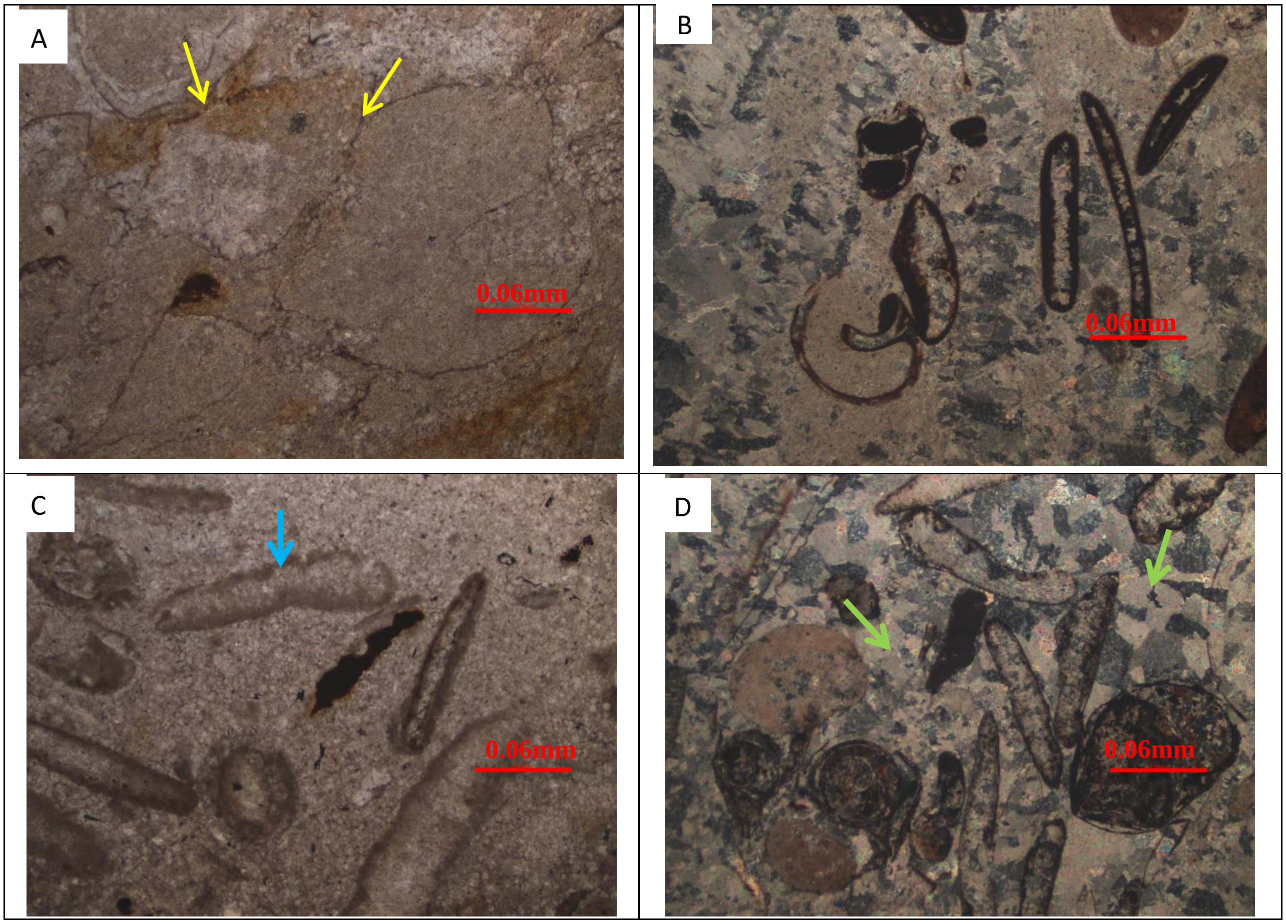

Figure 4. 5 The photomicrographs indicate mechanical compaction
A) Grain with grain contact indicated by yellowish arrow (sample KS_3-b4 in section D). B) (sample KS_3-b15) and C) shows micritization blue arrow (Sample KS_3-b8), D) shows Sparite cement the light green arrow the photomicrograph undertook, XPL; A, D, and PPL; B, C.

4.4.2.4 Neomorphism

Neomorphism is one of the late diagenetic processes that represent the gradual polymorphic transformation of older crystals to new crystals of the same mineral, through crystallization (Bathurst, 1975). The calcite crystals are coarse and gradual replacement of the original texture or carbonate grain. It is very coarse and with cloudy appearance and undulose extinction shows irregular distribution. Very coarse neomorphic calcite crystal replaced the original micrite however, there is the micrite relict that confirming the processes of neomorphic transformation

4.4.2.5 Recrystallization

Most of the microfacies contain highly crystalized fossil fragments, fractures filled by the calcite crystals and pore-filling coarse sparry calcite cement. The coarse calcite spars in most samples are anhedral with well-developed boundaries. Some of the calcite crystal has cleavages and twinning, with clear extinction (fig 4.5 C).

4.4.2.5 Dissolution

Dissolution is also an important process of diagenesis, that affects some microfacies, The dissolution structure identified from both outcrop scale and in thin sections includes molds, vugs, and channels (fig 4.5 A and B). There were identified from KS_3-b4, and KS_3-b10 in section D.

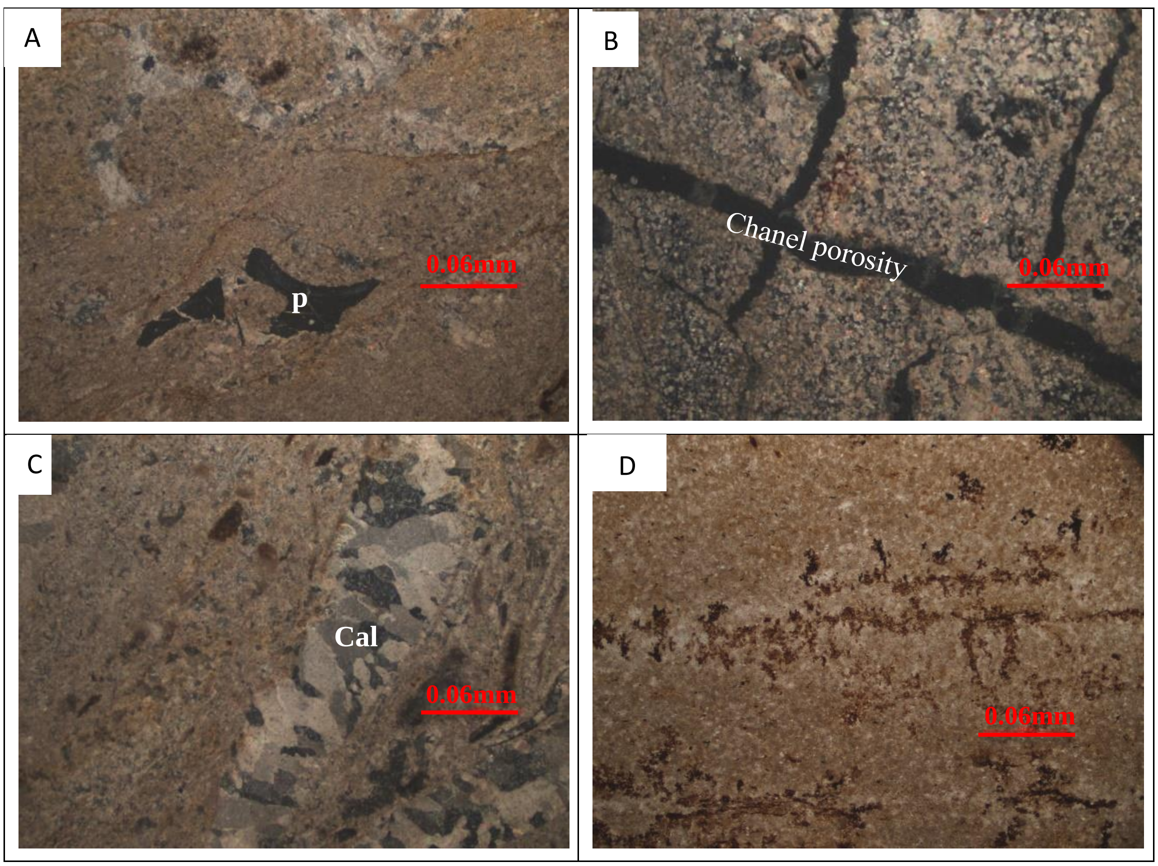

Figure 4. 6 The photomicrograph shows grain dissolution (KS_3-b4) A and, B sows channel porosity (KS_3-b10), C recrystallization (KS_3-b6), D Neomorphism (KS_3-b3A).P= porosity, Cal=calcite

CHAPTER FIVE

FACIES ANALYSIS

5.1 Introduction

The term "facies" is often used when describing sedimentary rocks in terms of their depositional settings. A body of rock with particular properties that represent the conditions of its formation is called a rock facies (Nichols 2009 and referenced therein). A sedimentary facies is described by recording all the features of its lithology, texture, sedimentary structures, and fossil content that can be used to infer formation processes. Hence terms such as marine facies, clastic facies, biofacies, and lithofacies can be used (Headberg, 1976; Krumbein and Sloss, 1951).

Based on field observation (the lithostratigraphic type) the sedimentary rocks are divided into three informal lithostratigraphic units, these are the sandstone unit, the mudstone unit, and the carbonate unit. In this section, several lithological, textural compositional variations were observed in the three lithostratigraphic units and their associations are systematically analyzed.

5.2 Lithofacies analysis

A total of 16 lithofacies were identified within the siliciclastic sedimentary unit. Among these, 11 lithofacies types were identified in the sandstone unit, while 5 lithofacies types were identified in the mudstone unit. The facies were identified, based on sedimentary structure, texture, and stratigraphic position at an outcrop and hand specimen scale. Each lithofacies is described and interpreted in the following section.

5.2.1 Thinly bedded sandstone facies (Facies 1)

Description: This bed is at the bottom of the section. The bed thickens up to 15 meters. Texturally, it consists of fine to medium-grain sand with well-sorting. It has reddish to light gray color. This bed contains a variety of thin bedding with varying thicknesses ranging from 1cm to 0.5m. The upper part of each bed is very thinly laminated within a single bed. Each bed is separated by thinly laminated fine-grain shale ranging in color from dark gray to greenish (fig. 5.1). This shale has a fissile nature. The bottom part of the bed is covered in vegetation, making it difficult to identify. The petrographic result of the thin section from this bed (sample: KS_2-b11) which were described as fine-grained, well sorted with rounded-sub-rounded, and grouped under quartz arenite based on the modal analysis of the framework grains(fig. 4.3).

Interpretation: the presence fine to medium grain sandstone with interbedded shale indicates a mixed lode-dominated low-energy depositional regime. The fine-grain sandstone and shale interbred with a fining upward cycle is interpreted to represent an overbank and crevasse play deposit (Dawit Lebenie 2010).

Figure 5. 1 Thinly bedded sandstone

Where (A) shows the whole unit exposure, (B) shows the intercalated shale, and (C) shows the upper white color sandstone subbed and lower reddish sandstone subbed within the thinly bedded sandstone bed.

5.2.2 Massive bed sandstone facies (facies 2)

Description: This bed is overlaying by the shale layer and overlays in the thinly bedded sandstone and has a maximum thickness of 15m. Texturally, it is medium to coarse grain, rounded to subrounded grain, moderately to well sorted, and reddish-brownish to light gray. This bed has a massively bedded upper section and a horizontally laminated bottom section (fig 5.2 A).

5.2.3 Shale facies (facies 3)

The fine-grained shale layer lies above massive to laminated sandstone and overlaying by massively bedded sandstone. It is 0.5m thick and ranges in color from light gray to dark gray (fig5.2 B).

5.2.4 Massive bedded sandstone facies (facies 4)

Description: This facies is overlaid by poorly consolidated sandstone facies and overlays on the shale facies and has a thickness of up to 20m. It is composed of medium to coarse grain sands with upward fining, moderately sorted with rounded to sub-rounded grains, high grain sphericity, reddish to light grey, purple color, with some scattered pebbles. Fine conglomerate lenses are prominent features of this bed (Fig. 5.2 C). The petrographic result of the thin section from this facies (sample: KS_2-b8) which were described as it is fine-coarse grain, rounded-subrounded with poorly sorted and it is categorized under sublitharenite (fig.4.3), compositionally matured, and texturally immature.

Interpretation: The characteristics including laminated to massive bedding bottom, the middle shale layer, and massive bedded sandstone with medium-coarse sand size, rounded-subrounded, well-moderately sorting are indicative of the fluctuation of energy. The presence of the shale layer indicates a low-energy environment with reduced water movement. The presence of a minor amount of scattered pebbles with coarse to medium-grained sandstone and the massive sandstone indicates the energy is changed to a high-energy bed load-dominated depositional regime. The absence of sedimentary structure and reddish to reddish brown color is a typical feature of alluvial fan deposits, and the presence of fine conglomerate lens common in high-energy environments such as river canals (Ahmed Wolela, 2008).

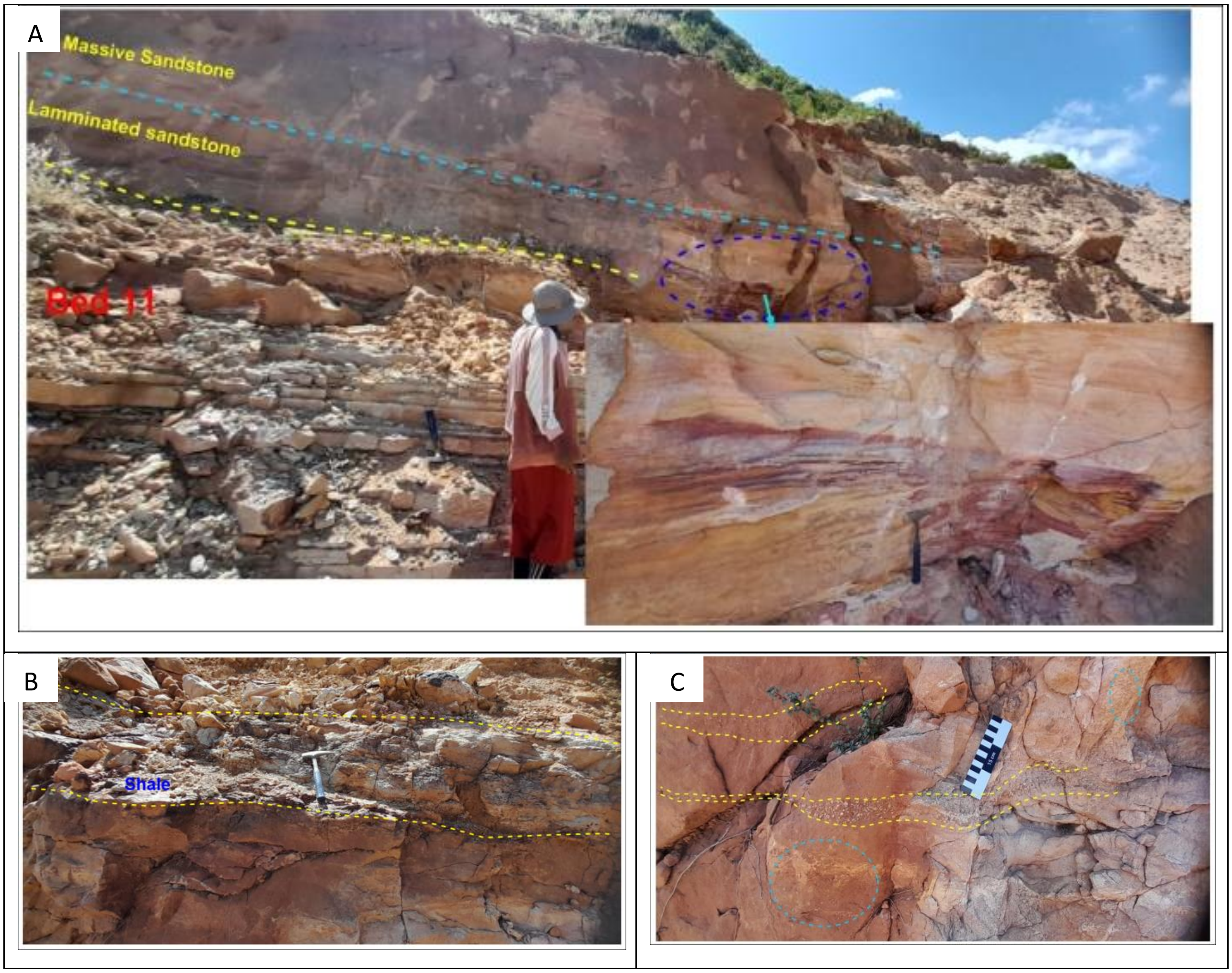

Figure 5. 2 A) The massive-laminated sandstone where the bottom part of the bed is laminated whereas the upper part is massive (the cyan broken line is the boundary). B) Shale layer in between the massive bedded sandstone and massive-laminated sandstone (indicated by yellow broken lines). C) The massive bedded sandstone where the yellowish broken line indicates lenticular bedding and the cyan circle shows bioturbation.

5.2.5 Poorly consolidated fine grain sandstone facies (facies 5)

Description: This is found below wavy bedding sandstone facies and above massive bedded sandstone facies and has a thickness of up to 5m. It is made of fine-grained sand with a light gray color and a friable texture. Conglomerate lenses and laminated strictures are present (fig.5.3).

Interpretation: the presence of laminated structure and fine-grained sand indicates deposited in reduced flow (Tucker 2001).

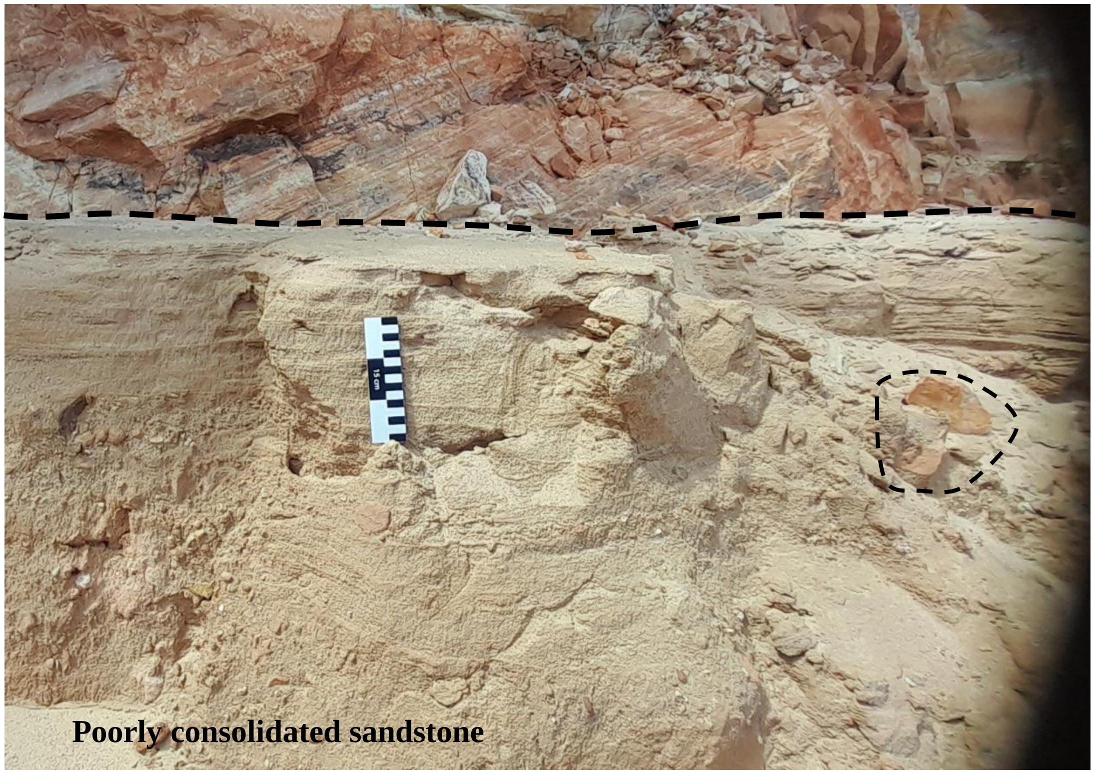

Figure 5. 3 Loosely-consolidated sandstone with very thin lamination, the black circles show the cobble size.

5.2.6 Wavy laminated fine to medium grain sandstone facies (facies 6)

Description: this facies overlay on the poorly consolidated sandstone facies with a maximum thickness of 5m. The grain morphology is fine to medium, well-sorted, and rounded. The color ranges from reddish brown to light gray. The bed's top is made of 0.1m thick shale with very fine grain and a light grey color. This bed commonly has thinly wavy with convolute bedding structure. Petrographically in this facies (sample KS_2-b6) shows texturally and compositionally immature to mature and classification under Litharenite (fig. 4.3).

Interpretation: the wavy laminated sandstone with a medium to fine grain texture and reddish to brownish color is typically associated with fluvial deposits and the textural and compositional immature to mature is also evidence of fluvial deposits (Tucker 2001).

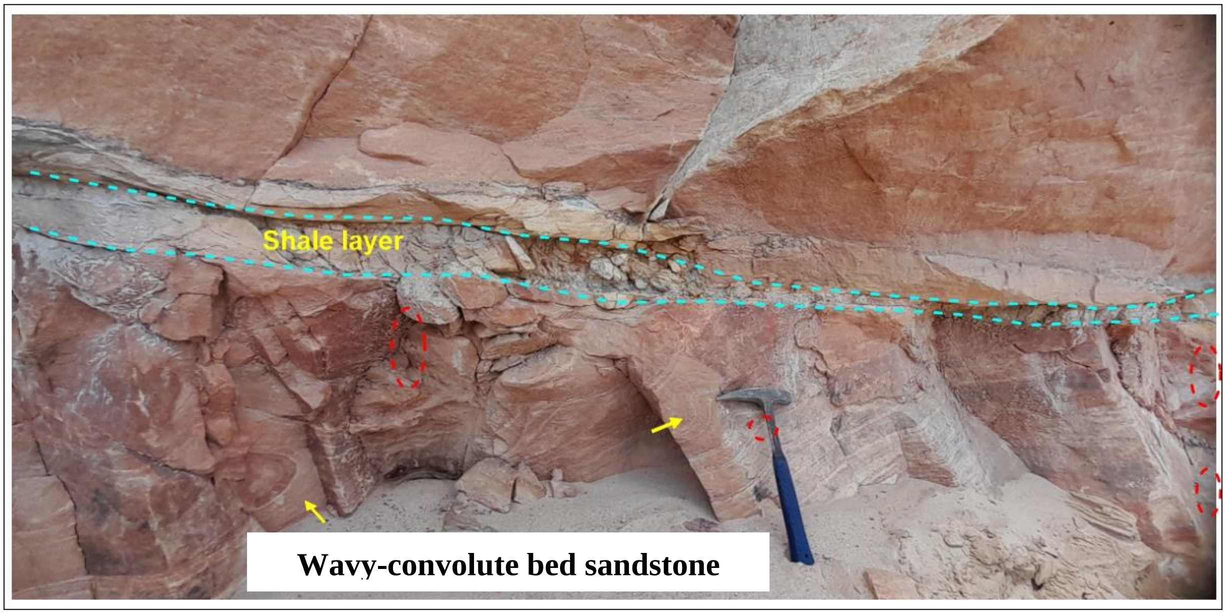

Figure 5. 4 Wavy laminated sandstone which is the bottom part, between the cross-bedding and the wavy bedding there is a very thin laminated shale layer
The yellowish arrow indicates convolute bedding.

5.2.7 Cross-bedded sandstone facies (facies 7)

Description: This facies is overlays on the wavy bedding sandstone facies and has a maximum thickness of 10m. Texturally, it consists of medium to coarse grain, moderately to well sorted, rounded to sub-rounded grain. It ranges from reddish brown to light gray. This facies is primarily composed of quartz on a hand spaceman scale. It has planar cross-beddings with the cross-beds in tangential contact with the lower bounding surface. The bottom of this facies has relatively low angle planer cross bed sandstone. Despite being separated by reactivation surfaces, these cross-bed sets no lithological or grain size differences between the foresets of this sand bed form or within the cross-bed set(fig 5.5). Petrographically this facies (sample KS_2-b5) shows texturally, medium-coarse grain with moderately to very good sorting and classification under Subarkose.

Interpretation: the presence of planar across-bedded to medium-coarse-grained sandstone facies is typically considered to be the coarser deposit of point bare facies. Planar to very low angle cross-bedded sandstone are interpreted as upper flow regime sand flat deposit Dawit Lebenie (2010). The cross bed set has the same orientation suggesting a consistent flow direction during the deposition of the sediment. The reactivation surface indicates fluctuating flow velocities, which causes erosion of the underlying bedform during low water flow stages. These surfaces are preserved by burial through the deposition of sediment during the high flow stage, which reactivates the deposition on the lee side.

Figure 5. 5 The cross-bedding sandstone has three sets the top and the bottom part is low angle relative to the middle part, the orientation one directional.

5.2.8 Laminated sandstone facies (facies 8)

Description: This bed is located above cross-bedded sandstone and it is 10m thick. Texturally, it is made up of medium to coarse-grained sand with reddish to whitish color, with moderate to well sorted and has rounded to sub-rounded grains with a coursing upward grading system, but small amounts of pebbles are randomly distributed throughout the bed. The sedimentary structures found in this bed are laminated and unidirectional cross-bedding. This bed has high quartz content on the hand spaceman scale. At the bottom of this bed, there is a shale layer that is fine-grained and gray (fig 5.6). This shale layer has a maximum thickness of 0.5m and disappears as you go north. The petrographic result of the thin section from this bed (sample: KS_2-b4) was described as fine-grained, well-sorted with well-rounded to sub-rounded, and grouped under Litharenite based on the modal analysis of the framework grains.

Interpretation: the presence of planar lamination indicates a quiet or low-energy environment whereas the presence of medium-coarse grain moderately to well-sorted coarsening upward grading system indicates the energy is changed to a high-energy environment (Dawit Lebenie 2010). The unidirectional small-scale cross-bedding in the upper indicates the sediment is deposited in wave action in a consistent direction and the coarsening upward grading system indicates the energy is gradually increasing.

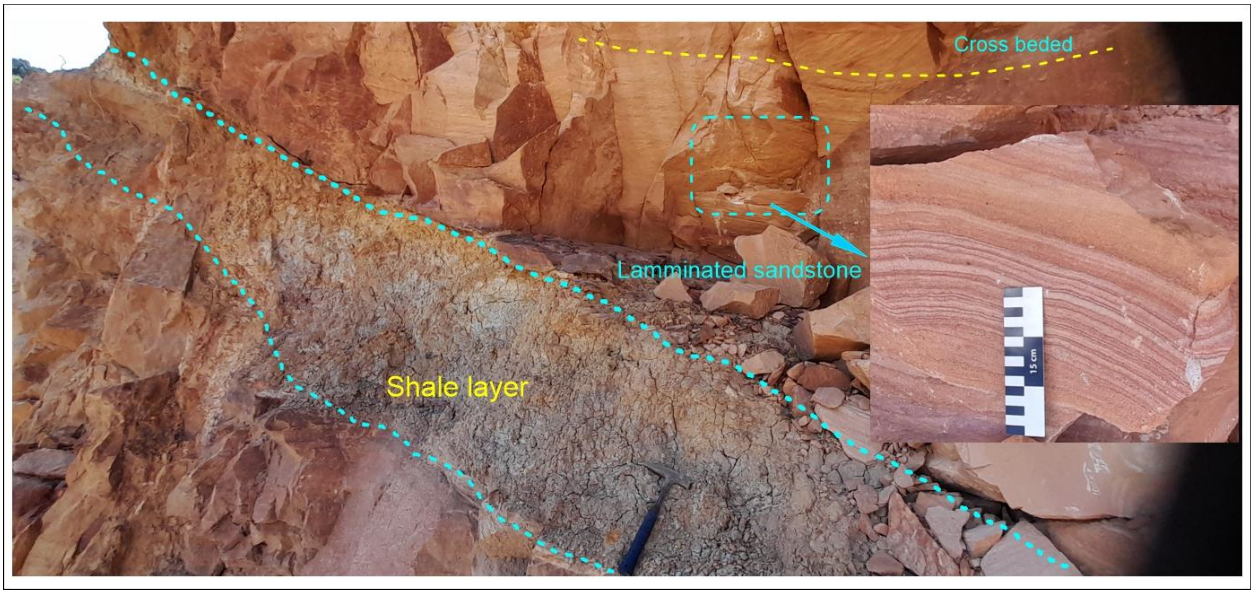

Figure 5. 6 Laminated sandstone beds, the upper part of the photo shows unidirectional cross-bedding, while the middle part shows lamination.
At the bottom, there is a shale layer that disappears as you move northward.

5.2.9 Massive bed sandstone facies (facies 9)

Description: The facies overlies on the thinly bedded sandstone facies and has a thickness of up to 15 meters. It is composed of coarse-very coarse randomly distributed sand grain, moderately-poorly sorted with rounded to sub-rounded grains, and high grain sphericity, the upper part of the bed is reddish, and the lower part is whitish. There is no observed sedimentary structure, indicating that the bed is structure less (fig.5.7A). The hand spacemen level is dominated by quartz. The petrographic result of the thin section from this bed (sample: KS_2-b3A and KS_2-b3B) was described as fine-grained, well-sorted with well-rounded to sub-rounded, and grouped under Subarkose based on the modal analysis of the framework grains

5.2.10 Massively to thinly bedded sandstone facies (facies 10)

Description: the facies have a thickness of up to 30m and are found above the massive bedded sandstone. It is texturally composed of medium to coarse grain sands with fining upwards, moderately sorted with rounded to sub-rounded grains, and reddish to whitish color. This bed also has randomly distributed pebbles at the middle. The sedimentary structure observed from this bed is massive at the top, with lenses of coarse sand in the middle and thinly laminated at the bottom (fig, 5.7B). The petrographic result of the thin section from this bed (sample: KS_2-b2A and KS_2-b2B) which were described as medium-coarse grained, poorly sorted with rounded-sub-rounded, and grouped under Subarkose based on the modal analysis of the framework grains(fig. 4.3).

Interpretation: the thinly laminated bottom portion suggests quieter, lower energy conditions. The randomly distributed pebbles with the lenses of coarse sand in the middle, the medium-coarse grain with coursing upward sequence, and massive bed sandstone in the upper part indicate the energy changed to a high bed load-dominated depositional regime.

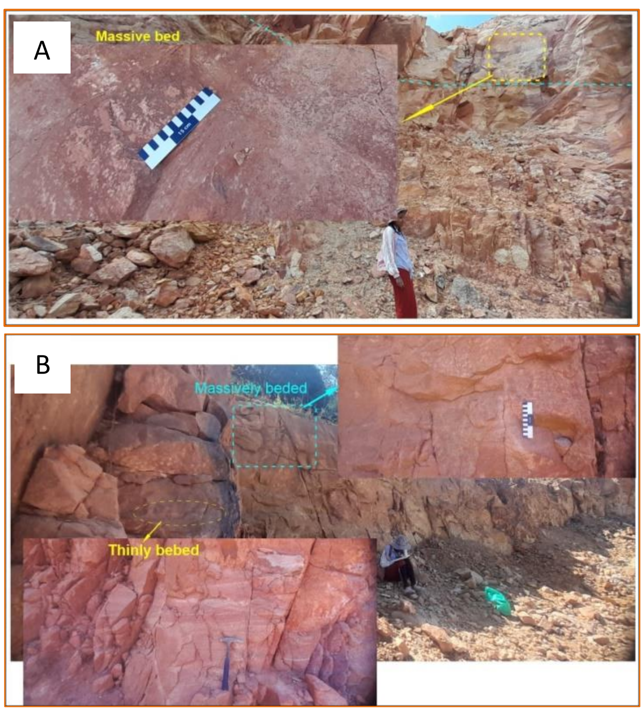

Figure 5. 7 Massive and massive to thinly bedded sandstone
A) Massive sandstone, the upper part of the photo displays sandstone with a massively bedded and random distribution of pebbles. B) Massive to thinly bedded sandstone, the upper part is a massive bed, while the lower part is thinly bedded. The structure seen in the image, resembling a joint or fracture, Is not a natural occurrence. It is man-made, as the area is an active quarry site

5.2.11 Wavy laminated to massive bedded sandstone facies (facies 11)

Description: The exposure is found at the top of the quarry site, where the cliff is forming, and the majority of it is covered in vegetation with a thickness of up to 35m. The bed is conformably overlying by the mudstone unit and is made up of medium-coarse-grained sandstone with randomly distributed quartz pebbles, which fins upwards into medium-fine grained sandstone with small fine conglomerate lenses sediment. These pebbles are rounded to sub-rounded, have a light color, and range in size from millimeters to centimeters. Moderately to poorly sorted, with rounded to subrounded grains and a whitish to reddish color. The sedimentary structure observed in this bed is thinly wavy laminated, unidirectional cross-bedded, and lenses of conglomerate at the upper part (fig5.8). Bioturbations and body fossils are absent. The petrographic result of the thin section from this bed (sample: KS_2-b1) which were described as coarse grain, poorly sorted with rounded-sub-rounded, and grouped under Subarkose based on the modal analysis of the framework grains(fig. 4.3).

Interpretation: the presence of coarse grain size, with a small fine conglomerate lens, and randomly distributed pebbles indicates formed in a high energy environment. The fine upward sequence suggests the meandering river deposits (Ahmed Wolela, 2008).

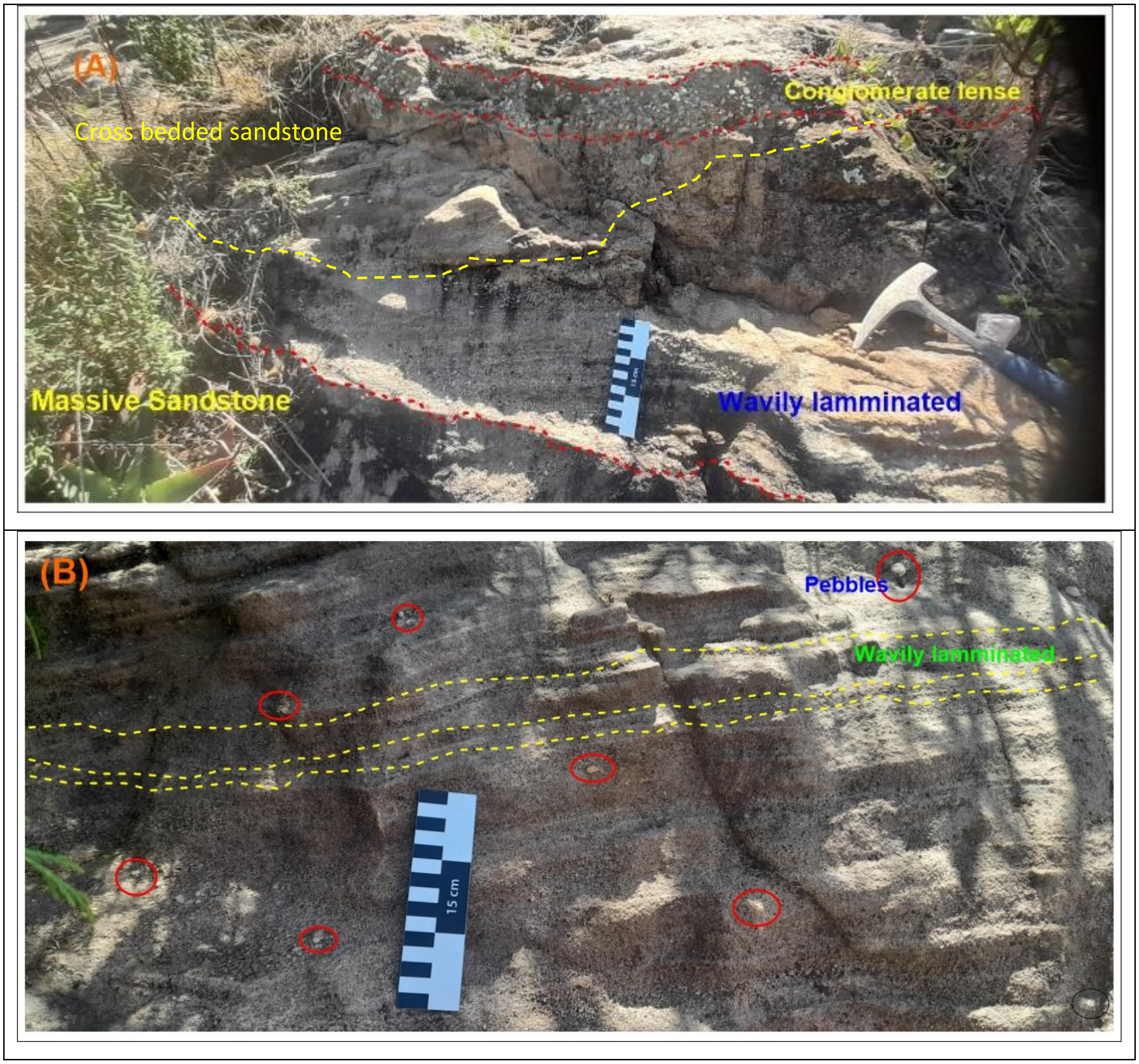

Figure 5. 8 Massive to thinly wavy bedded sandstone exposure
(A) The upper part of the image shows the conglomerate lenses. The middle part shows wave lamination and coarsening upward sequences and the lower part of the image shows a massive bed. (B) The red circle represents a random distribution of pebbles while the yellowish line depicts a thinly wavy lamination.

5.2.12 Poorly consolidated mudstone facies (Facies 12)

Description: This facies is the bottom part of the section which is 3m thick. It has a variegated color, with bioturbation (mottling), pseudofossil, and a siltstone layer. The siltstone layer is gray and measures 0.1m in thickness. The bottom section is obscured by vegetation, which makes identification challenging.

5.2.3 Shale intercalated mudstone facies (facies 13)

Description: This facies overlay the poorly consolidated mudstone facies and overlaying by silty-sand mudstone facies, and it has a thickness of up to 4m. This bed is composed of very fine Siliciclastic sediments. It is characterized by the intercalation of variegated shale, siltstone, and claystone. The interlamination between claystone, siltstone, and mudstone shows irregular to wavy lamination with fining upward bedding. The claystone wavy lamination within this bed shows a flame structure.

5.2.14 Silty-sand mudstone facies (facies 14)

Description: this facies is found between the loosely and poorly consolidated mudstone facies with a thickness of 3m and its color ranges from light gray to reddish. The layer is composed of silt-sized grains and shows a coursing upward sequence. Furthermore, it contains joints that are filled with reddish fine-grained secondary material. It shows localized slumping (fig 5.9)

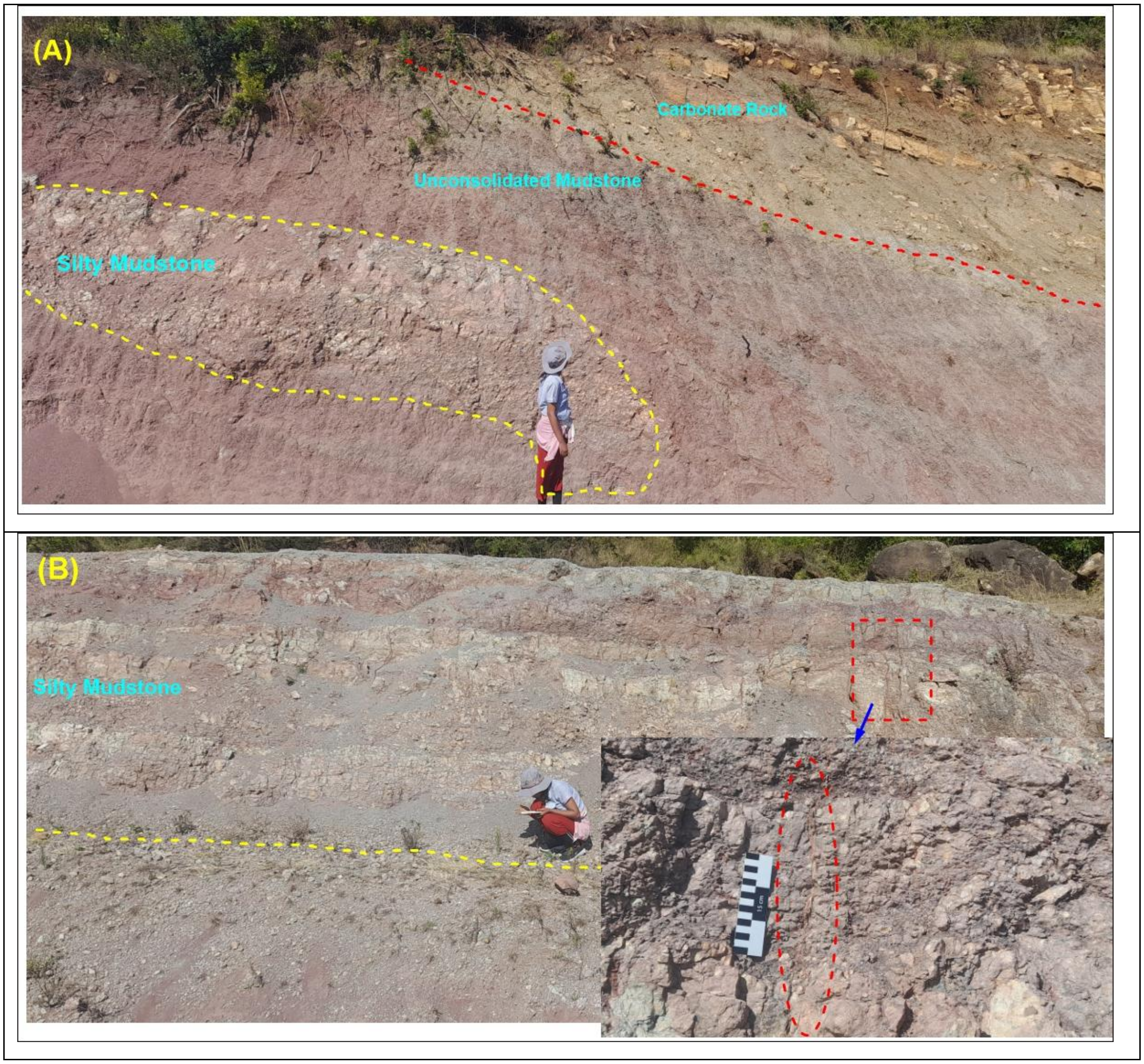

Figure 5. 9 Shows the silty mudstone
where (A) shows the contact between the silty mudstone, poorly consolidated mudstone and the carbonate unit, and (B) shows the silty mudstone exposure with a vein indicated by a red broken circle.

5.2.15 Loosely consolidated mudstone facies (facies 15)

Description: This layer is found next to the silty mudstone layer and has a thickness of up to 3m. It is made up of friable fine mud in a variety of colors, as well as clay stone, siltstone, and shale. Within this intercalation, the siltstone shows wavy and lenticular bedding s and fling upward sequence. Claystone ranges in color from reddish to gray and has a flame-like structure. The shale layer demonstrates fissility.

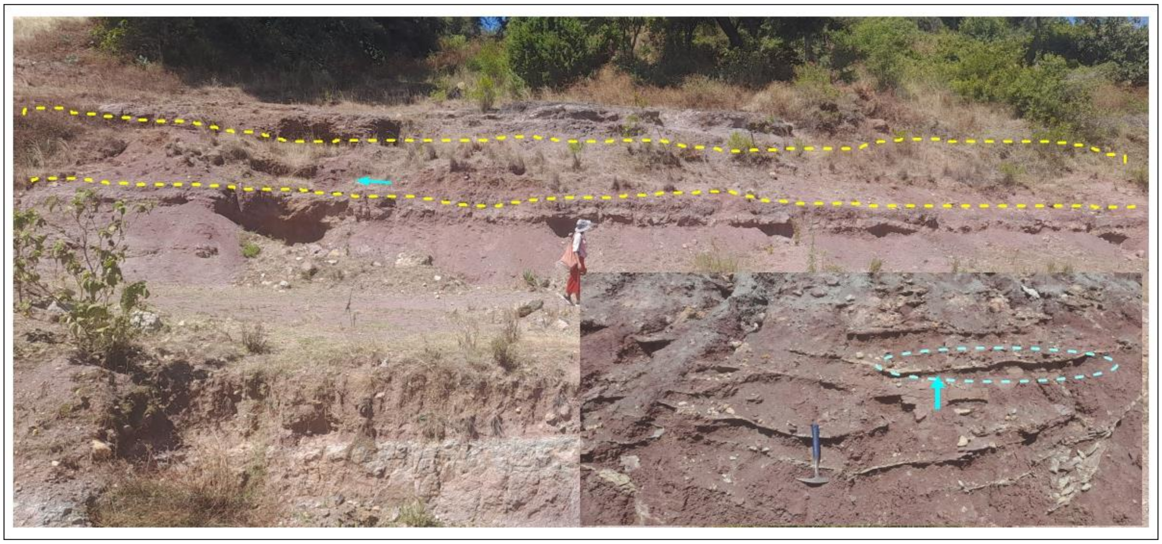

Figure 5. 10 Unconsolidated mudstone bed with wavy and lenticular bedding and fling upward sequence claystone (Indicated by the cyan broken circle and arrow).

5.2.16 Silty mudstone facies (facies 16)

Description: This is the uppermost part of the section, which is overlying by an ash-fall deposit in an unconformable manner. It has a thickness of 1m, but the thickness increases as you move north, and it shows localized slumping. It is characterized by a reddish color and is composed of fine-grained silt with a sequence that becomes coursing upwards.

Interpretation: facies (12, 13, 14, 15, and 16). The presence of loosely consolidated suggested that the sediment was primarily composed of fine-grained particles, such as clay and silt. The presence of mottling indicates the sediment was deposited with active organisms. The presence of fine gran siltstone layer typically formed in calm or low energy environments (Potter et al, 2005; Getaneh Assefa 1981). The dominancy of mudrock containing irregular lamination of silt and clay stone may indicate continental influence. In addition, flame structure and wavy lamination suggest a broad mudflat setting influenced by seasonal river floods and weak tidal currents (Potter et al, 2005). the lithology such as finer siliciclastic sediments such as silt, sandy silt, and mud types of sedimentary facies are typical characteristics of a back-barer tidal flat setting (Flamming 2012). The combination of localized slumping reddish color and fining upward sequence suggests variation in depositional energy and the fine grain silt composition suggests deposition in a low-energy environment.

5.3 Microfacies

5.3.1 Sandy Mudstone (MF 1)

Description: This contains 60-98% micrite, 2-10% fine sand size rounded to sub-rounded quartz grain, with undulose extinction and 10% calcite cement. It has a vein that is filled with calcite cement. One sample on the other limestone exposure 2 ($LS\text{-}S_1$) has high porosity (30%) (Fig. 5.10 C). This microfacies type was identified from section C (sample KS_1-b3A, KS_3-b3B) and on the other limestone exposure 2 (sample $LS\text{-}S_1$).

5.3.2 Carbonate Mudstone (MF 2)

Description: it contains a 100% non-laminated and homogenous micrite matrix, with very fine microspars or calcite crystals (Fig 5.10 D). These microfacies were identified in section D (sample KS_3-b2).

Interpretation: this type of microfacies (MF2 and MF1) are deposited in low-energy environments, which are shallow restricted intertidal areas of calm condition that have no water circulation (Flugel 1982) that radius the normal wave or current energy on shallow marine carbonate shelf. The absence of bioclast indicates deposition in near shore and tide condition is common. This microfacies corresponds to SMF-23 of Flugel (2010) and Wilson (1975) which was deposited in FZ 4 in restricted plate form area.

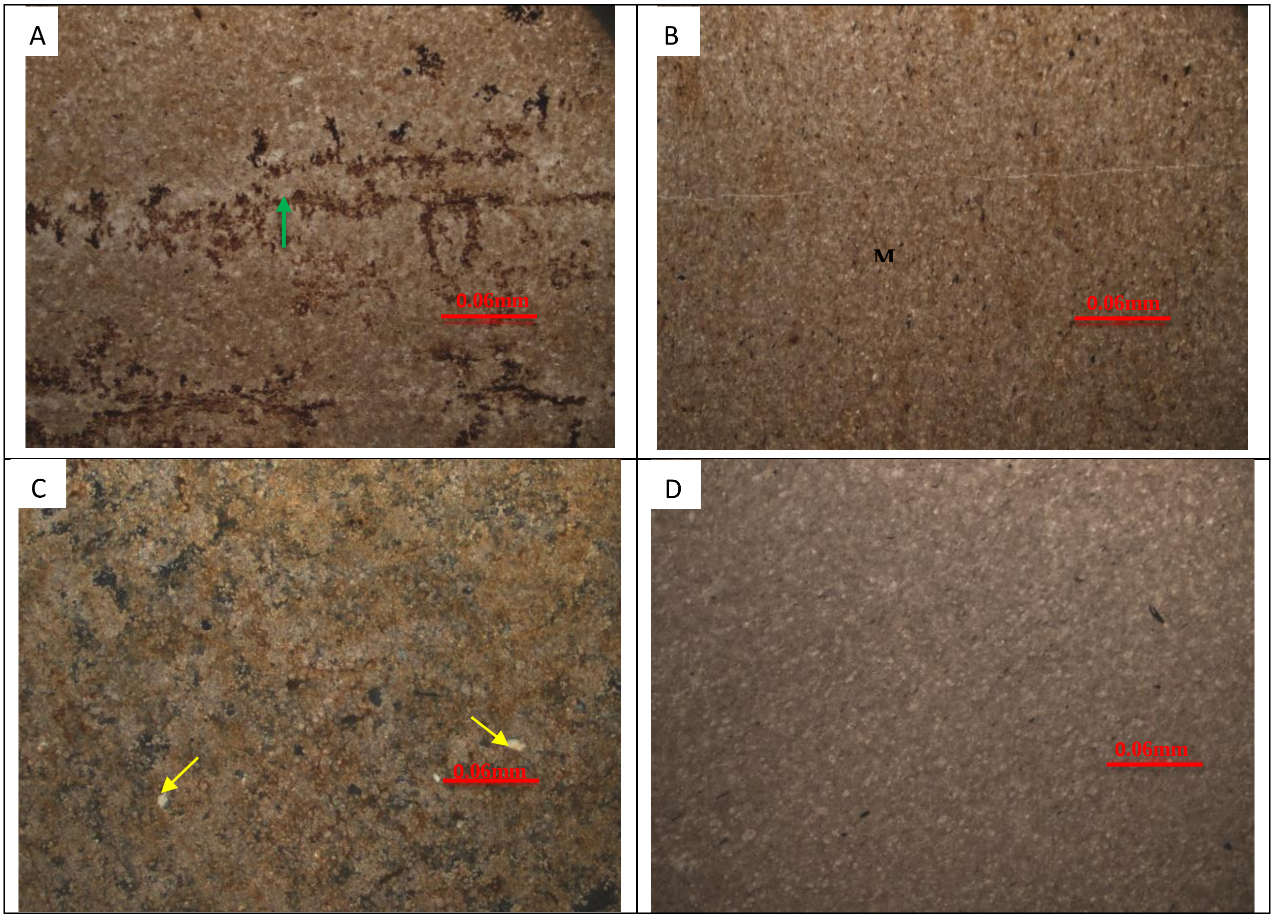

Figure 5. 11 The photomicrograph shows sandy mudstone.
A) Shows stylolite (KS_1-b3A), B) fine grain matric (KS_1-b3B), C) yellow arrow shows quartz grains (LS-s1), D) carbonate mudstone with fine grain micrite matrix (KS_3-b2). The thin section photomicrographs were taken under XPL.

5.3.3 Quartz bearing bioclastic packstone (MF 3)

Description: it contains 62-70% larger skeletal fragments of bivalve shells, echinoid spine with a variety of radial spines and gastropod shells (Fig. 5.11 A and B), 2-5% very fine sand-sized angular-subrounded quartz grains with undulose extinction, 20-30% micrite and 8% sparite, Most of the skeletal fragments are highly replaced by crystalized calcite with micritized fossils. The larger fossil fragment (0.12-1mm) is altered and crystalized with coarse, granular to blocky calcite crystals with cleavage. The grains are poorly sorted. This microfacies was identified from section C (sample KS_1-b2, KS_1-b4).

Interpretation: the presence of echinoid fragments indicates a marine environment, with normal salinity. Large skeletal bivalve shells formed in restricted platforms tidal flats and open platforms. This microfacies represents SMF 12 deposited in FZ 7and FZ 8(Flugel, 2004, 2010)

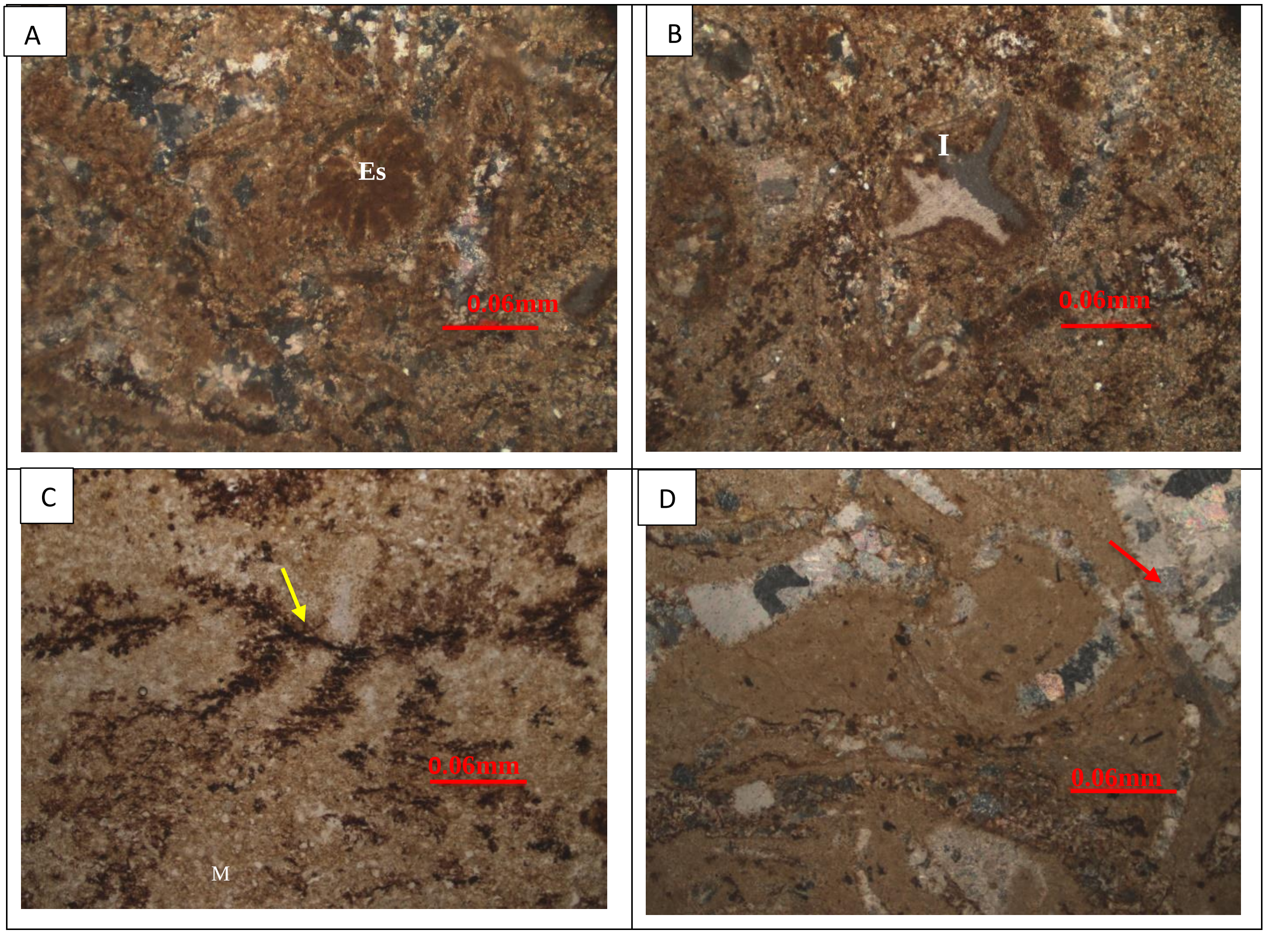

Figure 5. 12 Bioclastic Packstone microfacies
A) Echinoid spin with radial spins B) intraclast with recrystallization of calcite on the surface KS_1-b2. C) (sample KS_1-b4), D) The recrystallized bivalve shell (red arrow) and the thin section photomicrograph were taken under XPL, A, B, C D; ES =Echinoid spin, I= intraclast, M= micrite.

5.3.4 Coated biosparite grainstone (MF4)

Descriptions: It contains 62% of skeletal shell fragments of gastropod, brachiopod fragments, fibrous wall structure with pseidopunicat sectioned parallel to their length, with 35% fine to coarse calcite cement and fine-medium sand-sized quartz grain with undulose extinction (3%) (Fig5.11). Most of the shell fragments have micrite envelop or biogenic incrustation. Some recrystallized shell fragments are challenging for identification. This Microfacies was identified from section C (Sample KS_1-b 5).

5.3.5 Packstone mudstone (MF 5)

Description: It contains 60% coarse skeletal fragments of bivalves, gastropods, and brachiopods. Most of the skeletal fragments are recrystallized bivalve shells and some grains are coated and micritized, 35% of micrite without grain in one field of view, which is an interlocking mosaic of micro-sized equal calcite crystals and 5% of sparite. This microfacies is identified from section C (Sample KS_1-b6).

Interpretation: Coated biosparite grainstone (MF4) and packstone mudstone microfacies (MF5) represent SMF 11 which indicates shallow waters sand shoal depositional setting. The presence of large bivalves and gastropod shells with light color lithofacies and a significant amount of quartz grain also indicates in inner ramp sand shoal environment FZ 6 (Wilson, 1975; Flugel, 2004).

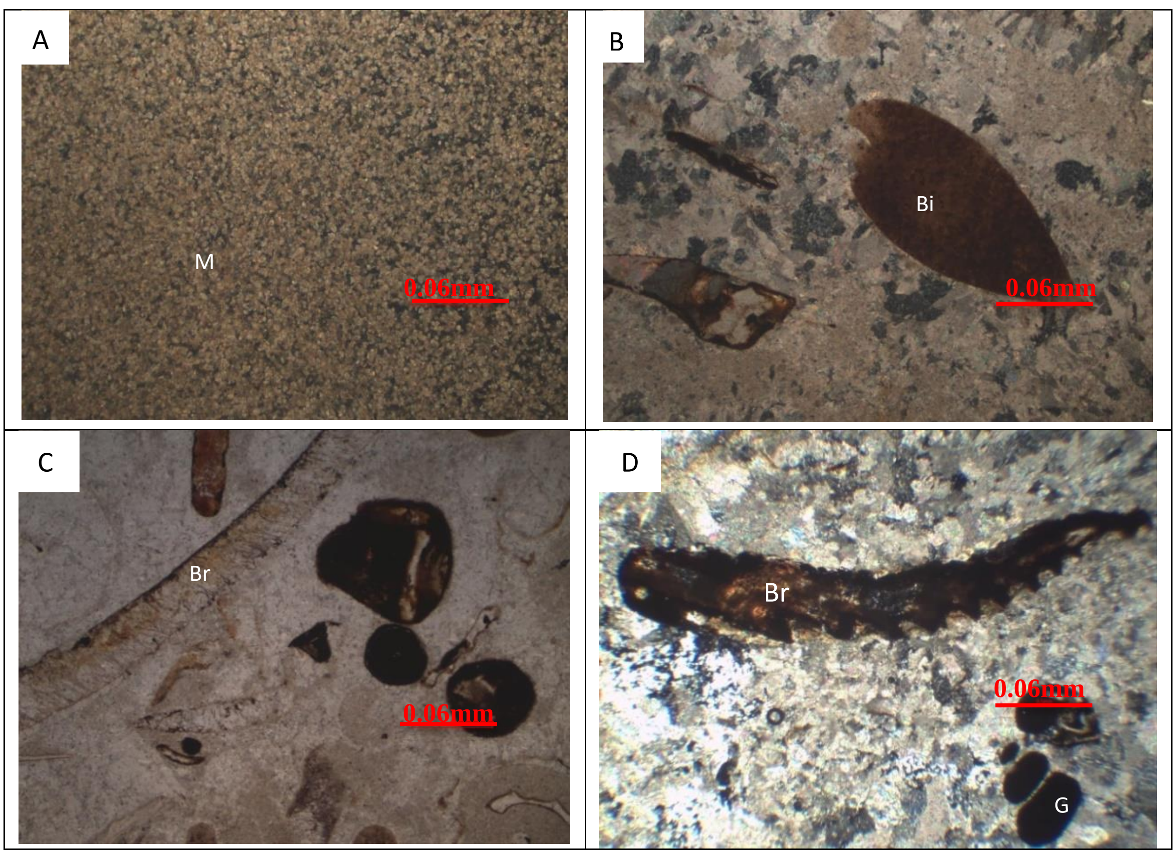

Figure 5. 13 The photomicrograph shows Packstone mudstone (KS_1 –b6) and biosparite grainstone (KS_1-b5) microfacies.
A) Some part of the thin section without grain only matrix B the bivalve grin with Sparite cement, C) the brachiopod skeletal grain and other dark grains , D) (KS_1-b5),the thin section photomicrographs were taken under XPL A&B; PPL C &D: G=gastropod, Bi= bivalves, Br= brachiopod, and M= micrite matrix

5.3.6 Oopelbiosparmicrite packstone (MF 6)

Description: it is coarse-grained facies, comprising 20-40 % bioclast which contains spongy, gastropoda, alga shell fragments, 5-15% Ooids which consist of nuclei and Oncoids with concentric layers, 5-20% peloids, 30-37% micrite, and 5-15% of sparite with porosity (5%) (Fig.5.15). These microfacies were identified from section C (sample KS_1-b7) and section D (sample KS_3-b8, KS_3-b13).

5.3.7 Daysclad grainstone (MF 7)

Description: It is coarse-grained, poorly sorted mud-free (micrite) facies, contains75% shell fragments of bivalve, gastropods, daysclad green algae, 2 % Peloids, and 20% of drusy calcite cement, filling the inter-granular pore spaces. These microfacies were identified from section C (sample KS_1-b8A) and section D (sample KS_3-b15).

Interpretation: dysclad green algae cortoids and Peloids, occur in restricted shallow water, open plate form, and inner ramp above the wave water base. Daysclad green algae prefer muddy and sandy substrates of the marine environment which are abundant, mainly in relatively shallow, protected lagoonal environments with depths ranging from several tens of meters (Damenu Adefirs, 2022 and referenced therein). Oopelbiosparmicrite Packstone (MF 6) and Daysclad Grainstone (MF 7) microfacies represent SMF18 and (FZ7 and FZ 8) (Flugel, 2004).

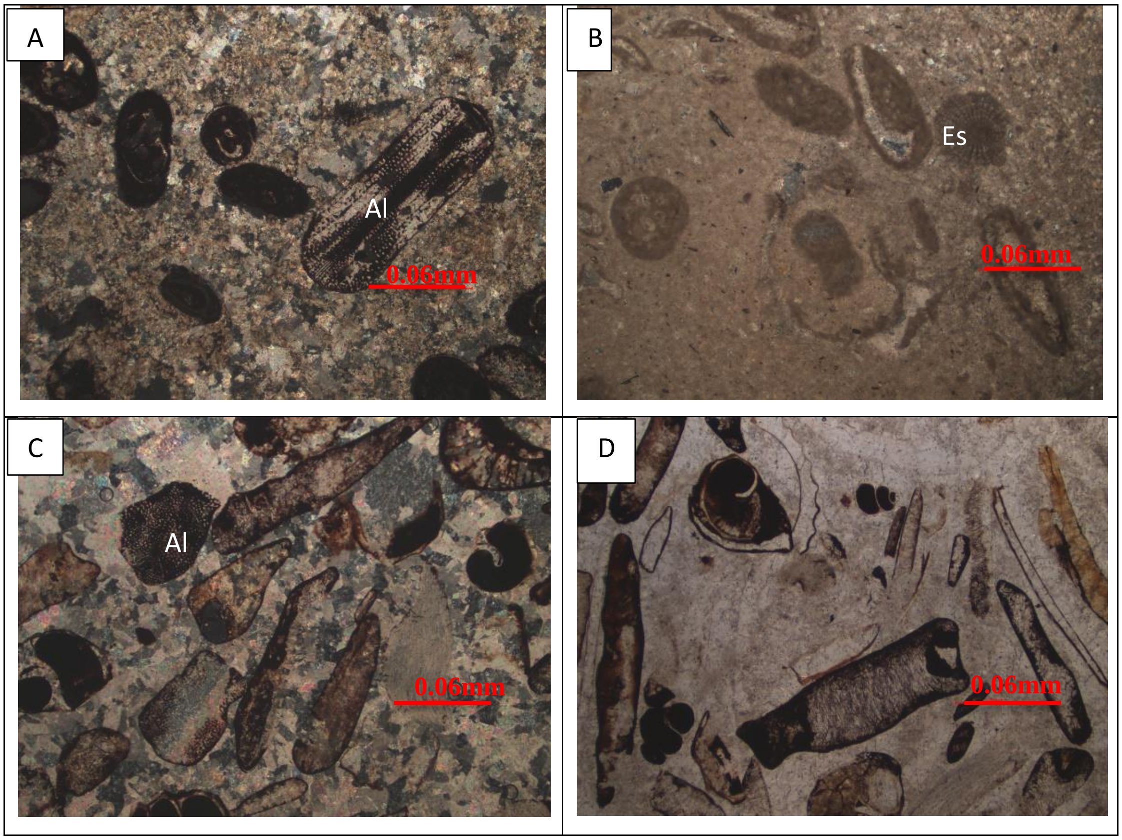

Figure 5. 14 The thin section photomicrographs were taken under XPL A, C; PPL B
Where, A&B (KS_1-b7) c &d (KS_3-b8) the thin section photomicrograph were taken under XPL A, B, C, and D. Al= Algie, Es= Echinoids

5.3.9 Biomicrite packstone (MF8)

Description: This microfacies consists of about 55-80% skeletal fragments of bivalve (1.5-2.3mm) and gastropods shells range from (0.5-2.8mm), 18-30% micrite, 10% of blocky calcite crystal cement, characterized by cleavage and 2-5% porosity. Most of the shell fragments are micritized and some recrystallized. These microfacies were identified from section D (sample KS_3-b4 and KS_3-b6).

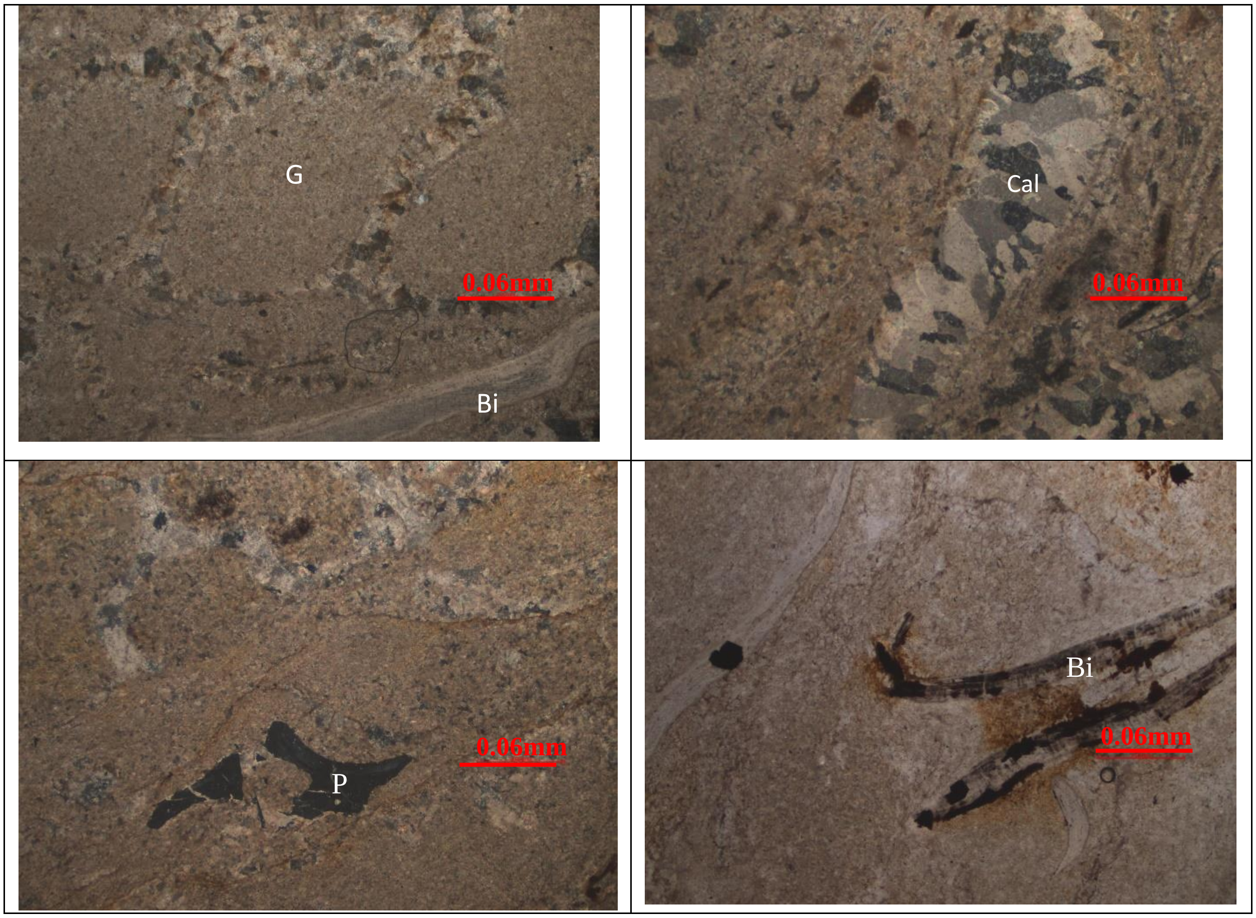

Figure 5.15 Biomicrite packstone. A(KS_3-b6) B(KS_3-b6) C(KS3-b4) D (KS_3-b4)The thin section photomicrograph was taken under XPL B, C; PPL A, D. Ga= Gastropod, Bi =Bivalve, Cal= Calcite, P =porosity

5.3.10 Bioclastic wackestone (MF9)

Description: these facies contains a 60% micrite matrix, with 20% randomly distributed large skeletal fragments of gastropods and brachiopods and 20% porosity and bioturbation. The brachiopods shell fragments are characterized by fine fibrous structures. This was identified from section D (sample KS_3-b10, KS_3-b17).

Interpretation: the coated and micritized coarse skeletal grains come from the inner-ramp shoal environment to the outer ramp setting, due to sea-wared offshore storm surge deposits (Flugel, 2010). The biomicrite packstone (MF 8) and bioclastic wackestone (MF9) microfacies represent SMF 12 and FZ 4 (Tucker and Wright 1990, Flugel 2004), which is the result of the re-deposition of allochthonous skeletal grain in the outer-ramp setting.

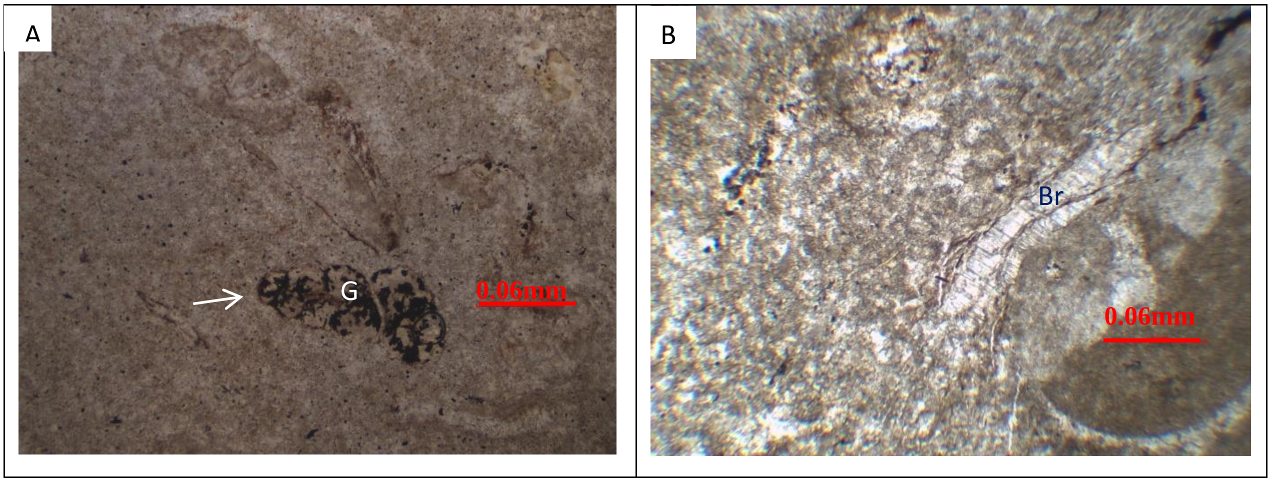

Figure 5. 16 Bioclastic wackestone facies, A) gastropods, B) brachiopods shell fragment with a fine fibrous structure. G gastropod

5.3.8 Biomicrite wackestone (MF10)

Description: it is made up of 40% micrite matrices, 30% recrystallized bivalve skeletal fragments, and 10% fine-medium sand-sized rounded-subrounded quartzes with undolusite extinction and 20% of calcite cement (Fig. 5.18 A&B.). This microfacies was identified from section C (Sample KS_1-b8B).

5.3.11 Bioclastic mudstone (MF11)

Description: this facies contains 60% micrite, with 5% bioclast, 25% fine grain sand-sized quartz grain with angular to sub-angular shape crystals and 10% opaque crystals. These microfacies were identified from section D (sample KS_3-b11).

Interpretation: the presence of a high percentage of quartz grain indicates shallow water, high energy, and intertidal environment (Damenu Adefris et al 2022).

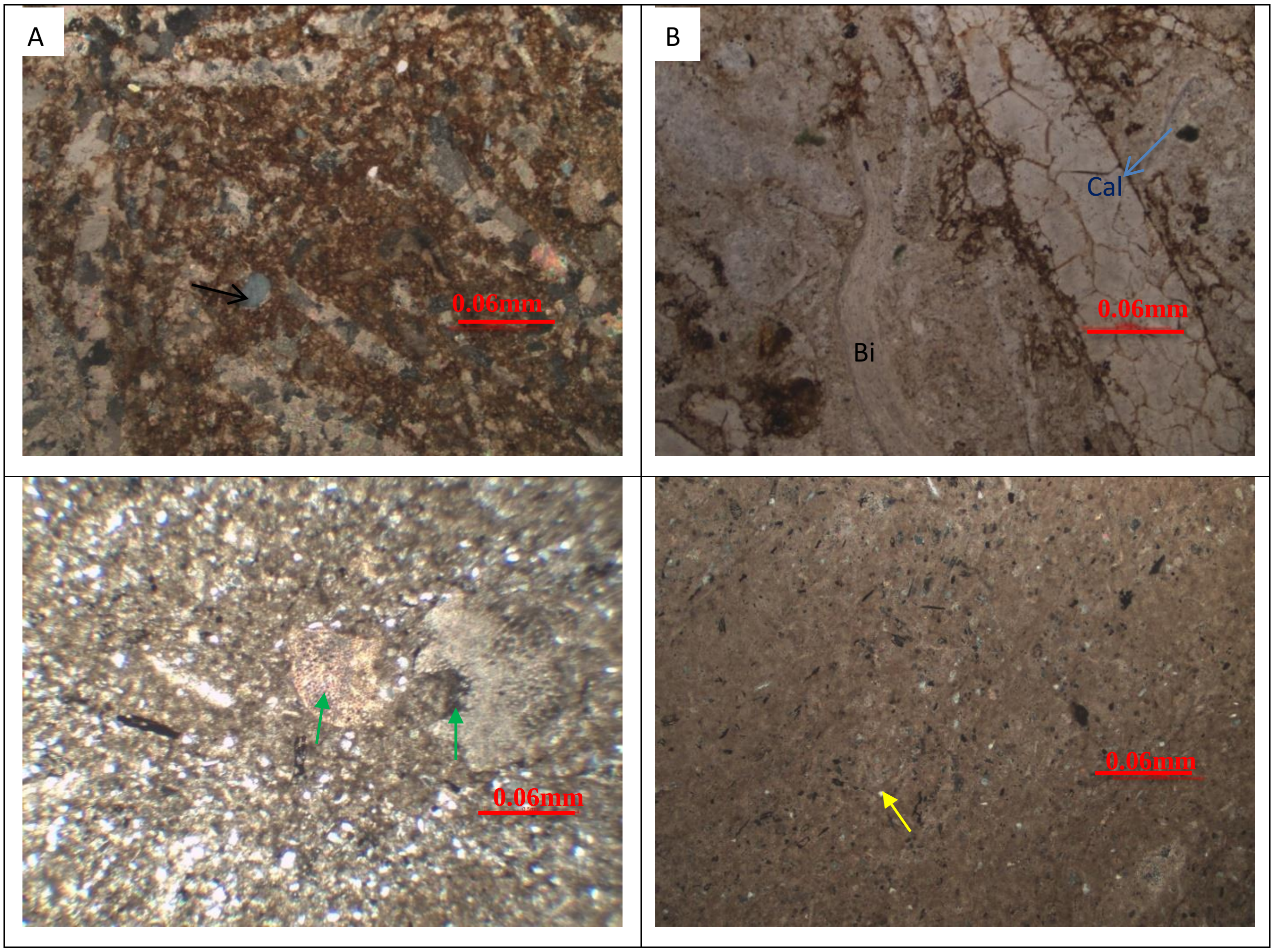

Figure 5. 17 The photo micrograph shows biomicrite wackestone facies.
A) The black arrow indicates the quartz grain with undulose extinction (KS_1-b8B). B) The bivalve shale fragments and the blue arrow indicate recrystallized skeletal fragments (KS_1-b8B). C and D represent bioclastic mudstone facies (sample KS3-b11) the yellowish arrow indicates the quartz grain (D). The thin section photomicrographs were taken under XPL A &D; and PPL B&C.

5.3.12 Radiolarian wackestone (MF12)

Description: This micro facies comprises 25% pelagic microfossils, dominantly radiolaria, with spherical-discoidal test (0.06-0.1 mm), pelagic bivalves (0.1-0.5mm) and sponge spicules (0.3-0.7mm), within about 75% micrite matrix. It was identified from a sample (KS-$Ls_{2)}$) on the other limestone exposure 3.

Interpretation: the abundant radiolaria and sponge spicules fossil, within the pelagic matrix, indicates a deep marine environment (Flugel, 2004). In this setting, the water is clear and calm with very little agitation. Radiolarian and sponge spicules microfossils are excellent indicators of normal marine salinity (Flugel, 1982, 2004). Therefore, these microfacies (MF12) indicate a deep basinal depositional environment (FZ1B), representing SMF3 (Wilson 1975).

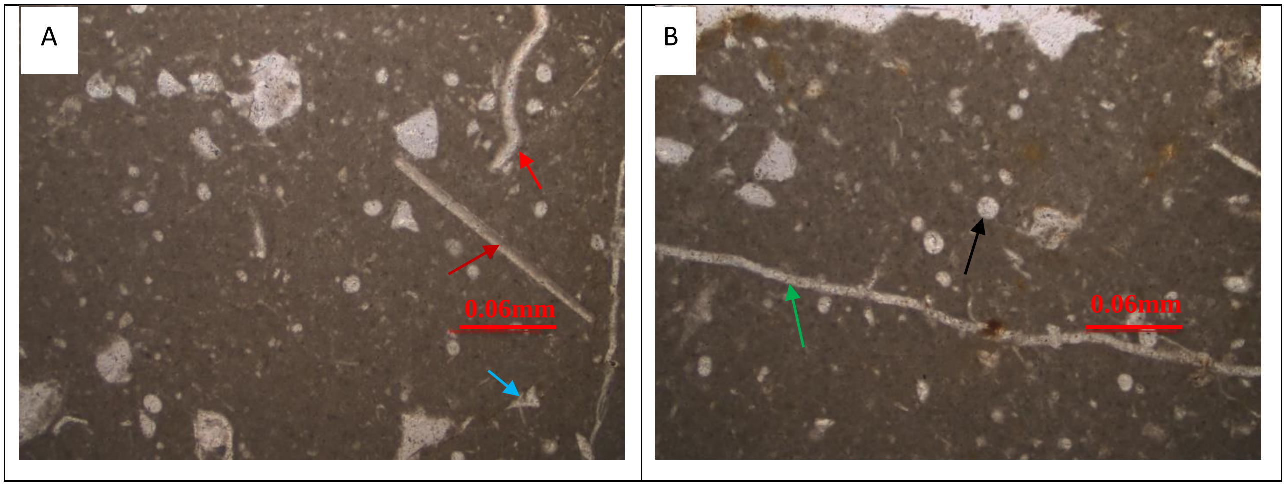

Figure 5. 18 Radiolarian rich facies

Where, A) the red arrow indicates pelagic bivalve shell fragment and the light blue arrow indicates sponge spicules. B) The light green arrow shows calcite vein and the black arrow shows radiolarian

CHAPTER SIX

DISCUSSION

6.1 Introduction

Based on field investigation and laboratory analysis of 31 thin section samples has been determined that the characteristics and depositional environments of the pre-volcanic sedimentary units in the Kella area. The siliciclastic sedimentary unit which has cliff-forming, quarry site, and road-cut exposure with consolidated to a semi-consolidated unit is observed. Although there is color variation in the siliciclastic unit in the studded section, the dominant color is red, which is caused by the presence of oxide. Additionally, there is also a presence of white to whitish-gray color in the section indicating a lower amount of oxide as cementing material. During the investigation, various lithofacies types were identified that provide evidence for interpreting the depositional environment. The petrographic analysis revealed that the sandstone unit is predominantly composed of quartz minerals.

The carbonate units predominantly consist of limestone with some marl and shall intercalation. The carbonate successions exhibit different distributions of skeletal and non-skeletal allochems, which are embedded within microcrystalline (micrite) and /or spray calcite cement. The range of microfacies within the carbonate succession extends from mudstone to grainstone/packstone.

6.2 Facies association and depositional environment

A depositional environment is a specific geographical area where sediment is deposited. These environments can be understood and categorized through facies analysis (Flugel 1982). A facies association is a combination of different facies types that plays a crucial role in interpreting the environment of sedimentary rocks. It involves interpreting the environment of a rock formation based on its specific characteristics and features, such as sedimentary structure, texture, lithological association, and fossils. The variation in facies succession, both horizontally and vertically, along with distinct lithological and paleontological features, reflect changes in the depositional environment. Walters's law (1894) states that the condition of deposition can shift laterally, indicating the overlapping of laterally related environments.

6.2.1 Facies association of siliciclastic sedimentary rock

The siliciclastic sedimentary unit (the sandstone unit and mudstone unit) in the Kella section after conducting a detailed filed investigation divided into sixteen (16) litho facies types based on sedimentary structure, texture, and sedimentological features. The identified lithofacies from this study include thinly bedded sandstone facies (F1), massive to laminated sandstone facies (F2), shale facies (F3), massively bedded sandstone facies (F4), poorly consolidated sandstone facies (F5), wavy laminated medium grain sandstone facies (F6), cross-bedded sandstone facies (F7), laminated sandstone facies (F8), massively bedded sandstone facies (F9), massive-thinly bedded sandstone facies (F10), thinly wavy laminated to massively bedded sandstone facies (F11), poorly consolidated mudstone facies (F12), shale intercalated mudstone facies (F13), silty-sand mudstone facies (F14), loosely consolidated mudstone facies (F15) and silty mudstone facies (F16). The identified lithofacies types are classified into three generalized facies associations, which include floodplain deposit, meandering river deposit, and peritidal deposits.

6.2.1.1 Floodplain deposit

This facies association comprises thinly bedded sandstone facies (F1), massive to laminated sandstone facies (F2), shale facies (F3), massively bedded sandstone facies (F4), and poorly consolidated sandstone facies (F5). The presence of intercalation of fine-grain sediments, the fine-grain sandstone and shale interbred with a fining upward cycle is interpreted to represent an overbank and crevasse play deposit. The presence of fine horizontally continuous to discontinuous lamination represents episodic suspension in terrigenous sediment supply and a variegated color can be the result of mixing of sediments of different colors (Ahmed Wolela, 2008 and Dawit Lebenie, 2010). The overall characteristics of these facies association are indicators of the floodplain deposits.

6.2.1.2 Meandering river deposit

Wavy laminated medium grain sandstone facies (F6), cross-bedded sandstone facies (F7), laminated sandstone facies (F8), massively bedded sandstone facies (F9), massive-thinly bedded sandstone facies (F10), thinly wavy laminated to massively bedded sandstone facies (F11) are grouped under this facies association. The wavy-convolute bed in the bottom, the planar cross-bedded in the middle, and the top shale layer with a fining upward sequence indicate the point bare deposits. A combination of cyclic sedimentation and fining upward sequence, bed load and suspension load deposits of channel and point bar, were an indicator of a meandering river deposit (Dawit Lebenie, 2010). The main reason for the upward fining and decrease in the scale of sedimentary structures within individual cycles can be best explained by a channel environment. During the period of lower flow or reduced sediment transport, fine-grained sediments settle.

6.2.1.3 Peritidal environment

The poorly consolidated mudstone facies (F12), shale mudstone facies (F 13), silty-sand mudstone facies (F14), loosely consolidated mudstone facies (F15), and silty mudstone facies (F16) grouped under this facies association. . As evidenced by field observation, the dominancy of mudrock contains irregular lamination of silt and clay stone, wavy lamination, and coarsening upward suggesting the presence of a tidal process. Mud deposition in a coastal environment can occur in areas that are protected from destructive waves and strong coastal currents). Finer siliciclastic sediments such as silt, sandy silt, and mud types of sedimentary facies are typical characteristics of a back-barer tidal flat setting (Flamming, 2012 and Potter et al, 2005). Getaneh Assefa (1981) interpreted the predominance of very fine sediment as evidenced by deposition in a low-energy environment in restricted lagoons or coastal lakes.

6.2.2 Microfacies association

Microfacies type and facies association must be taken into account for constricting models of carbonate depositional environment (Flugel, 2010). Three facies associations have been illustrated based on the identified microfacies and sedimentological characteristics.

6.2.2.1 Facies association one (FA 1)

Quartz bearings bioclastic packstone (MF 3), biomicrite wackestone (MF10**),** and bioclastic mudstone (MF11) microfacies are grouped under this facies association. The presence s of an alternating layer of clastic and carbonate materials is an indicator of the tidal flat setting. Carbonate tidal flats occur in specific environments that are shielded from the impact of open ocean waves. These areas are characterized by broad-shelf lagoons, which act as a barrier, reducing the force of incoming waves. This protective barrier separates the back shoal lagoons from the open ocean (Walker, 1992; Reading, 1996). Tidal flats are unique landscapes that exist partly underwater during high tides and are exposed during low tides.

6.2.2.2 Facies association two (FA 2)

Facies association 2 comprises oopelbiosparmicrite packstone (MF6), daysclad grainstone (MF7) and bioclastic wackestone (MF9) microfacies. The skeletal components of the lagoonal facies are varied and include different species of dayscladalen green algae, bivalves, and gastropods, which are typical indicators of a shallow water environment (Flugel, 1982; Shirazi et al 2013 and Damenu Adefris, 2022). Lagoons form along carbonates, where a beach barrier or partly encloses an area of shallow water, which has very limited connection to the open ocean. Sea water reaches a lagoon directly through a channel to the sea or via seepage through a barrier (Nichols, 2009).

6.2.2.3 Facies association three (FA 3)

The sandy mudstone (MF1), carbonate mudstone (MF2), coated biosparite grainstone (MF4) and packstone mudstone (MF5), biomicrite packstone (MF8) microfacies grouped under this facaies assosation. The skeletal grains, ooids, and coarse peloids sands indicate high-energy sand shoal environment which represents the plate form margin that separates the open marine from the restricted lagoon (Burchette and Wright, 1992, Flugel, 2004).

6.2.3 Depositional environment

Based on sedimentological and petrographic information, the vertical and lateral distribution of the facies type, as well as comparison from the modern facies, the carbonate succession suggests that they were deposited in a homoclinal carbonate ramp setting. According to Ahr (1973), the ramp environment was recognized as a major type of depositional setting for carbonate rock and used as an alternative to the carbonate shelf. The carbonate ramp is a gradually sloping surface that extends from near coastal land up to the basin. The slope of the ramp is less than 1^{o} and ranges smoothly from intertidal to basinal depth, with no significant change in gradient. In a ramp environment, the shallow water carbonate units gradually transition from offshore into progressively deeper water and finally into basinal environments.

6.2.3.1 Inner ramp

From the present study facies association 1, Facies association 2, and facies association 3 are found in shallow marine environment depositional environment. facies association 1 includes quartz bearings bioclastic packstone (MF3), biomicrite wackestone (MF10**),** and bioclastic mudstone (MF11) microfacies, facies association 2 comprises oopelbiosparmicrite packstone (MF6) and daysclad grainstone (MF7) microfacies and facies association 3 contains coated biosparite grainstone (MF4) from the studied section. The sample taken from exposure three is different from the other analyzed samples from the section. From the petrographic analysis of the sample from exposure three, radiolarian, sponge spicules and pelagic bivalves were identified and this indicates a deep marine environment. The inner ramp setting represents the euphotic zone between the upper shore face and fair wave base (FWWB), which is a zone of high energy and constant wave agitation (Tucker and Wright, 1990; Flugel, 2004). It includes areas from the shallow subtidal to the intertidal zone, such as the carbonate sands found in the agitated shallow subtidal shoreface zone (FWWB) and the low intertidal region. This encompasses tidal flat deposits, lagoon deposits, and barrier deposits (Ahr, 1973). The characteristics of sediments that formed in the inner ramp include predominantly Peloids of a sand shoal, ooids, and skeletal grains, in some cases with tidal flat, lagoons and beach environment, carbonate mudstone, wackestone, packstone, and evaporite facies formed.

6.3 Correlation

General stratigraphy of Ethiopian geology starts with a basement rock at the base covered by a Paleozoic Mesozoic sedimentary rock unit capped by a Tertiary trap series. The Mesozoic sediment of Ethiopia manly occurs in the Central Ethiopia (Getaneh Assefa, 1991; Russo et al., 1994; Ahmed Wolela, 2007, 2009), Mekelle basin (Bosellini et al., 1997; Beyth, 1971) and Ogaden basin (Bosellini et al., 2001). The present study of the pre-volcanic sedimentary unit in the Kella section is colorable with Blue Nile basin, Ogaden basin, and Mekelle basin based on the lithostratigraphic unit and stratigraphic position.

The sandstone unit in the Kella section is unconformably overlain on the basement unit (Giday WoldeGabriel et al., 1990; Tsegaye Abebe et al., 2010) and conformably overlaying by the mudstone unit as evidenced in the field and it is 165m thick. This unit comprises fine-coarse grain, poorly to well sorted, well rounded-sub-rounded grain size, thinly bedded, massively bedded with fine conglomerate lens and poorly consolidated sandstone, reddish-brownish, whitish, and light gray color in the bottom part of the section and it interpreted as a floodplain deposit. The middle and the upper part of the sandstone unit comprise poorly to well-sorted, well-rounded to sub-rounded grain with reddish-brown, whitish, and light gray color and the sedimentary structure that is found includes cross-bedded, lamination massive bedded, lens of conglomerate and the general fining upward sequence and it interpreted as deposited in the meandering river. Therefore the sandstone unit in the Kella section is coloreted with the Adigrat sandstone unit of the Blue Nile Basin, Ogaden Basin, and Mekelle Outlier (Ahmed Wolela, 2008). The Adigrat Sandstone Formation in the Blue Nile Basin has a maximum thickness of 100-700m and is interpreted as having continental origin (Aberra Mogessie et al., 2002; Russo et al., 1994; Ahmed Wolela, 2008,) in contrast Dawit Lebenie (2010, 2016) and Dawit Lebenie and Bussert (2009) proposed a storm dominated shore face to a barrier/ inlet spit as the depositional setting for this unit. In the Mekelle basin, the Adigrat sandstone has a thickness of 670m According to Bosellini et al. (1997) and Beyth (1972a, b) the Adigrat sandstone was deposited in a lacustrine-deltaic or estuarine environment, indicating continental origin. In contrast (Dainelli 1943; Merla et al 1979; Dawit Lebenie 2010) proposed shallow marine origin. In the Ogaden basin, this formation thickness ranges from 60-140m and the sandstone in this formation is typically quartzitic, well sorted, and mature, with a grain size that ranges from medium-coarse sand (Tamrat Worku and Astin, 1992).

The mudstone unit in the Kella section is conformably overlain by the carbonate unit and has a thickness of 24m. This unit comprises fine grain, variegated color, irregular wavy lamination with localized sampling, and it has fining upward sequences which are interpreted as deposited in a pretidal environment. This unit corresponds to the upper mudrock member of the Gohatsion formation in the Blue Nile basin. Recently, Samuel Getachew (2018) classified the Gohatsion Formation into lower mudrock member, a gypsum member (the middle member), and the upper mudrock member. The middle member and the lower member of the Gohatsion Formation were not observed in the Kella section.

During the early Jurassic-Oxfordian period, there was a significant transgression, most likely linked to the subsidence phase. This lead to a major rise in sea levels across East Africa, resulting in the submergence of the carton. The evidence for this can be found in the carbonate deposit in various basins, as documented by Bosellini (1989) and Russo et al. (1994). Extensive carbonate deposits are manly exposed in the three regions of Ethiopia, the Ogaden basin, the Blue Nile basin, and the Mekelle outlier.

The carbonate unit in the Kella section unconformably overlying by the volcanic unit (ignimbrite) with a thickness of 20m. This unit comprises the shale and the limestone intercalation. This unit is characterized by mudstone, wackestone, packstone, and grainstone microfacies and it contains the clastic input and coarse skeletal grain including brachiopod, gastropods, echinoid fragments, bivalve and it is formed in shallow marine environment. Therefore, it can be correlated with the Antalo Limestone of the Blue Nile basin, Mekelle basin, and Carbonate Formation in the Ogaden basin. The general correlation between the regional and the present study is presented below (Fig. 6.1)

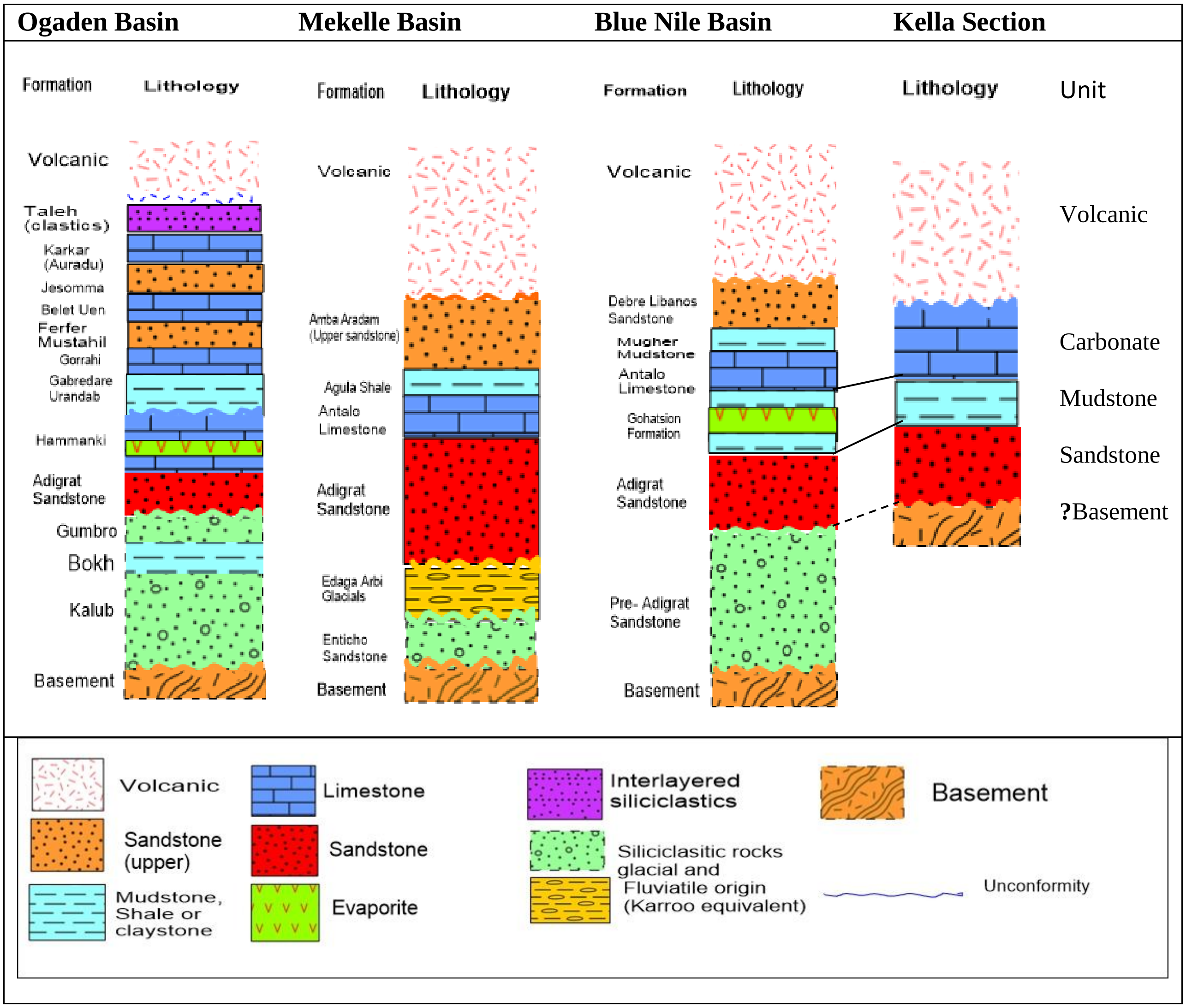

Figure 6. 1 The correlation of the Kella section with a regional lithostratigraphic unit of the Blue Nile, Ogaden, and Mekelle basin (After Beyth, M. 1972, Getaneh Assefa, 1981, and Dawit Lebenie, 2010)

6.4 Paleogeographic setting

In the late Triassic, east Africa was affected by the Karoo rift that developed in the east Africa margin along the southern flanks, in the crustal uplifting takes place after the Karoo rift (Hankel, 1994). In North-East Africa including the north and Central Ethiopia also Arabian plate formed under the stable margin of the Neotethyan Ocean. The Precambrian Orogenic belt, Karroo rifting, and Cretaceous and Tertiary rift tectonics are used to explain the distribution and rock associations. Following pre-existing lines of weakness in the basement, the Karroo rifts opened under oblique shear (Morley et al., 1999). N-S, NW-SE, and NE-SW oriented rift basins including the Ogaden and Abay Basins in Ethiopia, were formed as a consequence of the Karroo rift (Raaben et al., 1979; Tamirat Worku and Astin, 1992; Ahmed Wolela, 1997, 2008; Hunegnaw et al., 1998; Tadeesse Ketsela, 2007). Mesozoic sediments have been extensively deposited in Ethiopia due to a continuous period of land subsidence in the Ogaden and sea migration from the east to the west and north, encompassing the country's central and northern regions (Russo et al., 1994; Wolela Ahmed, 2007, 2009).

Therefore, as it is clearly described by Russo et al (1994) and Gani et al, (2009), the sedimentary successions in the Blue Nile basin and the Ogaden basin were formed at the same basin. The Kella section, which was the focus of the study, has great significance in understanding the depositional history of the Blue Nile and Ogaden basins. From the results of the current study, the pre-volcanic sedimentary units are correlated with the two basins and concluded that it was formed at the same basin as the Blue Nile and Ogaden basins.

CHAPETR SEVEN

CONCLUSION AND RECOMMENDATION

7.1 Conclusion

The detail sedimentological characteristics and stratigraphic works of the Pre-volcanic sedimentary unit in the Kella section were investigated. Based on a detail field investigation, three sedimentary unis were identified. These are sandstone unit, mudstone unit and carbonate unit. The volcanic unit overlies sedimentary unit and the basement unit underlies the sandstone unit.

Thirty-one (31) rock samples were prepared for thin sections and examined under a petrographic microscope. The petrographic analysis results of 10 sandstone samples show that the sandstone unit is classified into Subarcose (KS_2-b1, KS_2-b2A, KS_2-b2B, KS_2-b3A, KS_2-b3B, KS_2-b5), Litharenite (KS_2-b4, KS_2-b6), Sublitharenite (KS_2-b8), and Quartz arenite (KS_2-b11). Compositionally sandstone unit is mature to supper mature and texturally it ranges from immature to mature. Based on field description and petrographic results, the siliciclastic rocks are classified into 16 lithofacies types and these are classified under 3 litho facies association groups. These are: thinly bedded sandstone facies (F1), massive to laminated sandstone facies (F2), shale facies (F3), massively bedded sandstone facies (F4), poorly consolidated sandstone facies (F5), wavy laminated medium grain sandstone facies (F6), cross-bedded sandstone facies (F7), laminated sandstone facies (F8), massively bedded sandstone facies (F9), massive-thinly bedded sandstone facies (F10), thinly wavy laminated to massively bedded sandstone facies (F11), poorly consolidated mudstone facies (F12), shale intercalated mudstone facies (F13), silty-sand mudstone facies (F14), loosely consolidated mudstone facies (F15) and silty mudstone facies (F16) and the facies associations are Floodplain deposit, meandering river deposit, and peritidal environment.

From the carbonate unit, 20 thin sections were examined under a petrographic microscope. The analysis results reveal that the unit is classified into 12 microfacies types and grouped under 3 microfacies associations. This is sandy mudstone (MF1), carbonate mudstone (MF2), quartz bearings bioclastic packstone (MF 3), biosparite Grainstone (MF4), Packstone mudstone (MF5), Oopelbiosparmicrite Packstone (MF6), Daysclad Grainstone (MF7), biomicrite packstone (MF8) bioclastic wackestone (MF9) biomicrite wackestone (MF10**)** and bioclastic mudstone (MF11), and Radiolarian wackestone (MF12). The microfacies association of the carbonate unit is classified into three groups. Thus are; facies association 1 (MF3, MF10, MF11), facies association 2 (MF6, MF7, MF9), and facies association 3 (MF1, MF2, MF4, MF5, MF8) generally, the carbonate unit described in the Kella section was deposited in the shallow marine environment.

In the Kella section, the overall identified facies type, lithologic unit, depositional system, and their characteristics led to the conclusion of continental to shallow marine depositional environment. The Kella section, which was the focus of the study, has great significance in understanding the depositional history of the Blue Nile and Ogaden basins. From the results of the current study, the pre-volcanic sedimentary units are correlated with the two basins and concluded that it was formed at the same basin as the Blue Nile and Ogaden basins.

7.2 Recommendation

From the results of this thesis work, the following recommendation is given;

- The type of data for the analysis and interpretation of this study were primarily petrographic data and field investigation. The study area is highly affected by diagenesis processes and rift related faults which makes the area difficult to understand the sedimentological processes and to interpret the environment of formation. Therefore, it is recommended that to use additional geochemical data for further investigation.

References

Abbate, E., Bruni, P. and Sagri, M. (2015). Geology of Ethiopia: A Review and Geomorphological Perspectives. In: Billi, P. Landscapes and Landforms of Ethiopia, World Geomorphological Landscapes. Springer Science+Business Media Dordrecht .33-64.

Abera Mogessie, Krenn, K., Schaflechner, J., Koch, U., Egger, T., Goritchnig, B., Kosednar, B., Pichler, H., Ofner, L., Bauernfeind, D., Tadesse, S., Hailu K., and Demessie, M. (2002). Geological excursion to the Mesozoic sediments of the Abay Basin (Blue Nile), recent volcanics of the Ethiopian Main Rift and basement rocks of the Adola area, Ethiopia. Mitt.Österr.Miner.Ges. **147:** 43-74.

Aberash Habte, (2023). Stratigraphy and petrography of western rift escarpment volcanics sequence around Butajira Kella area, Central Main Ethiopian Rift. Unpublished MSc thesis, Addis Ababa Ethiopia.

Adefris, D., Nton, M. E., Boboye, O. A., Atnafu B. (2022). Stratigraphy and facies analysis of the Antalo limestone (Callovian–Tithonian), Mekele Basin, northern Ethiopia. Journal of Sedimentary Environments, **7(3):** 539-578. https://doi.org/10.1007/s43217-022-00110-w.

Ahr, W. M. (1973). The carbonate ramp: An alternative to the shelf model. Trans Gulf Coast Association of Geological Society, **23**: 221–225.

Armstrong-Altrin, J., Lee, Y.I., Verma, S.P. and Ramasamy, S. (2004). Geochemistry of sandstones from the upper Miocene Kudankulam Formation, southern India: Implications for provenance, weathering, and tectonic setting. J. Sediment. Res. **74**, 285–297.

Arno V., Di Paola G.M, Berhe Seife Michael (1981). The Kella Horst; its origin and significance in crustal attenuation and magmatic processes in the Ethiopian rift valley. First international symposium of crustal movements in Africa. Proceedings: Addis Ababa, United nations.

Asfawosson Asrat, Barbey, P. and Gleizes, G. (2001). Precambrian geology of Ethiopia: a review. Africa Geoscience Review, **8(3)**:271-288.

Beyth, M. (1971). The Geology of Central and Western Tigrai. Unpublished Manuscript. Ministry of Mines, Addis Ababa. Ethiopia.

Beyth, M. (1972). Paleozoic-Mesozoic sedimentary basin of Mekele Outlier, Northern Ethiopia. American Association of Petroleum Geologists Bulletin, **56(12):** 2426–2439. https:// doi. org/ 10. 1306/ 819A4 22A- 16C5- 11D7- 86450 00102 C1865D

Boccaletti, M., R. Mazzuoli, M. Bonini, T. Trua, and Bekele Abebe (1999). PlioQuaternary volcano-tectonic activity in the northern sector of the Main Ethiopian Rift (MER): relationships with oblique rifting, Journal of African Earth Sciences, 29, 679–698.

Boggs, S. (2009). Petrology of Sedimentary rocks, 2nd ed, Cambridge University Press, New York, 612pp.

Bonini, M., Corti, G., Innocenti, F., Manetti, P., Mazzarini, F., Tsegaye Abebe, and Z. Pecskay (2005), Evolution of the Main Ethiopian Rift in the frame of Afar and Kenya rifts propagation, Tectonics, 24, TC1007, doi:10.1029/ 2004TC001680.

Bosellini, A. (1988). The continental margins of Somalia. In: Geology and Geophysics of continental margins. AAPG Memoir **53**, 185–205.

Bosellini, A., Russo, A., and Getaneh Assefa. (2001).The Mesozoic succession of Dire Dawa, Harar Province, Ethiopia, Jafrearsc.32: 403-417.

Bosellini, A., Russo, A., Fantozzi, P.L., Getaneh Assefa and Solomon Tadesse. (1997). The Mesozoic succession of the Mekele Outlier (Tigrai Province, Ethiopia), Mem. Sci. Geol.49:95–116.

Bunter, M.G., Debretsion, T. and Woldegiorgis, L. (1998). New development in the pre-rift prospectively of the Eritrean Red Sea. J. Pet. Geol. **21**: 374–400.

Burchette, T. P., & Wright, V. P. (1992). Carbonate ramp depositional systems. Sedimentary Geology, **79**: 3–57.

Cannon, R.J., Simiyu-Sianbu, W.M.N. and Karanja, F.M. (1981). The proto-Indian Ocean and a probable Paleozoic/Mesozoic triradial rift system in East Africa. Earth Planet, Sci. Lett. **52**: 419–426.

Choquette, P.W., and James, N.P. (1981). Diagenesis 12. Diagenesis in limestone-3. The deep burial environment. Geoscience Canada. 14: 3-35.

Choquette, P.W., and James, N.P. (1990). Limestone - the burial diagenetic environment. In Diagenesis. Edited by I.A. Mcllreath and D.W. Morrow. Geoscience Canada Series. 4: 75-1 12.

Chorowicz, J. (2005). The East African Rift System. Journal of African Earth Sciences **43**: 379–410.

Coffin, M.F. and Rabinowitz, P.D. (1988). Evolution of the conjugate East African-Madagascan margins and the Western Somali Basin. Geological Society of America, Special Paper 226, 1–78.

Collinson, J.D. and Reading, H.G. (1996). Clastic Coasts. In: Sedimentary Environments: Processes, Facies and Stratigraphy, Reading H.G. (edn), 3rd edn, Blackwell, USA, pp. 154 231.

Corti, G. (2009). Continental rift evolution: From rift initiation to incipient break-up in the Main Ethiopian Rift, East Africa, Earth-Science Reviews **96**: 1–53.

Dainelli, G. (1943). Geologia dell'Africa Orientale (p. 464). Real Accademia Italia.

Daniel Meshesha, Takele Chekol, and Sileshe Negussia (2021). Major and trace element compositions of basaltic lavas from western margin of central main Ethiopian rift: enriched asthenosphere vs. mantle plume contribution, Heliyon, **7**: e08634. https://doi.org/10.1016/j.heliyon.2021.e08634 .

Dawit Lebenie Enkurie and Bussert, R. (2009). Stratigraphy and facies architecture of Adigrat Sandstone, Blue Nile basin-central Ethiopia, Zbl.Geol.Palaont.Teil I, **3 (4):** 217- 232.

Dawit Lebenie Enkurie, (2010). Adigrat Sandstone in Northern and Central Ethiopia: stratigraphy, facies, depositional environments and palynology. Unpublished Ph.D. thesis Technische Universität, Berlin. 166 pp.

Di Paola, G. M. (1972). Ethiopian Rift Valley (between 7° and 8° 40' lat. North): Bulletin Volcanologique, v. 36, p. 517-560

Dickinson, W.R. (1985). Interpreting provenance relations from detrital modes of sandstones. Provenance Arenites, **148**: 333–361.

Dunham, R.J. (1962). Classification of carbonate rocks according to depositional texture. Pet. Geol., **1**: 108-121.

Ebinger, C., Tilahun Yemane, Harding, D., Samson Tesfaye, Kelley, S. and Rex, D. (2000). Rift deflection, migration, and propagation: linkage of the Ethiopian and Eastern rifts, Africa. Geological Society of America Bulletin, **112**: 163–176.

Ebinger, C.J., Tesfaye Yemane, Gidey WoldeGabriel, Aronson, J.L. and Walter, R.C. (1993). Late Eocene Recent volcanism and faulting in the southern Main Ethiopian Rift. Journal of the Geological Society of London, **150**: 99–108.

Embry, A. and Klovan, J.E. (1971). A late Devonian reef tract on Northeastern Banks Island, Northwest Territories. Pet. Geol., **19**: 730-781.

Fairhead, J.D. (1988). Mesozoic plate tectonic reconstructions of the central South Atlantic Ocean: the role of the West and Central African rift system. In: Scotese, C.R., Sager, W.W. (Eds.), Mesozoic and Cenozoic Plate Reconstructions. Tectonophysics, 155pp. 181–191.

Flemming, B.W. (2012). Silicicalstic back-barrier tidal flasts (Chapter 10), In: Davis, R.A. (Jr) and Dalrymple, R.W (2012). Principles of Tidal Sedimentology, Springer Science+Business Midea B.V. DOI 10.1007/978-94-007-0123-6_10.

Flügel, E. (1982). Microfacies analysis of limestones. Springer.

Flügel, E. (2004). Microfacies of Carbonate Rocks: Analysis, Interpretation and Application. Springer, Berlin, 976 pp.

Flügel, E. (2010). Microfacies of Carbonate rocks: Analysis. Springer

Folk RL (1959) Practical petrographic classifcations of limestones. AAPG Bull 43:1–38.

Folk,RL. (1980). Petrology of sedimentary rocks. Austin, texas;Hemphill publishing campany. 184pp.

Gani N.D., Abdelsalam, M. G., Gera, S., Gani, M. R. (2009). Stratigraphic and structural evolution of the Blue Nile basin, Northwestern Ethiopian plateau.Geol.J.**44 (1):**30-56.

Gani, N.S., Abdelsalam, M.G., Gera, S. and Gani, M.R. (2008). Stratigraphic and structural evolution of the Blue Nile Basin, Northwestern Ethiopian Plateau. Geol. J. 1–27.

Gebrehiwot, S.G., Ilstedt, U., Gardenas, A. I. and Bishop, K. (2010). Hydrological characterization of watersheds in the Blue Nile Basin. Hydrol. Earth Syst. Sci. Discuss. **7**: 4089–4111.

Geological Survey of Ethiopia (GSE) (2010). Geology of the Akaki - Beseka area. Unpublished technical report, GSE, Addis Ababa, Ethiopia, 93pp.

George, R., Rogers, N. (2002). Plume dynamics beneath the East African plate inferred from the geochemistry of the Tertiary basalts of southern Ethiopia. Contrib. Mineral. Petrol. **144**: 286–304.

Getaneh Assefa (1979). Clay mineralogy of the Mesozoic sequence in the Upper Abbay (Blue Nile) River valley region, Ethiopia. SINET, Ethiop.J.Sci.,**3 (2)**: 37-65.

Getaneh Assefa (1981). Gohatsion Formation. A new Lias-Malm lithotratigraphic unit from the Abay River basin, Ethiopia. Geosci. J. **2**: 63–68.

Getaneh Assefa (1981). Gohatsion Formation. A new Lias-Malm lithotratigraphic unit from the Abay River basin, Ethiopia. Geosci. J. **2:** 63–68.

Getaneh Assefa (1991). Lithostratigraphy and environment of deposition of the Late Jurassic-Early Cretaceous sequence of the central part of Northwestern Plateau. N. Jb. Geol. Paläont. Abh. 182, Stuttgart.

Gezahegn Yirgu, Ebinger, C.J., and Maguire, P.K.H. (2006). The Afar volcanic province within the East African Rift System. Geological Society, London, Special Publications, **259**: 327pp.

Giday Woldegabriel, Aronson, J.L., Walter, R.C. (1990). Geology, geochronology, and rift basin development in the central sector of the Main Ethiopia Rift. Geol. Soc. Am. Bull. **102 (4)**: 439–458.

Hankel, O. (1994). Early permian to middle jurassic rifting and sedimentation in East Africa and Madagascar. Geol. Rundschau, **83**: 703–710.

Headberg, D. Hollis. (1976). International Stratigraphic Guide: A Guide to stratigraphic classification, Terminology and Procedure. John Wiley & Sons. Inc, Canada, 200 pp.

Hofmann, C., Courtillot, V., Feraud, G., Rochette, P., Gezahegn Yirgu, Ketefo, E. and Pik, R. (1997).Timing of the Ethiopian flood basalt event and implications for plume birth and global change, Nature, 389: 838-841

https://en.wikipedia.org/wiki/ Sodo (woreda. accessed on 28.12. 2023.

https://www.worldweatheronline.com/kela-weather-averages/et.aspx Accessed on Tue 16th Apr 11:42 am

Hunegnaw, A., Sage, L. and Gonnard, R. (1998). Hydrocarbon potential of the intracratonic Og-aden Basin, SE Ethiopia. J. Petr. Geol. **21**: 401–425.

Jepsen, D.H. and Athearn, M.J. (1964). Land and water resources of the Blue Nile River Basin, Appendix II-Geology. US Department of Interior/ Ethiopia's Water Resources Department, Addis Ababa.

Jepsen,D.H. and Athearn,M.J.(1961). Geologic plane and section of the left bank of the Blue Nile canyon near crossing of Addis Ababa-Debre Markos road. U.S.Dept. interior, Ethiopia's Water Res., Addis Ababa.

Kazmin, V. (1972). The Geology of Ethiopia. Unpublished Report, EIGS, Addis Ababa, Ethiopia.

Kazmin, V., Alemu Shiferaw and Tilahun Balcha (1978). The Ethiopian Basement: Stratigraphy and possible manner of evolution. Geol. Rundusch, **67**:531–546.

Kieffer, B., Arndt, N., Lapierre, H., Bastien, F., Bosch, D., Pecher, A., Gezahegn Yirgu, Dereje Ayalew, Weis, D., Jerram A.D., Keller, F. and Meugniot, C. (2004). Flood and shield basalts from Ethiopia: magmas from the African super swell. Journal of Petrology, **45**: 793-884.

Klerkx, J, Theunissen, K. and Delvaux, D. (1998). Persistent fault controlled basin formation since the Proterozoic along the Western Branch of the East African Rift, Journal of African Earth Sciences. **26(3)**: 347-361.

Klerkx, J., Theunissen, K. and Delvaux, D. (1998). Persistent fault-controlled basin formation since the Proterozoic along the Western Branch of the East African Rift. Journal of African Earth Sciences 26(3):347-361.

Krumbein, W.C. and Sloss, L, L. (1950). Stratigraphy and Sedimentation. W.H. Freeman & Co., San Fransisco, USA, 497 pp.

McConnel, R.B. (1972). The geological development of the rift system of Eastern Africa. Geol. Soc. Am. Bull. **83**: 2549–2572.

Mengesha Tefera, Tadiwos Chernet and Workineh Haro (1996). Explanation of the geological map of Ethiopia (Scale 1:2,000,000) 2nd ed. Unpublished technical report, Ethiopian Institute of Geological Surveys, Addis Ababa, Ethiopia, 85pp.

Merla, G., Abbate, E., Azzaroli, A., Bruni, P., Fazzuoli, M., Sagri, M. and Tacconi, P. (1979). Geological Map of Ethiopia and Somalia and Comment with a Map of Major Landforms (Scale 1:2 000 000). Consiglio Nazionale delle Ricerche, Rome, 95.

Merla, G., Abbate, E., Canuti, P., Sagri, M. & Tacconi, P. (1979). Geological map of Ethiopia and Somalia and comment with a map of major landforms (scale 1:2,000,000). Rome: Consiglio Nazionale delle Ricerche 95.

Ministry of Water Resources: Abbay River Basin Integrated Development Master Plan Project: Data Collection – Site Investigation Survey and Analysis, Phase 2. BECOM in collaboration with BRGM and ISL Consulting Engineers, Ministry of Water Resources, Ethiopia, Addis Ababa, Ethiopia, 1998.

Mohr, P. and Zanettin, B. (1988). The Ethiopian flood basalt province. In: Continental flood basalts, J. D. Macdougall (ed), Springer, Netherlands, pp. 63-110.

Mohr.P.A. (1962). The geology of Ethiopia. Addis Ababa University press, Addis Ababa, Ethiopia.

Morley, C.K., Ngenoh, D.K. and Ego, J.K. (1999). Introduction to the East African Rift System, in C.K. Morley ed., Geoscience of Rift Systems—Evolution of East Africa: AAPG Studies in Geology, **44**: pp. 1–18.

Nichols, G. (2009). Stratigraphy and Sedimentology, 2nd ed., John Wiley & Sons.

Peccerillo, A., Donati, C., Santo, A., Orlando, A., Gezahegn Yirgu and Dereje Ayalew (2007). Petrogenesis of silicic peralkaline rocks in the Ethiopian rift: geochemical 112 evidence and volcanological implications. Journal of African Earth Sciences 48(2):161-1

Pettijohn, F.J., Potter, P.E., and Siever, R. (1972). Sand and Sandstone, Springer-Verlag, Berlin', Heidelberg.

Pettijohn, F.J., Potter, P.E., and Siever, R. (1987). Sand and Sandstone, Springer-Verlag, NewYork, 553pp.

Pik, R., Daniel, C., Coulon, C., Gezahegn Yirgu, Hofmann, C. and Dereje Ayalew (1998). The northwestern Ethiopian plateau flood basalts: classification and spatial distribution of magma types. Journal of Volcanology and Geothermal Research, 81: 91- 111.

Pik, R., Marty, B., Carignan, J., Gezahegn Yirgu and Teklewold Ayalew (2008). Timing of East African Rift development in southern Ethiopia: Implication for mantle plume activity and evolution of topography. Geology, **36**: 167–170.

Potter, P.E ., Maynard, J.B., Depetris, P. J. (2005). Mud and Mudstones. Springer, p.305

Raaben, V.P., Komenyev, S.P., Lissin, V.N., Kitachew W.T. (1979). Preliminary Report on the Evaluation of Petroleum Prospects of the Ogaden Basin, Ethiopia. Ethiopian Inst. Geol. Surv., Note No. 112.

Reading, H.G. (1996) Sedimentary Environments: Processes, Facies and Stratigraphy. 3rd eds. Blackwell.

Russo, A., Getaneh Assefa. and Balemwal Atnafu (1994). Sedimentary evolution of the Abay River (Blue Nile) Basin, Ethiopia. N. Jb. Geol. Palaont. Mh. **5**:291-308.

Salman, G. and Abdula, I. (1995). Development of the Mozambique and Ruvuma sedimentary basins, offshore Mozambique. Sed. Geol. **96**: 7–41.

Samuel Getachew (2018). Stratigraphic, Petrographic and geochemical characteristics of the Gohatsion formation in the Blue Nile basin, Central Ethiopia Implication for paleoenvironmental reconstruction. Unpublished MSc Thesis, Addis Ababa University, Addis Ababa, Ethiopia, 103pp.

Scotese, C.R. and Chatterjee, S. (1999). The breakup of Gondwana and the evolution and biogeography of the Indian Plate. PINSA, **65 A (3**): 397–425.

Shackelton, R.M. (1978). Structural development of the East African Rift System. In: Bishop, W.W. (Ed.), Geological Background to Fossil Man: Recent Research in the Gregory Rift. Scottish Academic Press, East Africa, 55p.

Shirazi, M. P., Jahromi, F. D., & Bahrami, M. (2013). Microfacies and sedimentary environments of the fahliyan formation from the Southwest of Iran (Shiraz, Zagros). Open Journal of Geology, **3**: 49–53.

Sileshe Negussia, (2019). Petrology and Geochemistry of Basaltic Rocks from Midre Kebd Area, Main Ethiopian Rift Southern Ethiopia, Unpublished MSc thesis, Addis Ababa Ethiopia.

Tadesse Ketsela (2007). Integrated geophysical data processing and interpretation of crustal structure in Ethiopia with emphasis on the Ogaden Basin and adjacent areas. Unpublished PhD Dissertation, the University of Texas at El Paso, pp238

Tamirat Worku and Astin, T.R. (1992). The Karroo sediments (Late Palaeozoic to Early Jurassic) of Ogaden Basin, Ethiopia. Sediment. Geol. **76**: 7–21.

Tamiru Alemayehu, (2006). Groundwater Occurrence in Ethiopia, Addis Ababa University, Ethiopia.

Tamrat Worku and Astin, T.R. 1992. The Karroo sediments (Late Palaeozoic to early Jurassic) of Ogaden Basin, Ethiopia. Sediment. Geol. **76:** 7–21.

Tao, H., Sun, S., Wang, Q., Yang, X. and Jing, L. (2014). Petrography and geochemistry of Lower Carboniferous greywacke and mudstones in Northeast Junggar, China: Implications for provenience, source weathering and tectonic setting. Journal of Asian Earth Sciences, **87**: 11-25.

Teklewold Ayalew (1997). Metamorphic and structural evolution of the Gore-Gambella area western Ethiopia. SINET, **20**:235-259.

Tesfaye Korme, Acocella,V. and Bekele Abebe (2004). The role of pre-existing structures in origin, propagation and architecture of faults in the Main Ethiopian Rift. Gondwana Res. **7**: 467–479.

Tsegaye Abebe, Balestrieri, M.L. and Bigazzi, G. (2010). The Central Main Ethiopian Rift is younger than 8 Ma: confirmation through apatite fission-track thermochronology. Terra.Nova, **22 (6)**: 470–476.

Tsegaye Abebe, Mazzarini, F., Innocenti, F. and Manetti, P. (1998). The Yerer–Tullu Wellel volcanotectonic lineament: a transnational structure in central Ethiopia and the associated magmatic activity. J. Afr. Earth Sci., 26, 135–150.

Tucker, M. E., and Wright, V. P. (1990). Carbonate sedimentology (p. 482). Blackwell.

Tucker, ME. (2001). Sedimentary Petrology: An Introduction to the Origin of Sedimentary Rocks. 3rd eds, Great Britain at the Alden Press, Oxford and Northampton The Blackwell Science.

Walker, R. G., & Plint, A. G. (1992). Wave and storm-dominated shallow marine systems. In R. G. Walker & N. P. James (Eds.), Facies models response to sea level change Geological Association of Canada. 219–238pp.

Wanas, H.A., Abu El-Hassan, M.M. (2006). Paleosols of the upper cretaceous-lower tertiary maghra el-bahari formation in the northeastern portion of the Eastern Desert, Egypt: their recognition and geological significance. Sed. Geol. **183**: 243–259.

Wilson, J. L. (1975). Carbonate facies in geologic history (p. 471). Springer

Wolela Ahmed (2007). Source Rock Potential of the Blue Nile (Abay) Basin, Ethiopia. Petroleum Geology, **30(4):** 389-402.

Wolela Ahmed (2008). Sedimentation of the Triassic-Jurassic Adigrat Sandstone Formation, Blue Nile (Abay) basin, Ethiopia: Journal of African Earth Sciences, **52:**30-42

Wolela Ahmed (2009). sedimentation and depositional environments of the Barremian-Cenomanian Debre Libanos Sandstone, Blue Nile (Abay) Basin, Ethiopia. Cretaceous Research, **30**: 1133-1145.

Wolela Ahmed (2014). Diagenetic contrast of sandstones in hydrocarbon prospective Mesozoic rift basins (Ethiopia, UK, USA). Journal of African earth science, **99:** 529–553.

Wolela, A. (1997). Sedimentology, diagenesis and hydrocarbon potential of sandstone in hydrocarbon prospective Mesozoic basins (Ethiopia, UK, USA). Ph.D. Thesis, the Queen's University of Belfast. United Kingdom, 228p

Wolela, A. (2007). Source rock potential of the Blue Nile (Abay) basin, Ethiopia. Journal of Petroleum Geology, **30(4):** 389-402.

Wolela, A. (2009). Sedimentation and depositional environments of the BarremianCenomanian Debre Libanose sandstone, Blue Nile (Abay) basin, Ethiopia. Cretaceous Research, **30(5):** 1133-1145.

Wolfenden, E., Ebinger, C., Gezahegn Yirgu, Deino, A. and Dereje Ayalew (2004). Evolution of the northern Main Ethiopian rift: birth of a triple junction. Earth and Planetary Science Letters, **224**: 213–228.